กลยุทธ์ในการยิงทะลุท่อกรุสำหรับแหล่งกักเก็บก๊าซธรรมชาติที่มีหลายชั้น

นายรณศักดิ์ โมมิน

วิทยานิพนธ์นี้เป็นส่วนหนึ่งของการศึกษาตามหลักสูตรปริญญาวิศวกรรมศาสตร์มหาบัณฑิต
สาขาวิชาวิศวกรรมปิโตรเลียม ภาควิชาวิศวกรรมเหมืองแร่และปิโตรเลียม
คณะวิศวกรรมศาสตร์ จุฬาลงกรณ์มหาวิทยาลัย
ปีการศึกษา 2552

ต้นฉบับไม่มีหน้านี้
NO THIS PAGE IN ORIGINAL

Thesis Title	PERFORATION STRATEGY FOR MULTILAYERED GAS RESERVOIRS
By	Mr. Ronasak Momin
Field of Study	Petroleum Engineering
Thesis Advisor	Assistant Professor Jirawat Chewaroungroaj, Ph.D.
Thesis Co-advisor	Yothin Tongpenyai, Ph.D.

Accepted by the Faculty of Engineering, Chulalongkorn University in Partial Fulfillment of the Requirements for the Master's Degree

.... Dean of the Faculty of Engineering
(Associate Professor Boonsom Lerdhirunwong, Dr.Ing.)

THESIS COMMITTEE

.... Chairman
(Associate Professor Sarithdej Pathanasethpong)

.... Thesis Advisor
(Assistant Professor Jirawat Chewaroungroaj, Ph.D.)

.... Thesis Co-Advisor
(Yothin Tongpenyai, Ph.D.)

.... Examiner
(Assistant Professor Suwat Athichanagorn, Ph.D.)

.... Examiner
(Vinit Hansamuit, Ph.D.)

รณศักดิ์ โมมิน: กลยุทธ์ในการยิงทะลุท่อกรุสำหรับแหล่งกักเก็บก๊าซธรรมชาติที่มีหลายชั้น (PERFORATION STRATEGY FOR MULTILAYERED GAS RESERVOIRS)
อาจารย์ที่ปรึกษาวิทยานิพนธ์หลัก: ผศ. ดร. จิรวัฒน์ ชีวรุ่งโรจน์, อาจารย์ที่ปรึกษาวิทยานิพนธ์ร่วม: ดร.โยธิน ทองเป็นใหญ่, 125 หน้า

ลักษณะของแหล่งผลิตก๊าซธรรมชาติในอ่าวไทยเกิดจากการสะสมตัวของชั้นตะกอนแม่น้ำและปากแม่น้ำโบราณในขณะเดียวกันแหล่งกักเก็บดังกล่าวก็ได้ถูกรอยเลื่อนทางธรณีตัดเป็นโครงสร้างกักเก็บเล็กๆ ความซับซ้อนทางธรณีวิทยาดังกล่าวส่งผลต่อเนื่องมาถึงกรรมวิธีการผลิตก๊าซจากชั้นหินกักเก็บเหล่านี้ เนื่องจากชั้นหินกักเก็บมีหลายชั้นในบริเวณเดียวกัน ชั้นหินกักเก็บแต่ละชั้นมีความต่างกันทั้งในแง่ของขนาดและคุณสมบัติ ในขณะเดียวกันก็มีแรงผลักดันต่างกัน ทั้งแรงผลักดันจากตัวเอง และแรงผลักดันจากชั้นน้ำบาดาลที่ต่อกับชั้นก๊าซ เนื่องจากปัญหาดังกล่าวจึงจำเป็นต้องมีการศึกษากลยุทธ์ในการผลิตที่เหมาะสมสำหรับแหล่งกักเก็บก๊าซธรรมชาติที่มีหลายชั้น การศึกษานี้จะใช้แบบจำลองเป็นตัวศึกษา โดยมุ่งไปที่ลักษณะและคุณสมบัติของหินกักเก็บต่างๆ เพื่อที่จะวิเคราะห์ถึงปัจจัยที่มีผลต่อการผลิต และทำการหากลยุทธ์ที่เหมาะสมที่สุดในแง่ต่างๆ

จากการศึกษาพบว่าเมื่อชั้นก๊าซธรรมชาติทุกตัวอยู่ภายใต้แรงผลักดันจากตัวเอง การผลิตจากทุกๆชั้นพร้อมๆกันจะให้ผลลัพธ์ที่ดีที่สุดทั้งในแง่ของประสิทธิภาพและเวลาในการผลิต ในขณะเดียวกัน เมื่อชั้นก๊าซทุกตัวอยู่ภายใต้แรงผลักดันจากน้ำบาดาล น้ำบาดาลจะมีผลกระทบต่อความสามารถในการผลิตก๊าซธรรมชาติมาก การศึกษาพบว่าการผลิต พร้อมๆกันทุกชั้นโดยทำการปิดชั้นที่ผลิตน้ำมากไปทีละชั้นจะให้ผลลัพธ์ที่ดีที่สุด ในกรณีที่แหล่งผลิตก๊าซธรรมชาติประกอบด้วยชั้นก๊าซที่ผลิตภายใต้แรงขับจากตัวเอง และชั้นก๊าซที่ผลิตภายใต้แรงขับดันจากน้ำบาดาลอยู่ด้วยกัน พบว่าการแยกการผลิต ระหว่างผลิตจากชั้นก๊าซที่อยู่ภายใต้แรงขับดันจากน้ำบาดาล และชั้นก๊าซที่อยู่ภายใต้แรงผลักดันจากตัวเอง โดยทำการปิดชั้นที่ผลิตน้ำมากไปทีละชั้นจะให้ผลลัพท์ที่เหมาะสมที่สุด การศึกษายังพบว่าค่าความซึมผ่านของชั้นหินแต่ละชั้นมีผลมากต่อประสิทธิภาพในการผลิต

ภาควิชา วิศวกรรมเหมืองแร่และปิโตรเลียม	ลายมือชื่อนิสิต......................................
สาขาวิชา วิศวกรรมปิโตรเลียม	ลายมือชื่อ อาจารย์ที่ปรึกษา......................................
ปีการศึกษา 2552	ลายมือชื่อ อาจารย์ที่ปรึกษาร่วม......................................

4971618521 : MAJOR PETROLEUM ENGINEERING
KEYWORDS: MULTILAYERED GAS RESERVOIRS/ DRIVE MECHANISM/ CROSSFLOW/ RECOVERY FACTORS

RONASAK MOMIN: PERFORATION STRATEGY FOR MULTILAYERED GAS RESERVOIRS.
THESIS ADVISOR: ASST. PROF. JIRAWAT CHEWAROUNGROAJ, Ph.D.
THESIS CO-ADVISOR: YOTHIN TONGPENYAI, Ph.D., 125 pp.

The gas reservoirs in the Gulf of Thailand are generally hosted by fluvio-deltaic sands, which are generally limited in extent and dissected by numerous faults. This depositional environment and trapping mechanism result in multilayered reservoirs with different reservoir characteristics. The drive mechanisms associated with the reservoirs are either depletion or water drive. This study was initiated to determine the optimum depletion scenario for the multilayered reservoirs with different drive mechanisms. The study includes computer modeling of the reservoirs as well as several simulation runs to determine the effect of drive mechanism to the recovery performance under various perforation strategies.

The study reveals that when the multilayered reservoirs are under depletion drive mechanism, depletions from all reservoirs at the same time would provide optimal recovery performance in terms of production time and crossflow minimization between layers. When all reservoirs are under water drive mechanism, to produce from all layers and later on shut the layer with high water production off would provide optimal solution in terms of recovery efficiency, crossflow, and recovery time. For commingled production from both depletion drive and water drive reservoirs, separate production between different reservoir drive mechanisms, with early shutting-off the water producing reservoirs would provide optimal solution in terms of recovery efficiency, crossflow, and recovery time. It is also found that permeability plays important role in determination of recovery efficiency for each reservoir.

Department: Mining and Petroleum Engineering. Student's Signature: Ronasak M.
Field of Study: Petroleum Engineering. Advisor's Signature: J. Cheng
Academic Year: 2009 Co-advisor's Signature: Y. Ty

Acknowledgements

Many persons have contributed either directly or indirectly to my thesis; I wish to express my thanks to them sincerely.

Firstly and foremost, I would like to thank Dr. Yothin Tongpenyai and Dr. Jirawat Chewaroungroaj, my thesis advisors, for giving knowledge of petroleum engineering and invaluable guidance during this study. I also would like to express my sincere gratitude for his patience and encouragement throughout this work.

Secondly, I would like to thank all faculty members in the Department of Mining and Petroleum Engineering who have offered petroleum knowledge, technical advice, and invaluable consultation. I wish to thank the thesis committee members for their comments and recommendations that make this thesis formally complete.

I am extremely gratitude to my workplaces, PTT Exploration and Production Public Company Limited, who allowed me to study in this master degree program.

I would also like to thank Mr. Chavaphol Kamolsripanit, Ms. Jantakan Srisuriyon, Ms. Rossawan Chandakaew, Ms. Thanita Kiatrabile, Mr. Daniel de Verteuil, Ms. Kobkaeo Damri, Mr. Naruttee Kovitkanit, and Mrs. Suthinee Chaikawin for their kind help on using ECLIPSE reservoir simulation program, providing some important data used in this work, as well as helping on thesis administration.

Lastly, I would like to express my deep gratitude and thank to my family and friends who have always been my inspiration, hope, and faith.

Contents

CHAPTER Page

List of Tables

List of Figures

List of Abbreviations

API	degree (American Petroleum Institute)
bbl	barrel (bbl/d, bpd: barrel per day)
BHP	bottomhole pressure
CGR	condensate gas ratio
D	Darcy
GRV	Gross Rock Volume
GWC	Gas-Water Contact
K	kilo- (10^3 or 1,000)
M	thousand (1,000 of petroleum unit),
MSCF/D	thousand standard cubic feet per day
NTG	Net-To-Gross Rock Volume
OGIP	Original Gas In-Place
PVT	pressure-volume-temperature
PSIA or psia	pounds per square inch absolute
RF	Recovery Factor
SCAL	special core analysis
SGAS	gas saturation
STB or stb	stock-tank barrel
STB/D	stock-tank barrels per day
SWAT	water saturation
THP	Tubing Head Pressure

Nomenclature

A	cross-section area
B_g	gas Formation Volume Factor
Bw	water Formation Volume Factor
C_f	formation compressibility
d	differential operator
G	gas in place
G_p	cumulative gas production
h	*height*
k	permeability
k_{rg}	gas relative permeability
k_{rw}	water relative permeability
M	molecular weight
p	pressure
q	volumetric flow rate
Q	volumetric flow rate at standard conditions
r	radial direction
R	universal gas constant
S	saturation
t	time period (e.g.,year)
T	temperature
V	fluid volume
W_p	water production
W_e	water encroachment
x	^{1}distance in x direction, ^{2} x direction
y	y direction
z	^{1} compressibility factor, ^{2} z direction

GREEK LETTER

ϕ	porosity
ρ	fluid density (mass/volume)
μ	fluid viscosity

Δ	difference operator
∂	partial differential operator
υ	flow velocity

SUPERSCRIPTS

n	current time level
$n+1$	new time level

SUBSCRIPTS

A	areal
g	gas
i	initial
o	oil
r	radial
w	water

CHAPTER I

INTRODUCTION

Multilayered gas reservoirs in the Gulf of Thailand (GoT) are generally hosted by fluvio-deltaic sands, which are generally limited in extent and dissected by numerous faults. Thus a single area may consist of a large number of individual reservoirs. Trapping is generally achieved in faulted anticlines or sand lens structures.

The basins are generally gas prone, primarily as a result of high heat flows and relatively deep burial depths. The heat flow factor also appears to have resulted in the release of significant quantities of CO_2 from the breakdown of basement carbonates. This CO_2 is associated with most of Thailand's commercial gas accumulations.

The reservoir drive mechanism for each sand layer in the GoT is found to be either depletion drive or water drive mechanism. This is due to the multiple depositional environment of the basin.

Within a single compartment of the reservoirs, there can be numbers of reservoir sands. To find 20 hydrocarbon-bearing sands in a single well is not uncommon in the GoT. These reservoir sands can be either channel sands or bar sands. The channel sands are typically thicker than bar sands, and are often supported by aquifer. The bar sands are thinner, with the shape of thin lens (from delta front bars and crevasse spray deposits). The bar sands have been found with both aquifer support and no aquifer support. Figure 1.1 depicts the shape and patterns of bar and channel sands.

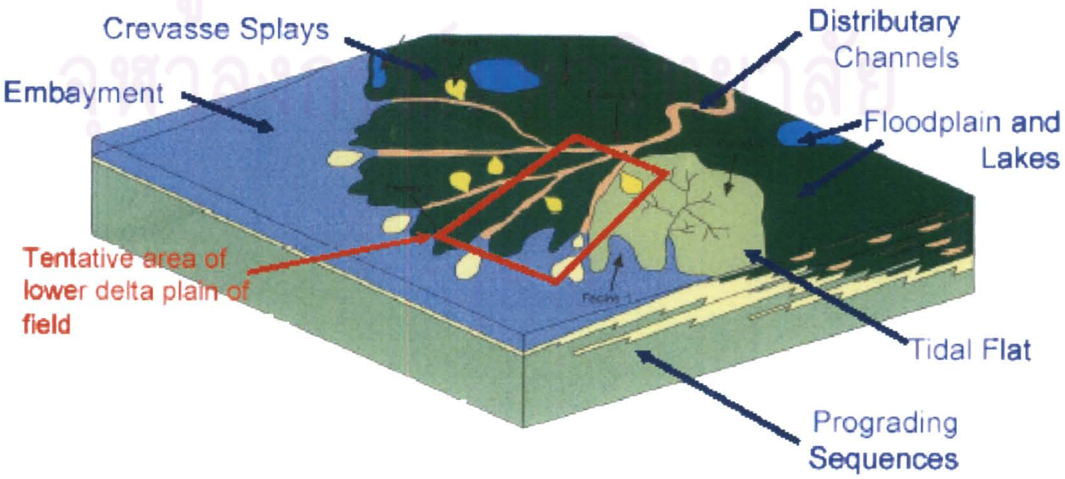

Figure 1.1 Shape & Patterns of Bar and Channel Sands

The channel sands encountered in the GoT multilayered gas reservoirs have porosity ranging from 8% to 30% and permeability ranging from 1 mD to 10 D. The channel sand thickness is in the range of 5 to 30 meters (16 to 100 feet). The channels are found both as isolated channel, interconnected groups and even multiple interconnected groups.

The bar sands have less porosity than the channel sands given the same depth. Their porosity lies in a range of 8% to 25% and permeability in the range of 1 mD to 10 D. The sand thickness is in the range of 1 to 20 meters (3 to 60 feet) in general.

Another complexity of the GoT multilayered gas reservoir is that the type of sand is not totally associated with drive mechanism i.e., a channel sand can be either water drive or depletion drive, depends on whether the sand is connected to an aquifer. The drive mechanism for specific sand layer will only be known once the sand is put into production. This complexity leads to the difficulty in selection of the sand to perforate.

In terms of petroleum engineering, the two sands type is not distinguished between each other. There are only thin or thick reservoirs, with either depletion or water drive mechanism. Yet the complexity encountered on both Bar and Channel reservoir's rock and fluid properties, and with different drive mechanism creates difficulties for engineers to find optimum production/perforation scenario to be applied. Especially where these multiple reservoirs are to be produced through common well.

Current GoT practice is to produce from bottommost reservoirs upwards and shut any reservoirs with excessive water productions. This method allows the gas to be produced from deepest reservoir first and produce the next upper reservoirs in sequence. This method's strong point is that since it allows the bottom reservoir to be produced first, the shutting-off of the depleted reservoir can be done easily without concerns that the non-depleted reservoirs will have to be isolated.

Given the complexity of the reservoir characteristics, the GoT gas fields possess one of the most challenging reservoir management aspects for reservoir engineers. The multilayered characteristics of the reservoirs in combination with two main drive mechanisms; depletion and water drive, and a number of production constraints (CO_2, H_2S, water production) that added difficulties for the reservoir management.

1.1 Outline of Methodology

In order to improve the multilayered gas reservoirs management, this thesis has been initiated to find the various method of perforation strategy such that the well's production can be optimized. This includes modeling of drive mechanism and determination of its impact on the reservoir performance, study of optimal perforation sequencing under different drive mechanisms, and study of optimal perforation under production constraints.

The study is carried out in following steps:

1) Set up of Actual Reservoir Model

The study starts with setting up of actual reservoir model. An objective of this step is to obtain real dynamic reservoir response such as pressure and production rate. This real dynamic response is used as basis for the simplified reservoir model to be prepared in next step. The model will be constructed based on available geological data such as structural map and isopach map through the employment of Petrel Geological Modeling Software. The PVT and SCAL data are based on available GoT reservoirs data. The resulting model is considered as representative model for GoT multilayered gas reservoirs.

In performing the actual model set up, the pre-assumptions is that the drive mechanism associated with each sand layer is known. This pre-assumption has to be made because the type of sand deposition is not associated with drive mechanism. i.e., the bar sand can be either water drive or depletion drive, depending on whether the sand is connected to the aquifer. This pre-assumption leads to the need for simplified model to allow for the change in drive mechanism from the pre-specified input.

2) Generate simplified model that matches the actual model

In the next step, the simplified version of reservoir model possessing similar response to the actual model is created. The purpose of this step is to ensure that there can be a simplified model that possess similar response to actual model, and therefore for the study conducted, the simplified model will provide similar results to the actual model. This simplified model have the similar number of reservoirs, similar reservoir inclination (dip angle), and OGIP to the actual model.

The comparison of reservoir response between actual and simplified model is observed on the similar trend of response basis. A ±10% difference in value is considered acceptable.

3) Study/Optimize Various Scenarios

Better understanding of the performance of the multilayered reservoir is expected through this step. After simplified model has been decided to be a basis for the study, various perforation options are put into test through the model. This includes:

(a) The strategy to perforate the depletion sands alone.

(b) The strategy to perforate the water drive sands alone.

(c) The strategy to perforate both sand layers under depletion drive and sand layers under water drive. The options to study such as:

1. The option of dedicated well according to drive mechanism.
2. The option of sequenced perforation.
3. To study the optimal perforation strategy under different sand layer sequence.

These options are then compared to determine the best perforation strategy as well as the response and behavior of the reservoirs under each perforation option.

4) Result Analysis

After all steps have been carried out, the results are summarized and analyzed carefully to check the validity of each result in terms of:

(a) Practicality

(b) Operation ability

(c) Other concerns.

1.2 Thesis Outline

This thesis consists of six chapters.

Chapter II outlines a list of related works/studies on multilayered gas reservoirs and perforation strategy.

Chapter III describes the setting of reservoir model, theory of gas reservoirs, and drive mechanisms.

Chapter IV discusses the principle of reservoir simulation, original model generation, and simplified model generation and matching with actual model.

Chapter V discusses the cases studied and their results of reservoirs simulation obtained.

Chapter VI provides conclusion and recommendation.

CHAPTER II

LITERATURE REVIEW

This chapter discusses previous works that are related to multilayered gas reservoirs and perforation strategy.

2.1 Previous Works on the Subject

A number of literatures regarding behavior of multilayered reservoirs and perforation sequence have been reviewed as elaborated below. As a summary, only a small amount of the reviewed articles directly address the perforation sequence in multilayered gas reservoirs. This left the topics of interest becomes challenging.

Arianto *et al.* [1] have presented the completion solution for multilayered gas fields. The field of interest is Sanga-Sanga PSC offshore Kalimantan which is fluvial gas field consisting of:

1. Lower section: Low permeability (1-100 mD), Depletion drive reservoirs
2. Upper section: Higher permeability (100-1000 mD), Water drive reservoirs

The classical way of perforation is to carry out a bottom-up perforation approach. However, this leads to low gas rate (as the bottom has low permeability), liquid loading, and/or poor well performance. Alternatively, production from shallow reservoirs can be chosen, but the watered out perforation zone will be difficult to isolate. Their solution in the past was to use single selective completions. However, this solution is quite ineffective since their production tubing system has to be completed with various downhole equipment such as double tubing packer, sliding sleeve valve etc. which increase a risk of system leakage and subsequent problems. In their study, they have decided to use the dual completions, one for the shallow and one for the deep reservoirs which proves to be successful applications.

Al-Sheri *et al.* [2] has tested the commingled production from multilayered gas-carbonate reservoirs in Ghawar field, Saudi Arabia. They have highlighted that the key successful factors for commingled production is to keep the flowing bottomhole pressure of the system below the lowest static reservoir pressure. They further stressed that the best result would be obtained when similar static pressure zones are combined or when the lower static pressure zone exhibits higher productivity index. Along with several findings, they concluded from actual results that commingled production shows improvement both for production rate and recovery. This conclusion is made from comparing the commingled production vs. original selective zone production (i.e., to produce from only one reservoir zone at a time).

Fetcovich *et al.* [3] have presented the performance prediction of multilayered, depletion-drive gas reservoirs using material balance and radial flow equation. The study was based on actual field data with no crossflow between each layer and high contrast between layer permeability. The conclusions from the studies are that for multiple depletion drive gas reservoirs, to combine all reservoirs into single reservoir with average reservoir properties is possible in view of long term performance prediction. The conclusion hold true regardless of contrasts in reservoir properties among each reservoir layers.

A number of published literature regarding the multilayered gas reservoirs has been reviewed such as a study performed by Raghavan [4], Sansu *et al.*[5], and Gangdan *et al.* [6]. However, most literatures are irrelevant to the topic of interest.

From the available theses, Jiraratwaro [7] has studied the effect of different perforation sequence in multilayered oil & gas reservoirs. His work deals primarily on wellbore modeling using the Petroleum Expert's IPM software. He employs the history matching technique to fine-tune the model and used it for future prediction of reservoir performance under different perforation sequences. Based on his findings, no single strategy is best for all well models. He suggests that the current field practice, while provides minimum water production, yields low recovery efficiency. The highest recovery efficiency is the bottom up approach.

From the available senior project documents, two works are found to be related to the topic of interest. Thirawarapan *et al.* [8] studied the effect of partial perforations in multilayered gas reservoirs with an attempt to delay water production. Their work is carried out using both wellbore modeling (Petroleum Experts' IPM Software) and reservoir simulation (Schlumberger's Eclipse Software). Their study started with verification of each layer's production from existing well using PLT data. They found that apart from different reservoir properties encountered in each layer, the partial perforation contributes significant effect to reduction of water production. However, in terms of recovery efficiency, the results depend on other factors such as reservoir permeability. In high permeability reservoirs, the recovery efficiency is increasing with reducing partial perforation ratio and vice versa for low permeability reservoirs. From the economic point of view they found that almost all partial perforation approaches reduces the incremental NPV.

Another senior project reviewed is the work from Kiatrabile *et al.* [9]. They studied the production strategy emphasized on reservoir drive mechanism. In their study a simplified reservoir model has been built using reservoir simulator. Their reservoirs consisted of 7 layers, 4 depletion drive with 3 water drive in between. Homogenous reservoir properties were set. They categorized their study into three situations corresponding to the impact of permeability. The first is where the permeability of water drive layers is higher than the depletion drive layers. The second is where the permeability of water drive layers equal to the depletion drive layers. And the third situation is where the permeability of water drive layers is less than the depletion drive layers. For the first situation, they found that bottom up perforation approach is the best. For the second situation, they found that to perforate the depletion drive layer followed by the water drive would yield highest recovery. And in the third situation the simultaneous production using dedicated well for different reservoir drive mechanism would be the best.

2.2 Discussions

From a number of literatures surveyed, no articles have mentioned the treatment of multilayered gas-sandstone reservoirs similar to the GoT multilayered gas fields. The work carried out by Arianto *et al.* is based on different depositional environment. The study by Al-Sheri *et al.* is made on carbonate reservoirs. The work by Fetkovitch *et al.* is based on depletion drive reservoirs only.

From the available theses and senior project documents, related topics have been reviewed but these are differences to the topic of interest. Jiraratwaro's investigation deals with oil reservoirs with some gas layers. His focus is on the well model. Thirawarapan *et al.*'s work deals with effect of partial perforations in attempt to delay water production. It can be seen that there is still space for this study to improve understanding on perforations in multilayered reservoirs. Nevertheless, the literature reviewed provides a very good hindsight to this study.

CHAPTER III

THEORY AND CONCEPT

As the study approach relies on reservoir simulations technique, this chapter will explain the use of reservoir simulation in this study.

3.1 Reservoir Simulations

The reservoir simulation technique is used in this study because it offers advantage on phenomenon of gas and water flowing in reservoirs, the interaction between each reservoir in the multilayered reservoirs through the common producing well(s), and the effect of different drive mechanisms on the producing characteristics of the multilayered reservoirs. These advantage is important in order to understand the behavior of multilayered reservoirs, and ultimately, to determine the optimal production/perforation techniques to be applied.

The reservoir simulation software used in this study is the Eclipse software.

Black Oil model is used in this study as the reservoirs of interest are mostly wet gas reservoirs, the compositional change in the reservoir fluids through time is minimal and therefore Compositional model is not needed.

In the original model, the model is upscaled, and imported to reservoir model by geological modeling software. As a result, the reservoir shape is too complex to duplicate using simple reservoir modeling both from the areal extent and dip angle aspects. To reflect this complexity in simplified model, the corner-point grid needs to be used over simple Cartesian gridding system.

The well model is generated using Prosper software, which is commonly used because of its accuracy in predicting flow in wells in the GoT reservoirs.

The two important concepts that are used in the reservoir simulations are the concept of material balance and the concept of fluid flow in porous medium.

3.2 Material Balance Concept

The law of conservation of mass is the basis of material balance calculations. Material balance is an accounting of material entering or leaving a system. The calculation treats the reservoir as a large tank of material and uses quantities that can be measured to determine the amount of a material that cannot be directly measured. In its simplest form, the equation can be written on volumetric basis as:

Initial volume = volume remaining + volume removed

Measurable quantities include cumulative fluid production volumes for oil, water, and gas phases; reservoir pressures; and fluid property data from samples of produced fluids. Material balance calculations may be used for several purposes. They provide an independent method of estimating the volume of oil, water, and gas in a reservoir for comparison with volumetric estimates. The magnitude of various factors in the material balance equation indicates the relative contribution of different drive mechanisms at work in the reservoir. Material balance can be used to predict future reservoir performance and aid in estimating recovery efficiency.

3.3 Material Balance in Gas Reservoir

Reservoirs containing only free gas are termed gas reservoirs. Such a reservoir contains a mixture of hydrocarbons which exists wholly in the gaseous state. The gas reservoirs can be classified as dry gas reservoirs, wet gas reservoirs, and gas-condensate reservoirs, depending on the composition, pressure, and temperature at which the accumulation exists.

Gas reservoirs may have water influx from contiguous water-bearing portion of the formation or maybe volumetric (i.e., have no water influx). The general material balance equation applied to a gas reservoir is in the form of:

$$G(B_g - B_{gi}) + GB_{gi}\frac{\left(c_w S_{wi} + c_f\right)}{\left(1 - S_{wi}\right)}\Delta\bar{p} + W_e = G_p B_g + B_w W_p \qquad (3.1)$$

where

G = Initial gas in-place

G_p = Cumulative gas production

B_g = Gas formation volume factor

B_{gi} = Initial gas formation volume factor

c_w = Water compressibility

S_{wi} = Initial water saturations

c_f = Formation compressibility

Δp = Difference in reservoir pressure compared to original reservoir pressure.

W_e = Cumulative water encroached to reservoir

B_w = Water formation volume factor

W_p = Cumulative water production

Equation (3.1) is derived by applying the law of conservation of mass to the reservoir and associated production.

For gas reservoirs, the gas compressibility is much greater than the formation and water compressibility, and the second term on the left-hand side of Equation (3.1) becomes negligible.

The new equation becomes

$$G(B_g - B_{gi}) + W_e = G_p B_g + B_w W_p \tag{3.2}$$

When there is neither water encroachment into the reservoir nor water production from the reservoir, the reservoir is said to be volumetric. In this case Equation (3.2) reduces to

$$G(B_g - B_{gi}) = G_p B_g \tag{3.3}$$

But

$$B_g = \frac{p_{sc} z T}{T_{sc} p} \tag{3.4}$$

Substituting B_g into Equation (3.4), we have

$$\frac{p}{z} = -\frac{p_i}{z_i G} G_p + \frac{p_i}{z_i} \tag{3.5}$$

Because p_i, z_i and G are constants for a given reservoir, Equation (3.5) suggests that a plot of p/z as the ordinate versus G_p would yield a straight line with:

$$\text{slope} = -\frac{p_i}{z_i G}$$

$$\text{y intercept} = \frac{p_i}{z_i}$$

The *p/z* plot versus cumulative production is shown in Figure 3.1.

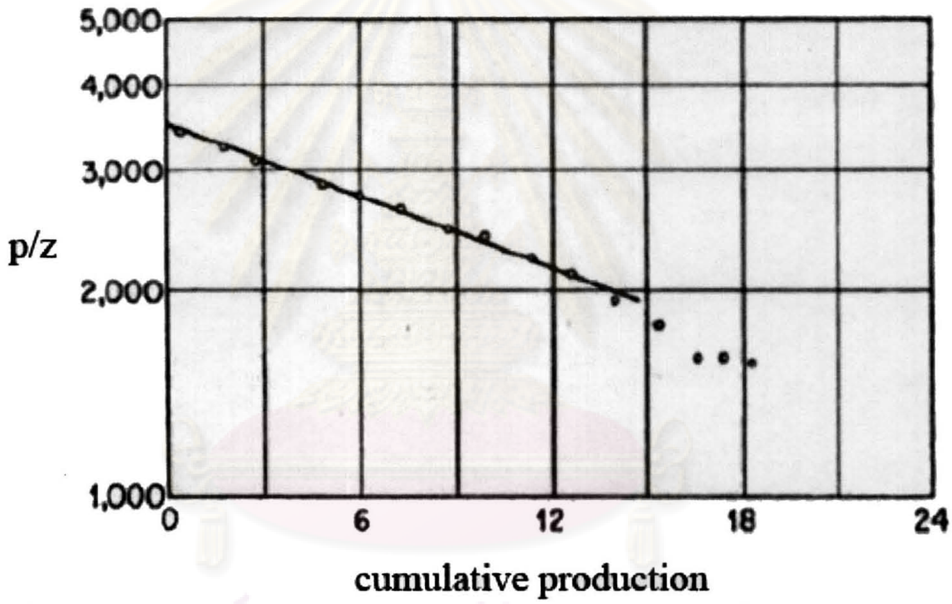

Figure 3.1: *p/z* plot versus cumulative production (Craft and Hawkins[11])

If p/z is set equal to zero, which would represent the production of all the gas from reservoir, then the corresponding G_p equals G, the initial gas in-place.

3.4 Fluid Flow in Porous Medium

The fluid flow equations that are used to describe the flow behavior in a reservoir can take many forms depending upon the combination of variables presented previously (i.e., types of flow, types of fluids, etc.). By combining the conservation of mass equation with the transport equation (Darcy's equation) and various equations of state, the necessary flow equations can be developed. Since all flow equations to be considered depend on Darcy's law, it is important to consider this transport relationship first.

3.4.1 Darcy's Law

The fundamental law of fluid motion in porous media is Darcy's law. The mathematical expression developed by Darcy in 1756 states that the velocity of a homogeneous fluid in a porous medium is proportional to the head (or potential), and inversely proportional to the fluid viscosity. For a horizontal linear system, this relationship is:

$$v = \frac{q}{A} = \frac{-k}{\mu}\frac{dp}{dx} \tag{3.6}$$

where

v = Apparent velocity in centimeters per second and is equal to q/A.

q = Volumetric flow rate in cubic centimeters per second.

A = Total cross-sectional area of the rock in square centimeters. In other words, A includes the area of the rock material as well as the area of the pore channels.

μ = Fluid viscosity, centipoise.

dp/dx = Pressure gradient, atmospheres per centimeter. Taken in the same direction as v and q.

k = Permeability of the rock, Darcy.

The negative sign in Equation (3.6) is added because the pressure gradient dp/dx is negative in the direction of flow. For a horizontal-radial system, the pressure gradient is positive and Darcy's equation can be expressed in the following generalized radial form:

$$v = \frac{q_r}{A_r} = \frac{k}{\mu}\left(\frac{\partial p}{\partial r}\right)_r \tag{3.7}$$

where:

q_r = volumetric flow rate at radius r

A_r = cross-sectional area to flow at radius r

$(\partial p/\partial r)_r$ = pressure gradient at radius r

v = apparent velocity at radius r

The cross-sectional area at radius r is essentially the surface area of a cylinder. For a fully penetrated well with a net thickness of h, the cross-sectional area A_r is given by:

$$A_r = 2\pi rh \tag{3.8}$$

Darcy's law applies only when the following conditions exist:

- Laminar (viscous) flow;
- Steady-State flow;
- Incompressible fluids;
- Homogeneous formation.

For turbulent flow, which occurs at higher velocities, the pressure gradient increases at a greater rate than does the flow rate and a special modification of Darcy's equation is needed. When turbulent flow exists, the application of Darcy's equation can result in serious errors.

3.4.2 Radial Flow of Compressible Fluids (Gases)

For a viscous (laminar) gas flow in a homogeneous radial system, the real-gas equation of state can be applied to calculate the number of gas moles n at the pressure p, temperature T, and volume V:

$$n = \frac{pV}{zRT} \tag{3.9}$$

At standard conditions, the volume occupied by the above n moles is given by:

$$V_{SC} = \frac{nz_{SC} RT_{SC}}{p_{SC}} \tag{3.10}$$

Combining the above two expressions and assuming $z_{sc} = 1$ gives:

$$\frac{pV}{zT} = \frac{p_{SC} V_{SC}}{T_{SC}} \tag{3.11}$$

Equivalently, the above relation can be expressed in terms of the reservoir condition flow rate q, in scf/day, and surface condition flow rate q_{sc}, in scf/day, as:

$$\frac{p \times q}{zT} = \frac{p_{SC} q_{sc}}{T_{SC}} \tag{3.12}$$

Rearranging:

$$\left(\frac{p_{SC}}{T_{SC}}\right)\left(\frac{zT}{p}\right) q_{sc} = q \tag{3.13}$$

where:

q = gas flow rate at pressure p in scf/day

q_{sc} = gas flow rate at standard conditions, scf/day

z = gas compressibility factor

T_{sc}, = standard temperature in ∘R and

p_{sc} = standard pressure in psia

Dividing both sides of the above equation by the cross sectional area A and equating it with that of Darcy's law, i.e., Equation (3.6), gives:

$$\frac{q}{A} = \left(\frac{p_{SC}}{T_{SC}}\right)\left(\frac{zT}{p}\right)\left(\frac{1}{2\pi rh}\right) q_{sc} = -0.006328 \frac{k}{\mu} \frac{dp}{dr} \tag{3.14}$$

The constant 0.001127 is to convert Darcy's units to field units. Separating variables and arranging yields:

$$\left[\frac{q_{sc}p_{SC}Tz\mu}{(0.006328)(2\pi)T_{SC}kh}\right]\int_{r1}^{r2}\frac{dr}{r} = -\int_{p1}^{p2} pdp = \frac{1}{2}(p_1^2 - p_2^2) \tag{3.15}$$

Assuming that the product of $z\mu_g$ is constant over the specified pressure range between p_1 and p_2, and integrating, gives:

$$\left[\frac{q_{sc}p_{SC}Tz\mu}{0.01988T_{SC}kh}\right]\ln(r_2/r_1) = (p_1^2 - p_2^2) \tag{3.16}$$

Then,

$$q = \frac{0.703533kh(p_1^2 - p_2^2)}{T(z\mu_g)\ln(r_2/r_1)} \tag{3.17}$$

where:

q = gas flow rate, scf/day

k = permeability, mD

T = temperature, ◦R

μ_g = gas viscosity, cp

h = reservoir thickness, ft

r = total length of the radial system, ft

If one considers the drainage radius of the well, and adding skin factor into account, the final equation is,

$$q = \frac{0.703533kh(p_r^2 - p_{wf}^2)}{T(z\mu_g)\ln((r_2/r_1) + S)} \tag{3.18}$$

It is essential to notice that those gas properties z and μ_g are very strong functions of pressure, but they have been removed from the integral to simplify the final form of the gas flow equation. The above equation is valid for applications when the pressure is less than 2000 psi. The gas properties must be evaluated at the average pressure.

3.5 Discussions

This chapter describes the basic theory and techniques used to describe the gas and water flow in the reservoirs. Reservoir simulations can be used to describe the flow in multilayered reservoirs. The analysis of study results carried out in Chapter V will utilize the basic theory outlined in this chapter.

CHAPTER IV

ORGINAL RESERVOIR MODEL AND SIMPLIFIED RESERVOIR MODEL

This chapter describes the selection of actual reservoir model for the study, their characteristics and resulting production profiles. Setting up of simplified model, assumptions used and matching results are also discussed.

4.1 Description of Original Reservoir Model

The reservoir model for the study is selected from available reservoir model in the GoT. The selection aims at the model that is best described in terms of geological setting/depositional environment as outlined in Chapter I. Two models have been picked: one for bar sand and another for channel sand. The bar sand reservoirs will be representative of thin, small reservoirs and the channel sand reservoirs will be representative for thick, large reservoirs which normally connected with aquifers.

4.1.1 Bar Sand Reservoir Model

Bar sand reservoir model has been well-identified from geological modeling in combination with 3D Seismic amplitude anomaly and well log correlations. The geological setting of bar sand reservoir is shown in figure 4.1

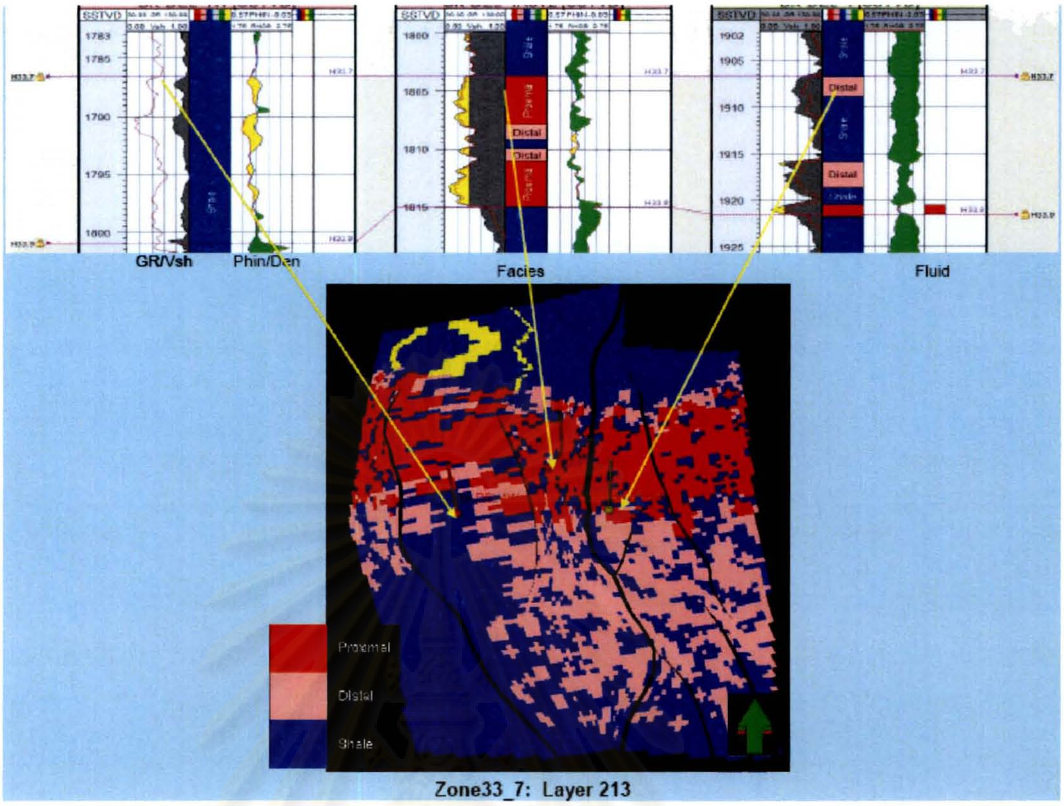

Figure 4.1: Mouth Bar Facies

Based on data collected and correlated, the reservoir possesses following reservoir characteristics:

1. Reservoir fluid type: Wet Gas
2. Top reservoir depth (ft): 6206
3. Average thickness (ft): 61.4
4. GWC depth (ft): 6360
5. GRV (MMrcf): 1,714
6. Net to Gross Sand(%): 0-100% (Average 25%)
7. Porosity (%): 10% - 35% (Average 21%)
8. Permeability (mD): 22-1000
9. Average reservoir pressure (psia): 2955
10. Reservoir temperature (°F): 294
11. Reservoir fluid SG (air = 1): 0.97
12. OGIP (Bscf): 8.57

The reservoir model was built based on the collected geological data. The details of input data for simulation are described in Appendix A. Summarized data for reservoir model including phase equilibrium data, reservoir and fluid properties are described below. PVT properties and rock properties are tabulated in Table 4.1.

a) Case Definition

Simulator:	Black Oil	
Model Dimensions:	Number of cells in the x direction	56
	Number of cells in the y direction	120
	Number of cells in the z direction	4
Grid type:	Corner Point	
Geometry type:	Block Centered	
Oil-Gas-Water Options:	Water, Gas	

b) Grid

Properties:	Porosity		=	10% - 35%	
	Permeability	k-x	=	22-1000	mD
		k-y	=	22-1000	mD
		k-z	=	2.2-100	mD
	Gross thickness		=	15.4 feet/ layer	
	Net to Gross Ratio		=	0-100% (Average 25%)	
Depth of Top face			=	6,206 ft	

Table 4.1: PVT properties of reservoir fluids and rock properties

Water Properties	Reference pressure(Pref)	4652.5	psia
	Water FVF at Pref	1.0636	rb/stb
	Water viscosity at Pref	0.1907	cp
	Water viscosibility	9.22 E-06	1/psi
Fluid Densities at Surface Conditions	Oil density	48.4 (50 °API)	lb/ft^3
	Water density	62.43	lb/ft^3
	Gas density	0.060	lb/ft^3
Rock Properties	Reference Pressure	4230	psia
	Rock Compressibility	5.4029E-6	1/psi

c) SCAL (Special Core Analysis)

Initial reservoir properties

Initial Water Saturation (SWAT) : 0.40

Initial Gas Saturation (SGAS) : 0.60

Initial Pressure : 2,955 psia

The gas saturation and relative permeability relation is tabulated in Table 4.2 and shown in Figure 4.2.

Table 4.2: Water saturation versus gas and water relative permeabilities

Sw	K_{rg}	K_{rw}
0.4000	1.0000	0.0000
0.4411	0.5549	0.0040
0.4822	0.2846	0.0183
0.5233	0.1317	0.0446
0.5644	0.0529	0.0840
0.6056	0.0173	0.1372
0.6467	0.0041	0.2049
0.6878	0.0005	0.2876
0.7289	0.0000	0.3859
0.7700	0.0000	0.5000
1.0000	0.0000	1.0000

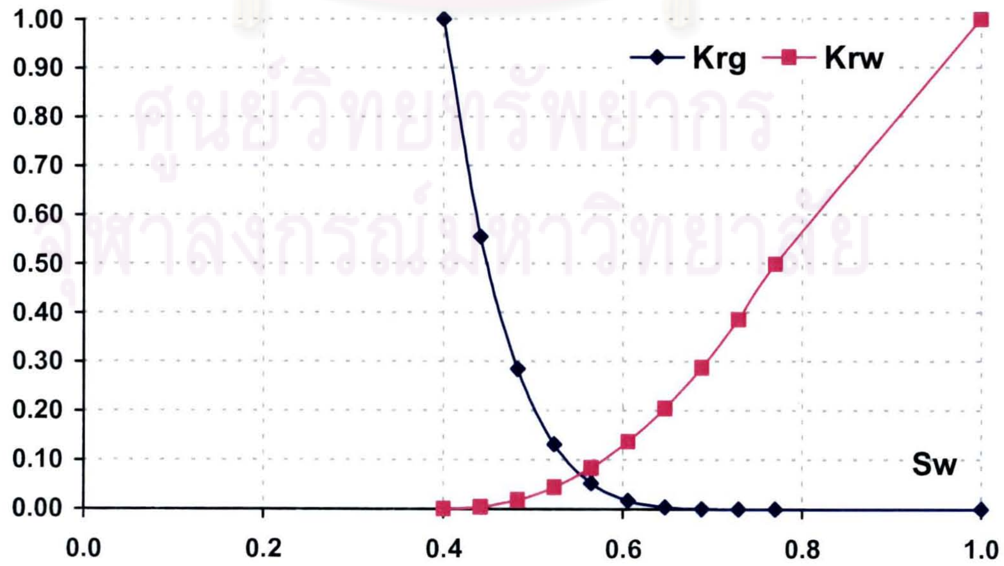

Figure 4.2: Bar sand reservoirs relative permeability function

The resulting reservoirs shape, net to gross distribution, porosity distribution and permeability distribution, pressure distribution, and gas saturation of the bar sand reservoir are shown in Figures 4.3 to 4.8. Histogram showing permeability distribution of the bar sand reservoirs are shown under Figure 4.9.

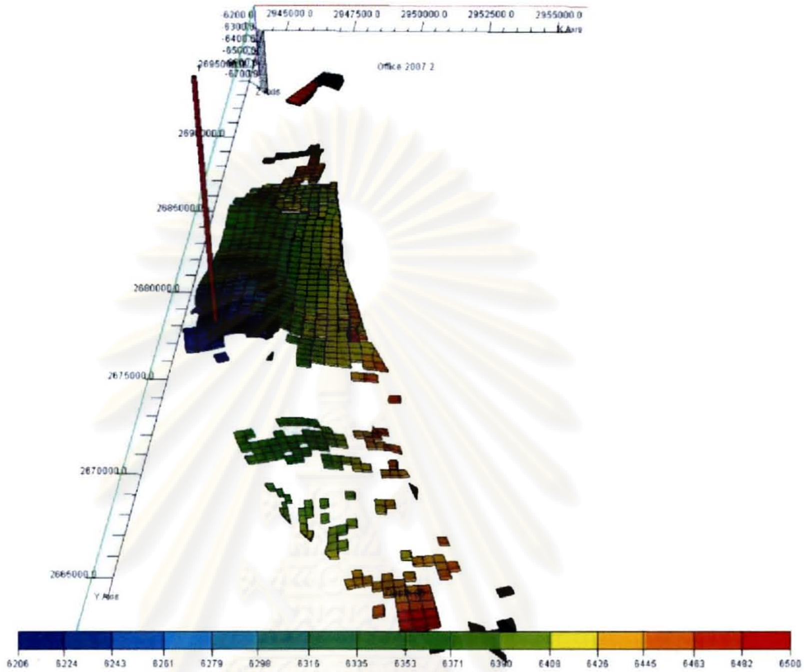

Figure 4.3: Bar sand reservoirs shape

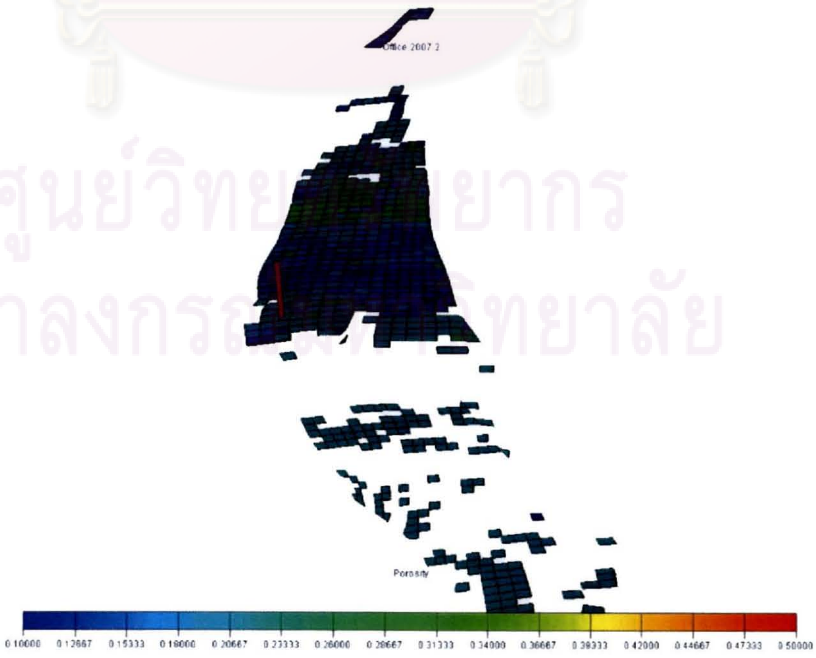

Figure 4.4: Bar sand reservoirs porosity distribution

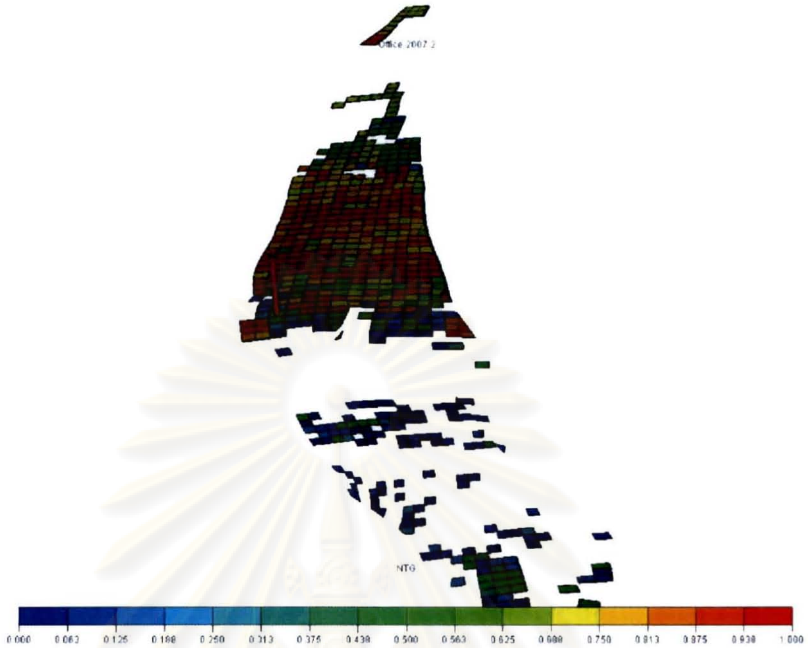

Figure 4.5: Bar sand reservoirs Net to Gross ratio distribution

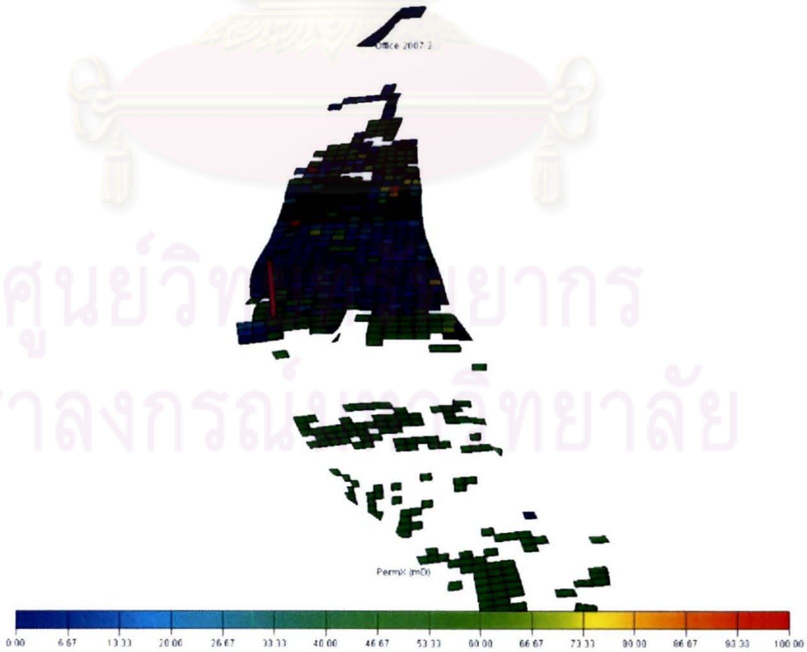

Figure 4.6: Bar sand reservoirs permeability distribution

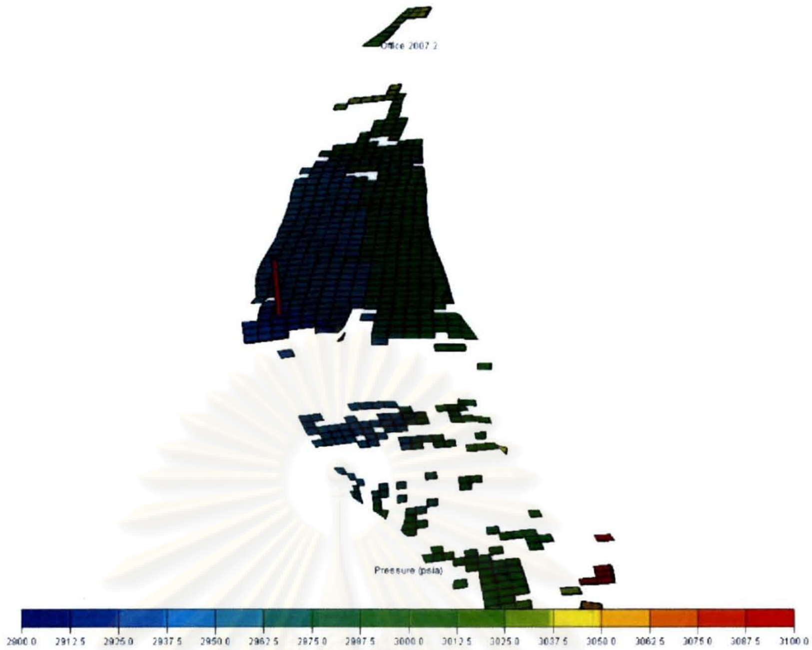

Figure 4.7: Bar sand reservoirs pressure distribution

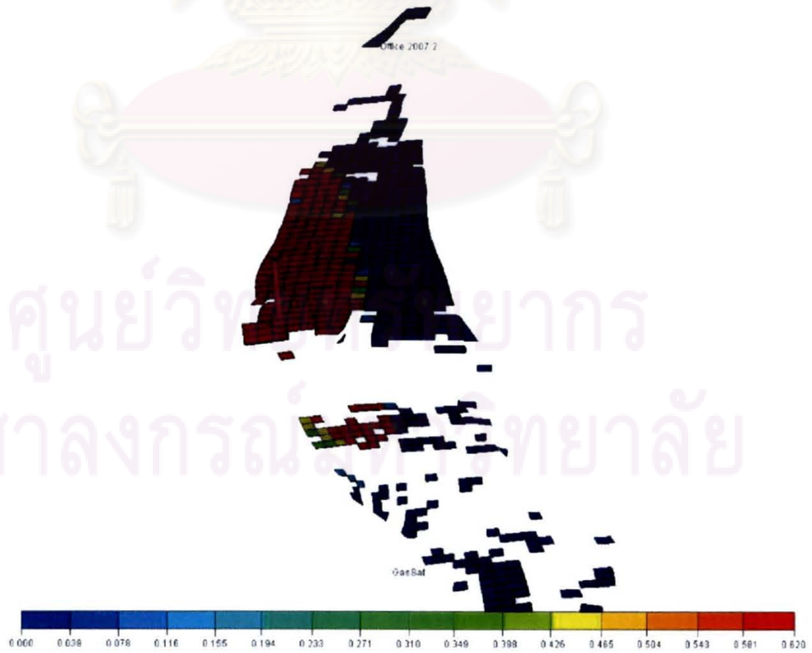

Figure 4.8: Bar sand reservoirs gas saturation distribution

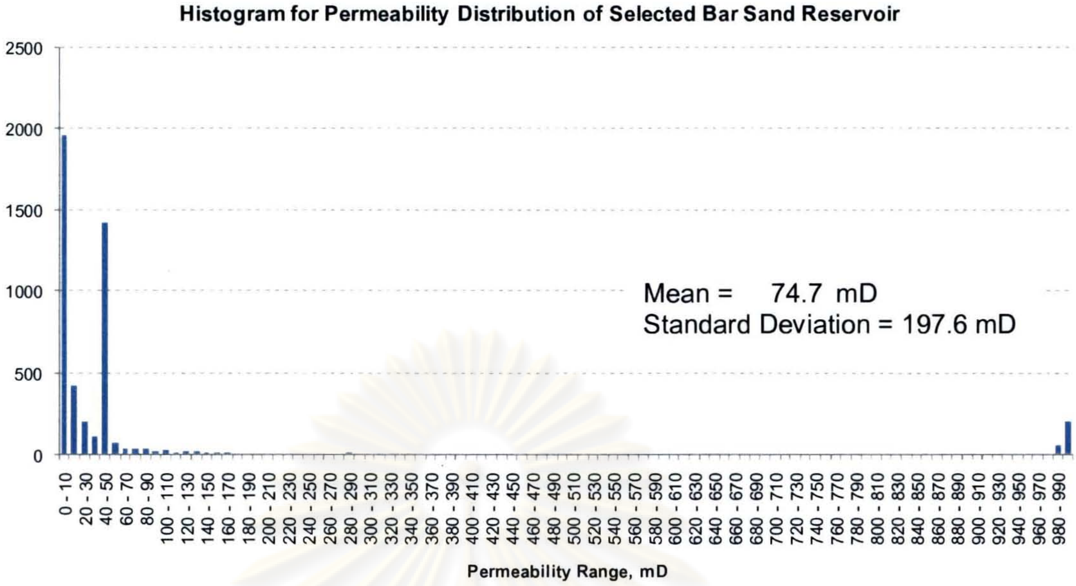

Figure 4.9: Histogram for bar sand reservoirs permeability distribution

The dynamic response of the selected bar sand reservoirs will be described under the model matching between original and simplified model section.

4.1.2 Channel Sand Reservoirs Model

Similar to bar sand reservoirs, the Channel sand reservoirs model picked has been well-identified from geological modeling in combination with 3D Seismic amplitude anomaly and drilled well log correlations. The geological setting of channel sand reservoirs is shown in figure 4.10.

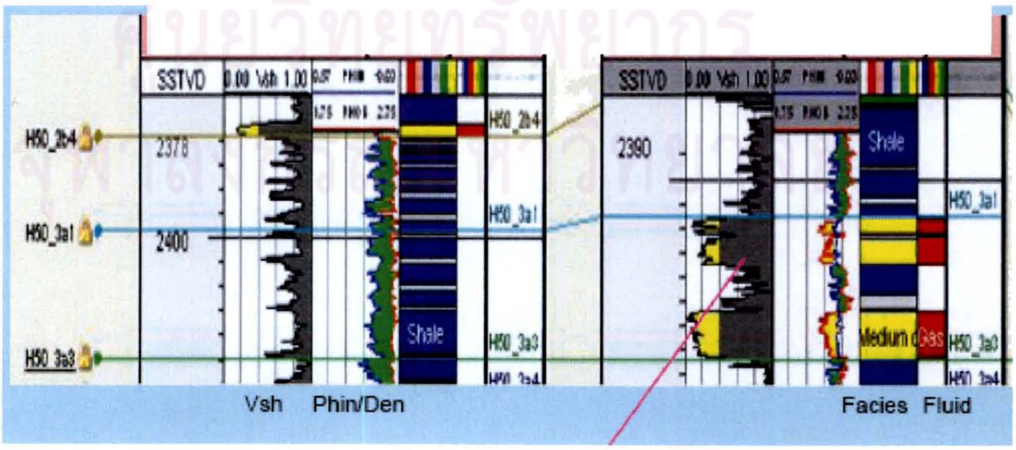

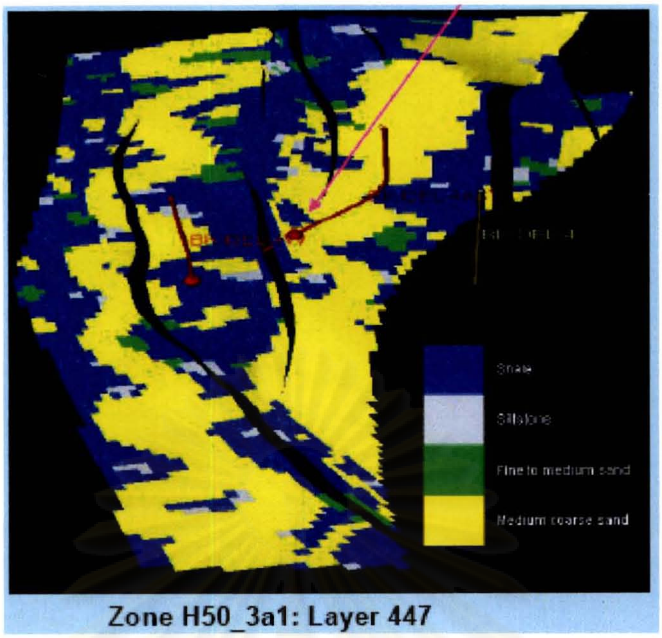

Figure 4.10: Fluvial Channel Facies

Based on data collected and correlated, the reservoirs possesses following reservoir characteristics:

1. Reservoir fluid type: Wet Gas
2. Top reservoir depth (ft): 7,875
3. Average thickness (ft): 98.7
4. GWC depth (ft): 8,420
5. GRV (MMrcf): 2,704
6. Net to Gross Sand(%): 0-100% (Average 40%)
7. Porosity (%): 15% - 34% (Average 21%)
8. Permeability (mD): 2.4-1000
9. Average reservoir pressure (psia): 3,785
10. Reservoir temperature (°F): 347
11. Reservoir fluid SG (air = 1): 1.1
12. OGIP (Bscf): 49.7

The reservoir model was built based on the collected geological data. The details of input data for simulation are described in Appendix A. Summarized data for reservoir model including phase equilibrium data, reservoir and fluid properties are described below. PVT properties and rock properties are tabulated in Table 4.3.

a) Case Definition

Simulator:	Black Oil		
Model Dimensions:	Number of cells in the x direction	56
	Number of cells in the y direction	120
	Number of cells in the z direction	5
Grid type:	Corner Point	
Geometry type:	Block Centered	
Oil-Gas-Water Options:	Water, Gas	

b) Grid

Properties:	Porosity		=	15% - 34%	
	Permeability	k-x	=	2.4-1000	mD
		k-y	=	2.4-1000	mD
		k-z	=	0.24-100	mD
	Gross thickness		=	18.9	feet/ layer
	Net to Gross Ratio		=	0-100% (Average 40%)	
Depth of Top face			=	7,875 ft	

Table 4.3: PVT properties of reservoir fluids and rock properties

Water Properties	Reference pressure(Pref)	3349	psia
	Water FVF at Pref	1.0897	rb/stb
	Water viscosity at Pref	0.1601	cp
	Water viscosibility	1.00 E-05	1/psi
Fluid Densities at Surface Conditions	Oil density	48.4 (50 °API)	lb/ft^3
	Water density	62.43	lb/ft^3
	Gas density	0.068	lb/ft^3
Rock Properties	Reference Pressure	3349	psia
	Rock Compressibility	5.4092E-6	1/psi

c) SCAL (Special Core Analysis)

<u>Initial reservoir properties</u>

Initial Water Saturation (SWAT) : 0.38

Initial Gas Saturation (SGAS) : 0.62

Initial Pressure : 2,955 psia

The gas saturation and relative permeability relation is tabulated in Table 4.4 and shown in Figure 4.11.

Table 4.4: Water saturation versus gas and water relative permeabilities

Sw	K_{rg}	K_{rw}
0.3800	1.0000	0.0000
0.4233	0.5549	0.0040
0.4667	0.2846	0.0183
0.5100	0.1317	0.0446
0.5533	0.0529	0.0840
0.5967	0.0173	0.1372
0.6400	0.0041	0.2049
0.6833	0.0005	0.2876
0.7267	0.0000	0.3859
0.7700	0.0000	0.5000
1.0000	0.0000	1.0000

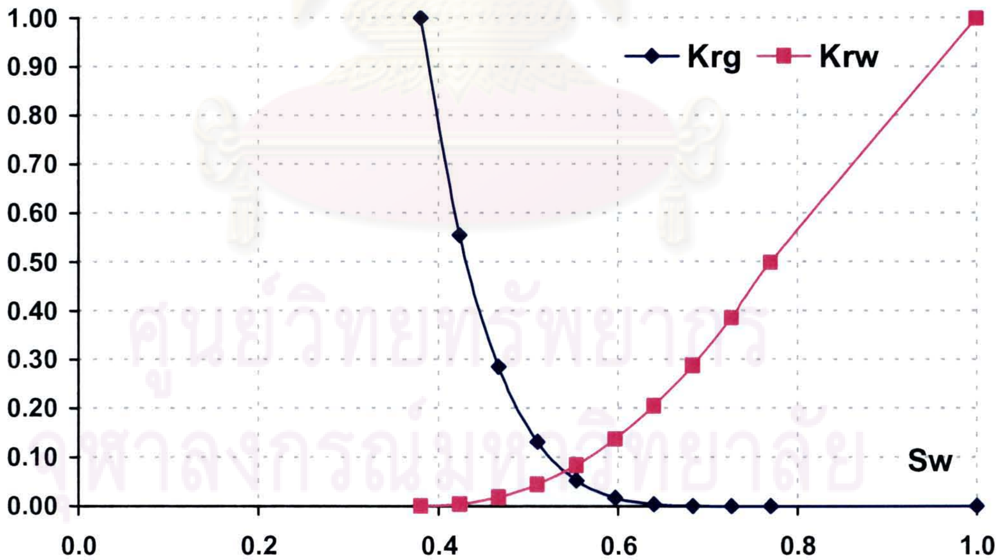

Figure 4.11: Channel sand reservoirs relative permeability function

The resulting reservoir shape, net to gross distribution, porosity distribution and permeability distribution, pressure distribution, and gas saturation of the channel sand reservoir are shown in Figure 4.12 to 4.17. Histogram showing permeability distribution of the bar sand reservoirs are shown under Figure 4.18.

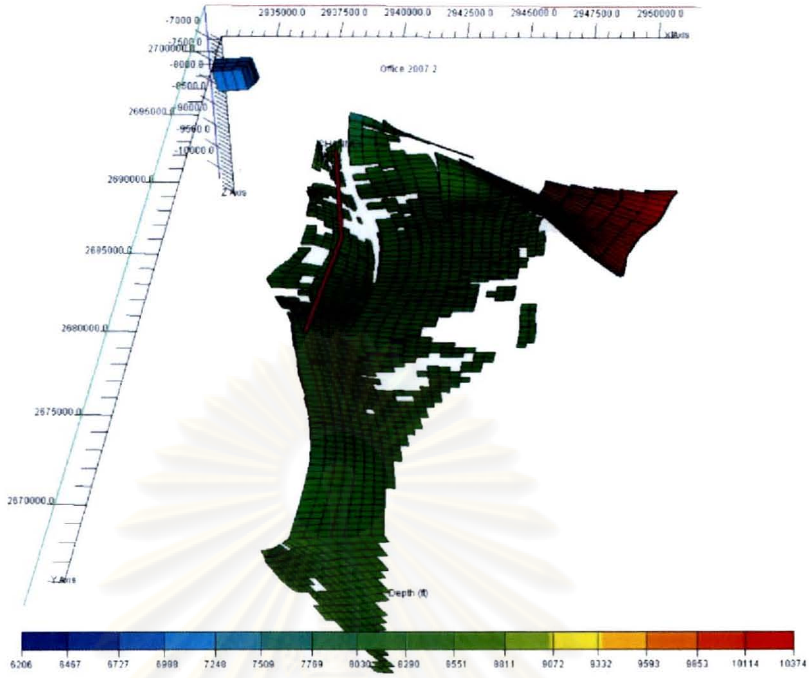

Figure 4.12: Channel sand reservoirs shape

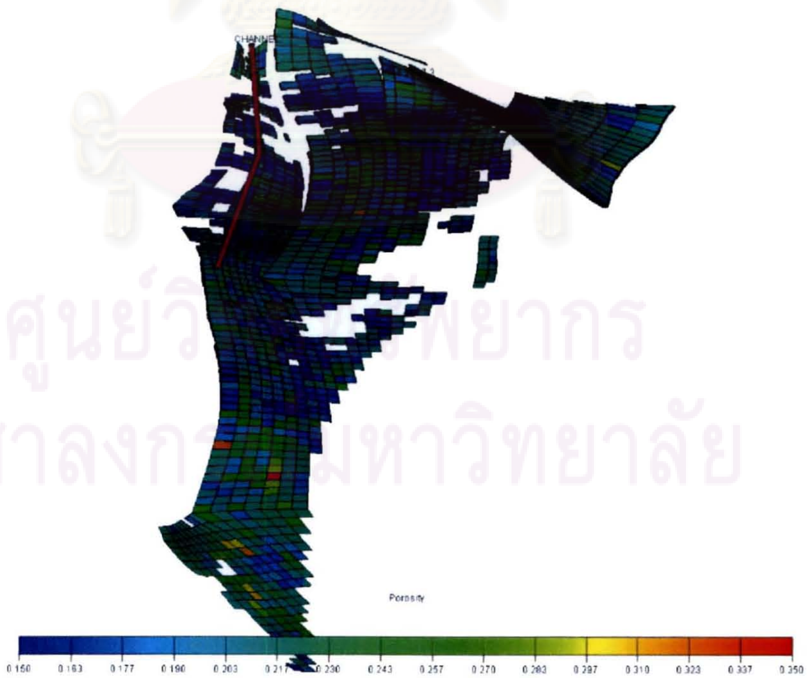

Figure 4.13: Channel sand reservoirs porosity distribution

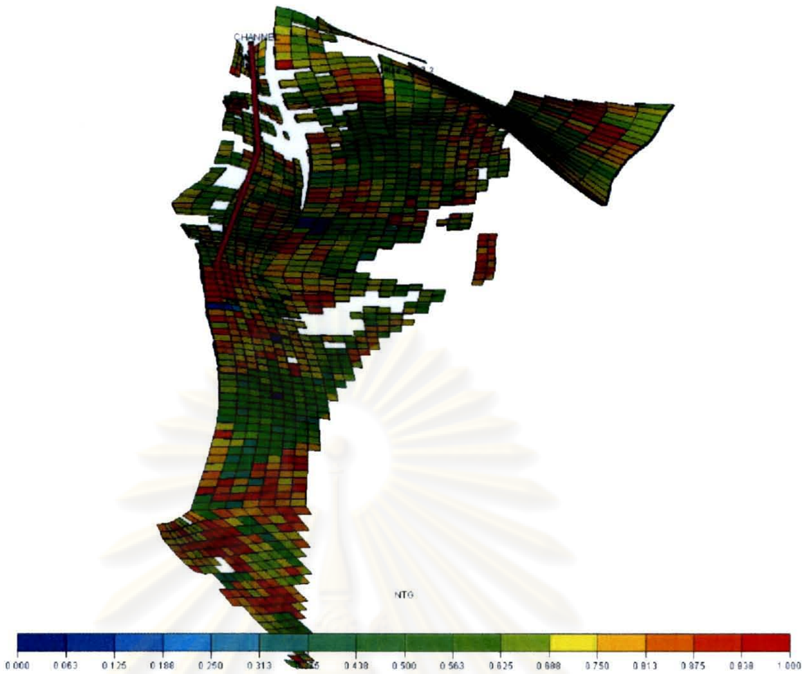

Figure 4.14: Channel sand reservoirs Net to Gross ratio distribution

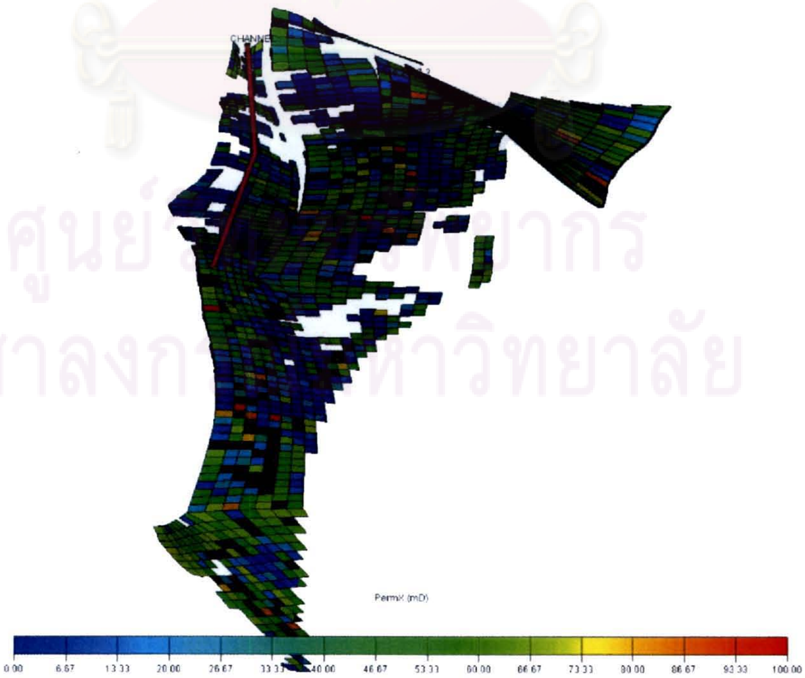

Figure 4.15: Channel sand reservoirs permeability distribution

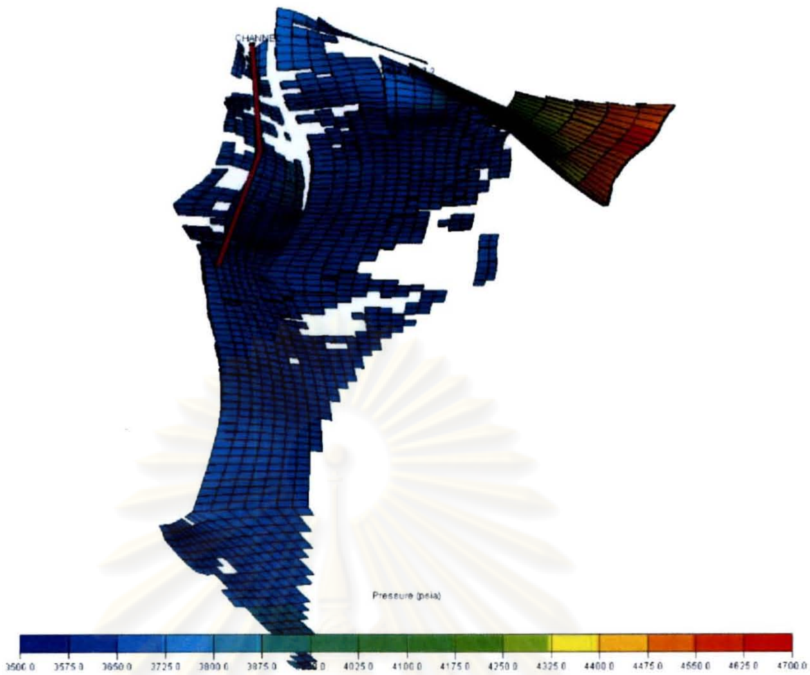

Figure 4.16: Channel sand reservoirs pressure distribution

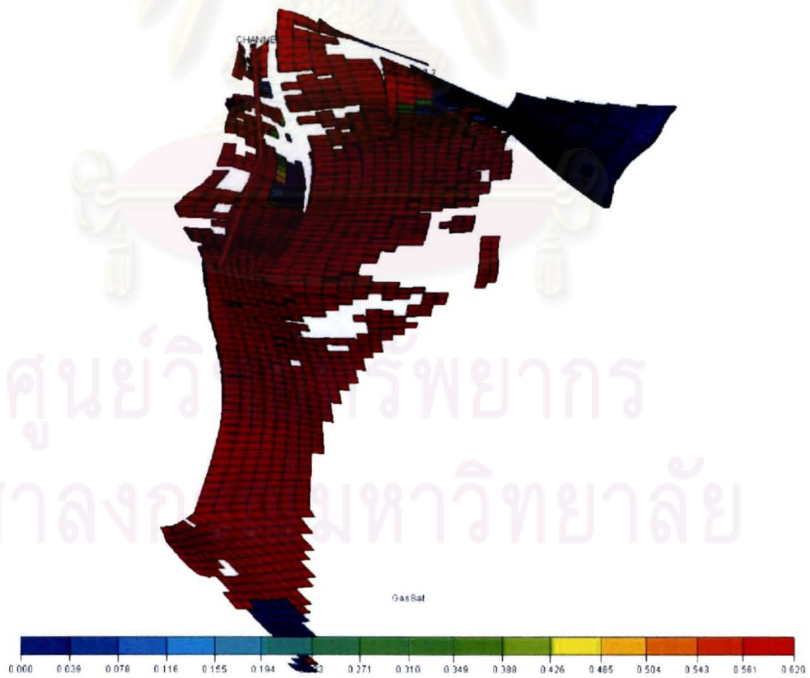

Figure 4.17: Channel reservoirs gas saturation distribution

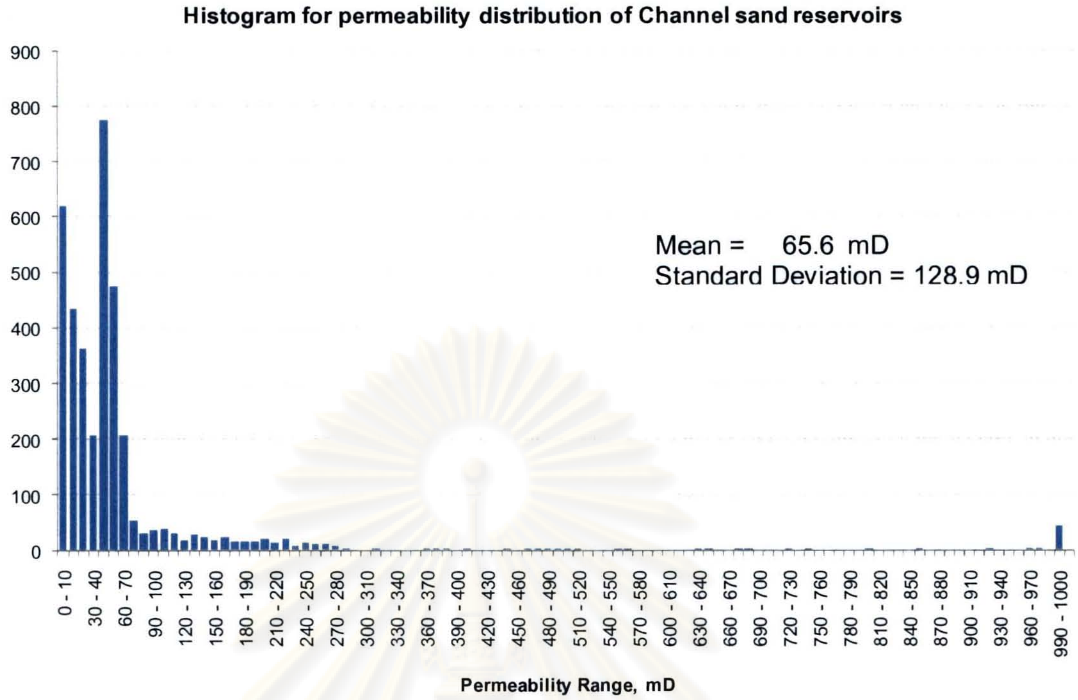

Figure 4.18: Histogram for bar sand reservoirs permeability distribution

The dynamic response of the selected channel reservoirs will be described under the model matching between original and simplified model section

4.2 Generation of Simplified Reservoir Model

The simplified version of reservoir model possessing similar response to the actual model is created using reservoir simulation software. This simplified model will offer benefit over the actual model as the reservoirs layers can be remodeled (such as changing the drive mechanism) and re-sequenced. Better understanding of the multilayered reservoir performance is expected through this model. The simplified model will have the similar number of reservoirs, similar reservoir inclination (dip angle), and OGIP to the actual model.

4.2.1 Homogenous Original Model

Although the OGIP of the simplified model would be matched with the original model, the number of cells would be reduced; the shape would be slightly different due to the simplification assumptions.

The homogenous version of the original reservoir model is set up using average value of the properties shown in table 4.5. Apart from these assumptions, no other modifications are made to the original reservoir model.

Table 4.5: Average properties used for original model modification and simplified model generation

Properties	Bar sand reservoirs		Channel sand reservoirs	
	Range	Average	Range	Average
Net to Gross (%)	0-100%	25%	0-100%	40%
Porosity (%)	10-35%	21%	15-34%	21%

4.2.2 Simplified Model

The simplified model has been generated using corner point gridding. In order to reflect the original reservoir's dip, the simplified model has been set with inclination angle in accordance with the original model. The dip angle of the original reservoir model is shown in Figures 4.19 and 4.20.

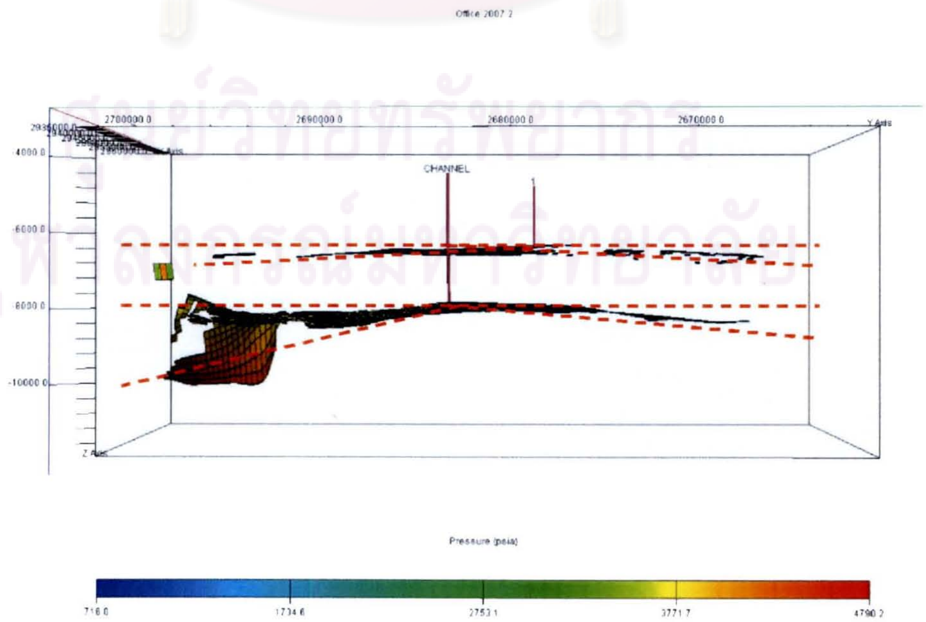

Figure 4.19: Bar and channel sand reservoirs dip along Y-Y axis

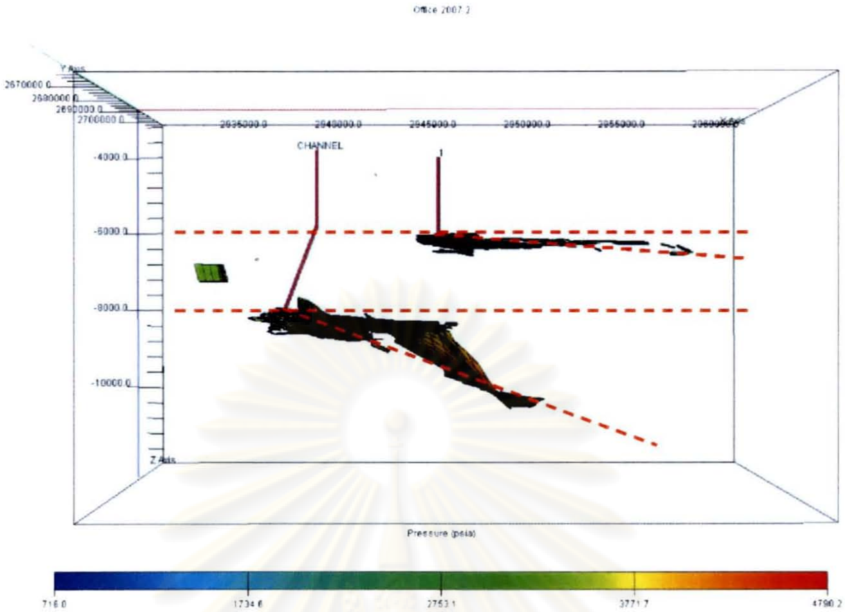

Figure 4.20: Bar and channel sand reservoirs dip along X-X axis

As both bar and channel reservoirs have to be constructed on the same model, the different in dip angle has to be normalized. As a result, the dip angle has been set to 2 ft/100ft for the Y-Y direction dip and 10 ft/100ft for X-X direction dip. The result reservoir plane is shown in Figure 4.21.

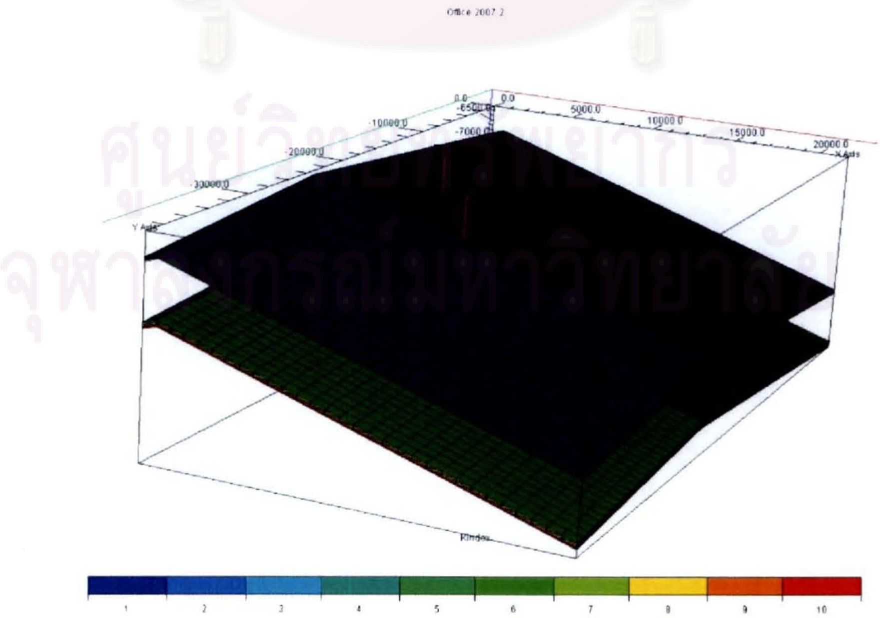

Figure 4.21: Simplified Model Reservoir Plane

The following data has been used for setting up of the simplified model.

a) Case Definition

Simulator:	Black Oil	
Model Dimensions:	Number of cells in the x direction	15
	Number of cells in the y direction	45
	Number of cells in the z direction	4 (Bar)
		5 (Channel)
Grid type:	Corner Point	
Geometry type:	Block Centered	
Oil-Gas-Water Options:	Water, Gas	

b) Grid

			Bar	Channel
Properties:	Porosity	=	21%	21%
	Gross thickness	=	15.4	18.9 ft/ layer
	Net to Gross Ratio	=	25%	40%
	Depth of Top face	=	6,206 ft	7,875 ft

The shape and size of the reservoir is obtained by setting active cell in close match to the original model. The comparison between the original model and simplified model is shown in Figures 4.22 and 4.23.

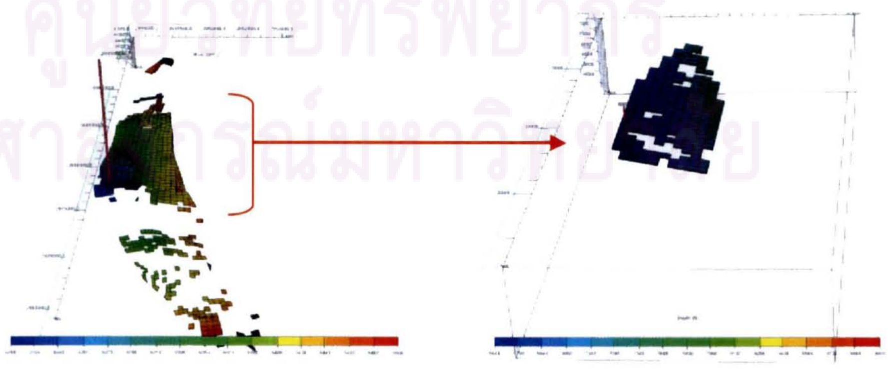

Figure 4.22: Shape matching between original and simplified model for bar sand reservoirs

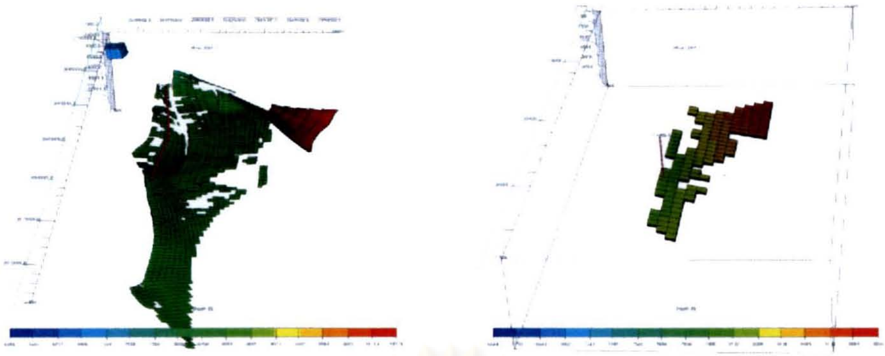

Figure 4.23: Shape matching between original and simplified model for channel sand

c) PVT Same as Original model, each for bar and channel sand reservoirs

d) SCAL Same as Original model, each for bar and channel sand reservoirs

The static model matching between original and simplified model has been made by adjusting the pore volume, OGIP, water in place and initial reservoir pressure to best match. Matching result is shown in Table 4.6 under section 4.2.4. The deviation for simplified model is less than 10% for all data investigated.

4.2.3 Well Model

In order to simulate the dynamic performance, the well model has been created using Prosper Software. The model is built based on monobore well design which is widely applied in the GoT. The well has a wellbore diameter of 6-1/8 inches with 3-1/2 inches production casing (inside diameter of 2.992 inches). The well is perforated from 6,000 ft. to 7,500 ft, depending on the reservoir depth in each case. The schematic of wellbore and configuration is shown in Figure 4.24.

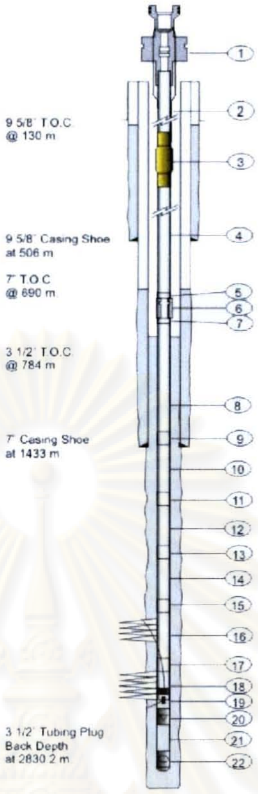

Figure 4.24: Monobore well schematics

The well's configuration detail and the set up of VFP model can be found in Appendix A. As a summary, the model set up including:

Fluid Type:	Dry & Wet Gas
Method:	Black Oil
Inflow Model:	Multilayered (Jones)
VLP Model:	PE2
Variables Run:	WHP: 14.5 – 3250 psig
	CGR: 0- 3000 stb/MMscf
	WGR: 0 – 3000 stb/MMscf

4.2.4 Matching of Original and Simplified Model

In matching of the original and simplified model, following steps are taken;

a) Static Model Matching

Since the rock and fluid properties are kept similar between the original and simplified model, the model is matched by 2 variables:

(a) Adjust the reservoir inclination angle until the GWC contact and initial reservoir pressure are matched.

(b) Adjust the reservoir shape until the pore volume, gas and water in place are matched.

After various adjustments, the final match is shown in Table 4.6. The result is further used for dynamic model matching.

Table 4.6: Static model matching result

Properties	Bar sand reservoirs		Channel sand reservoirs	
	Original	Simplified	Original	Simplified
Pore Volume, MMRB	64.111	64.395	101.120	101.104
OGIP, BSCF	8.573	8.575	49.751	49.999
Water In Place, MMbbl	50.754	51.170	48.436	48.286
Initial Reservoir Pressure, psia	2,955	2,991	3,773	3,785

b) Dynamic Model Matching

Because the reservoir size, shape, and inclination have been set in order to match static model, the parameter to match the dynamic model response is permeability. All other rock and reservoir fluid properties are set to be the same. The resulting permeability is found to be 100 mD for bar sand reservoirs and 80 mD for channel sand reservoirs.

The matching is carried out for gas production rates, reservoir pressures, bottomhole pressures, and *p/z* behavior of the reservoirs. The matching of water production is not carried out due to relatively low water production (< 0.001 bbl/d) from both reservoirs.

<u>Bar Sand Reservoirs Matching Results</u>

Original model and simplified model has been compared for gas production rates, reservoir pressures, bottomhole pressures, and *p/z* behavior. In matching of production rates, the production of bar sand in the reservoir is capped at 5 MMscf/d using single well with 3-1/2 inches production casing size. Although the erosion limit for this tubing size is at 20 MMscf/d. The matching is done at lower rate in order to see the behavior more clearly.

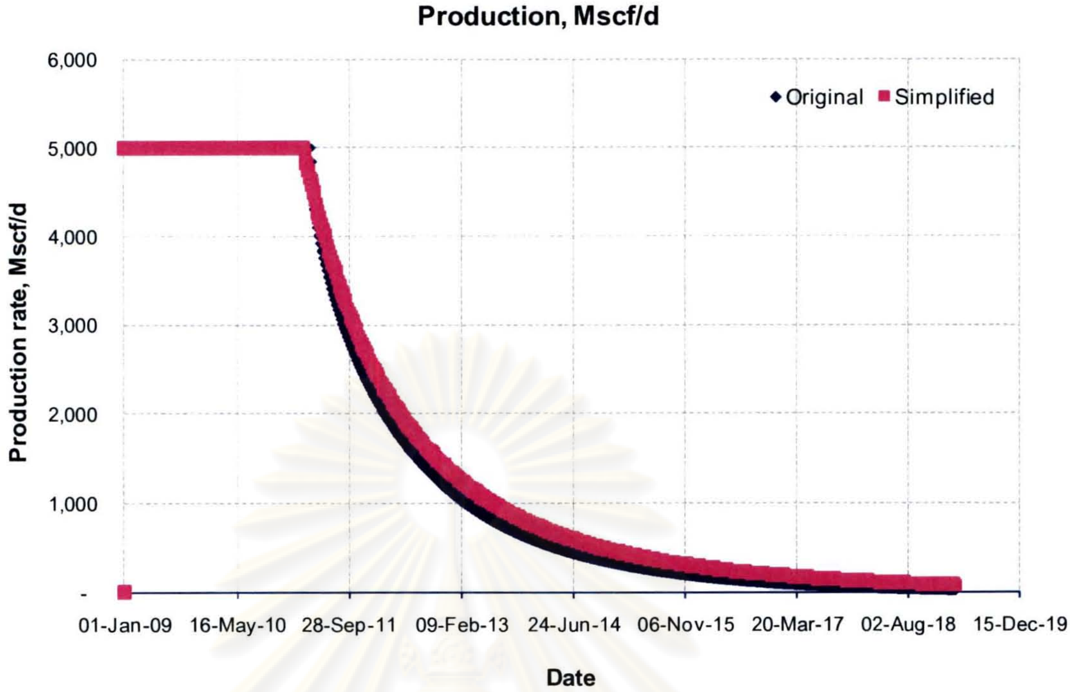

Figure 4.25: Result of model matching, Production rates

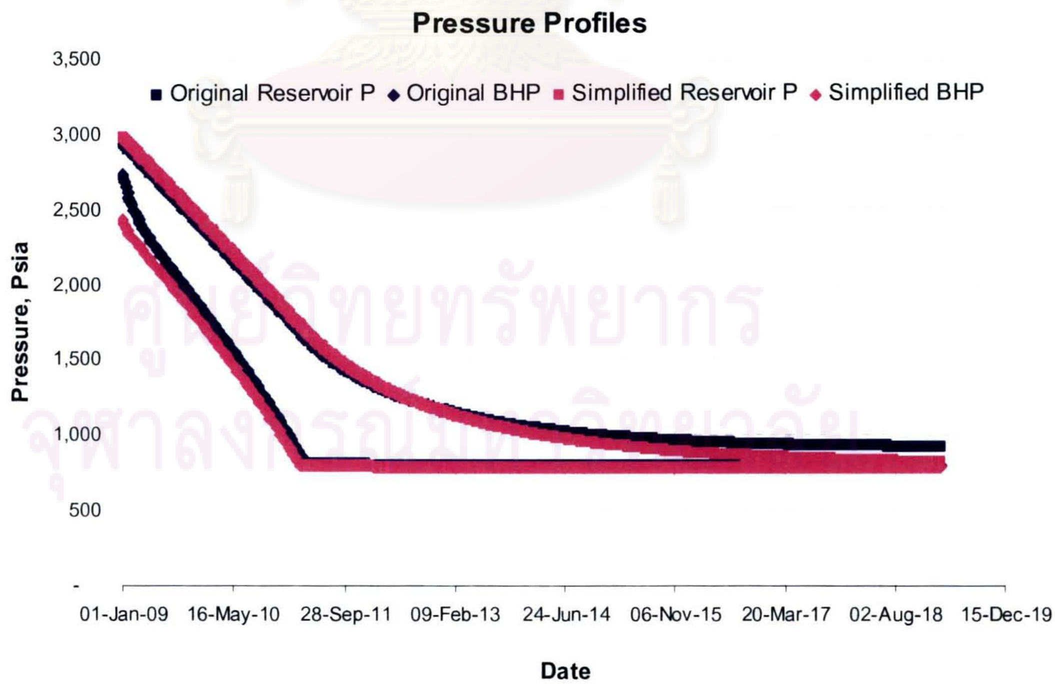

Figure 4.26: Result of model matching, Pressures

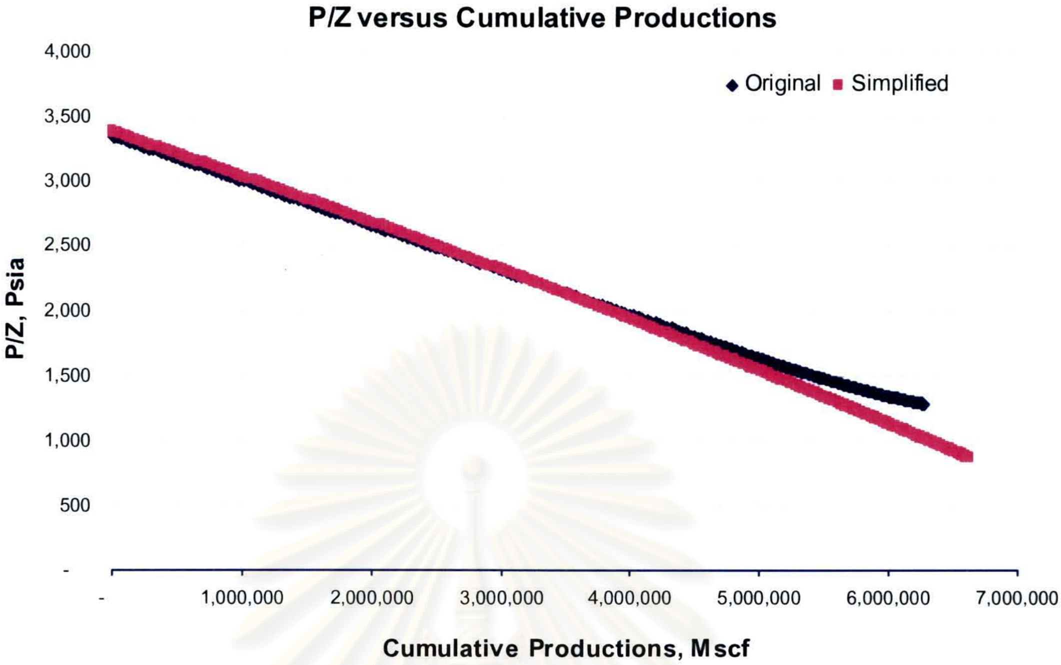

Figure 4.27: Result of model matching, *p/z*

The result deviation from matching between original and simplified model is shown in Figure 4.28. The deviation is plotted as percentage difference in production rates, reservoir pressures, and bottomhole pressures. Most results are found to be accurate within ±5% deviation. Although the production rate shows more than 10% deviation in the late life, it is associated with very low production rates at the time, which can be considered as insignificant. The deviation is, therefore, considered acceptable.

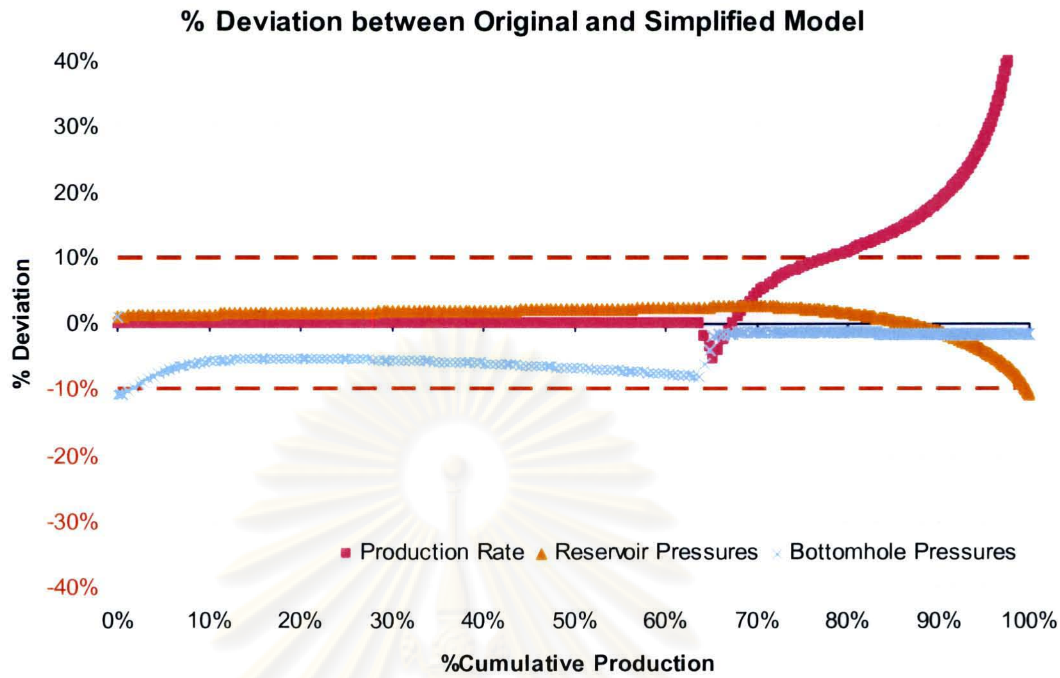

Figure 4.28: Result of model matching, deviation plot

Channel Sand Reservoirs Matching Results

In order to confirm the model, additional matching scenario has been set for channel sand reservoirs, where the reservoirs can be subjected to large connecting aquifer. Numerical aquifer has been set with 10 times and 20 times the size of gas reservoirs, connecting to the edge of the reservoir which is the direction of meandering channel.

As the performance matching is done based on single well. The well capacity is limited by erosion to 20 MMscf/d using 3½ inch production casing. The matched parameters are flowrate, reservoir and bottomhole pressure, and *p/z* behavior of the reservoirs.

The base case matching is shown in Figures 4.29 through 4.31.

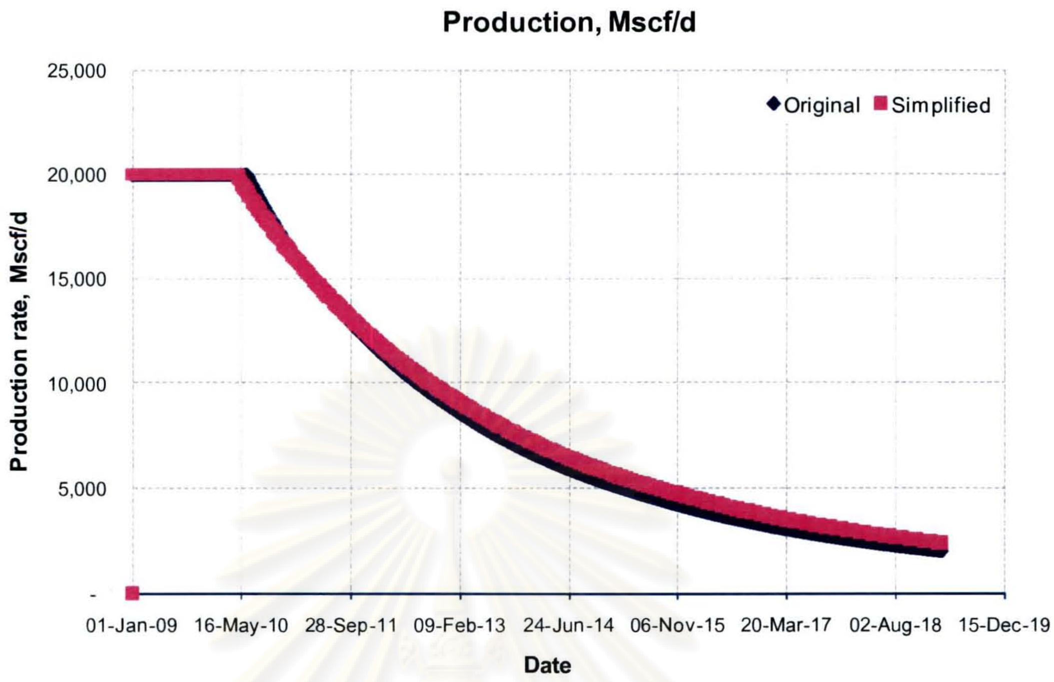

Figure 4.29: Result of model matching, Production rates

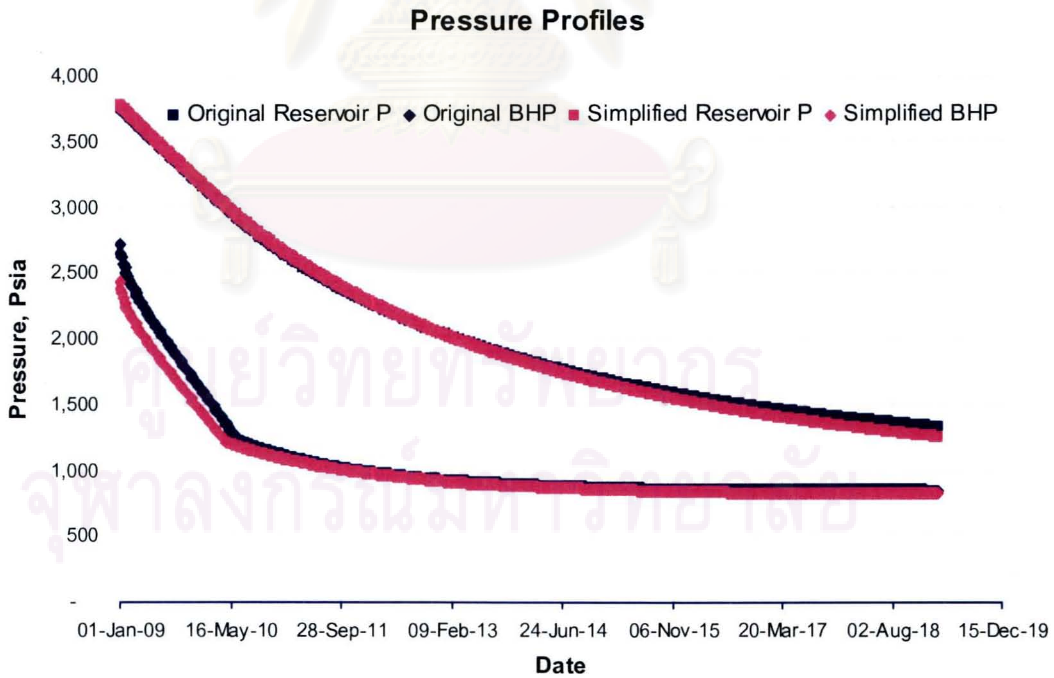

Figure 4.30: Result of model matching, Pressures

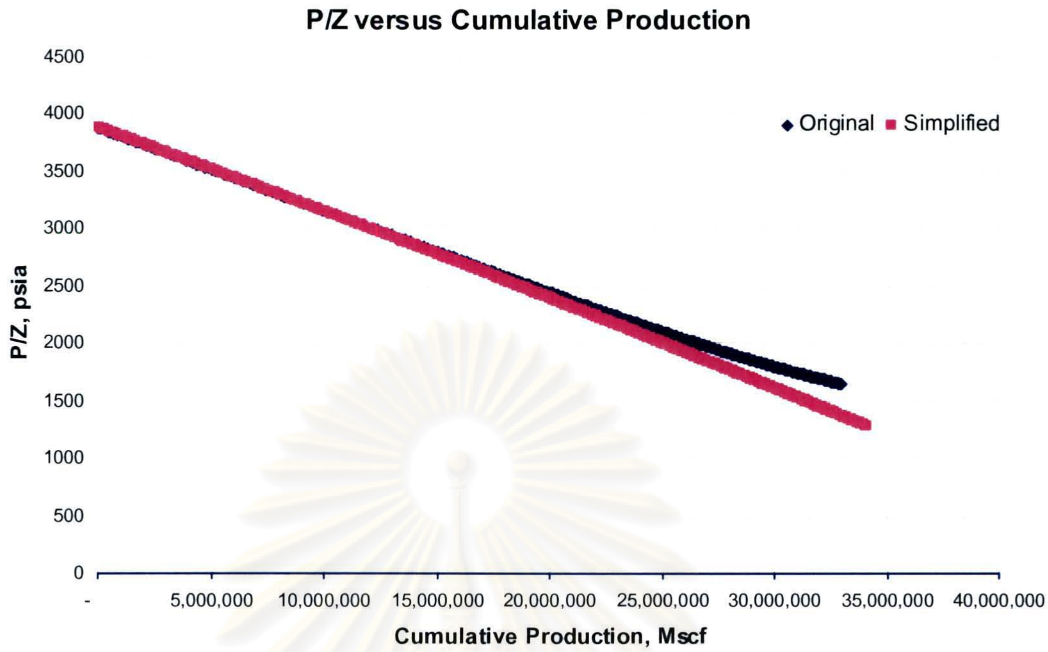

Figure 4.31: Result of model matching, *p/z*

The result deviation from matching between original and simplified model is shown in Figure 4.30. Similar to bar sand reservoirs, most results are accurate within ±5% deviation. Although the production rate shows more than 10% deviation in the late life, it is associated with very low production rates at the time. The deviation is, therefore, considered acceptable as well.

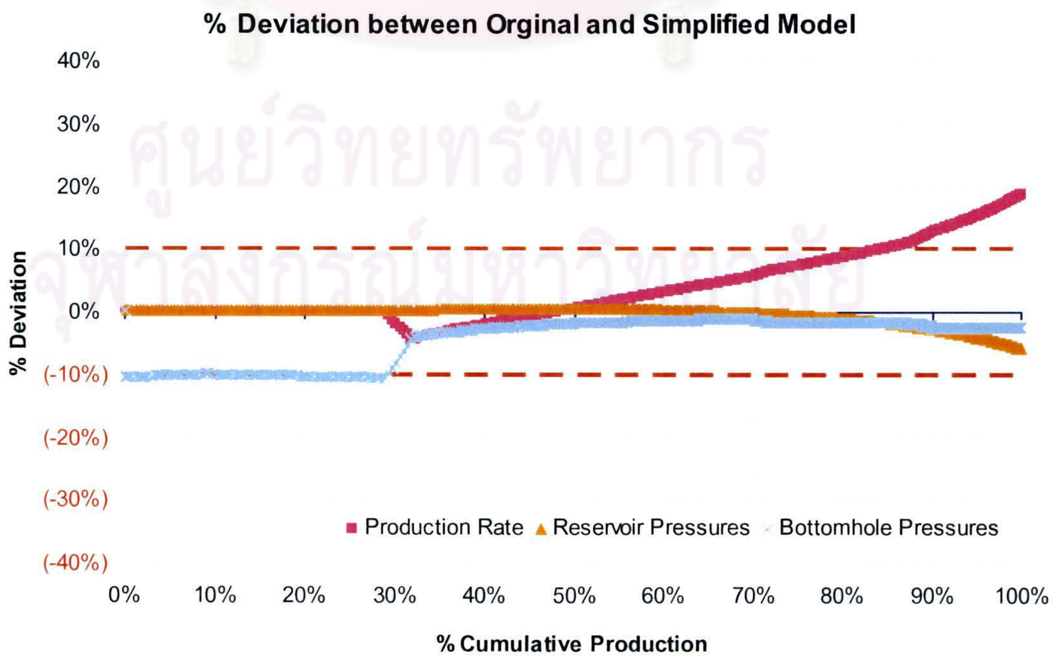

Figure 4.32: Result of model matching, deviation plot

Numerical Aquifer Matching Results for Channel Sand

For the additional simulation with large numerical aquifers, the model matching result are shown through Figures 4.33 to 4.35 for aquifer size of 10 times of gas reservoir size and 4.36 to 4.38 for aquifer size of 20 times of gas reservoir size. No change to either original or simplified model, including well location, is made apart from added aquifers.

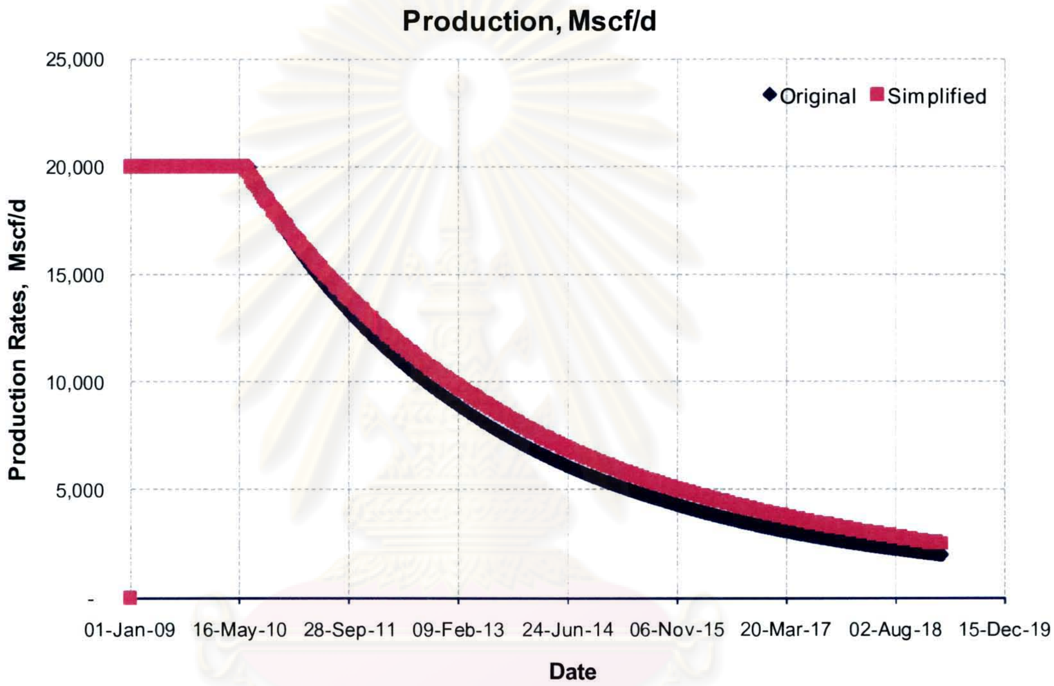

Figure 4.33: Result of model matching, Production rates. Aquifer size = 10 x gas reservoir size

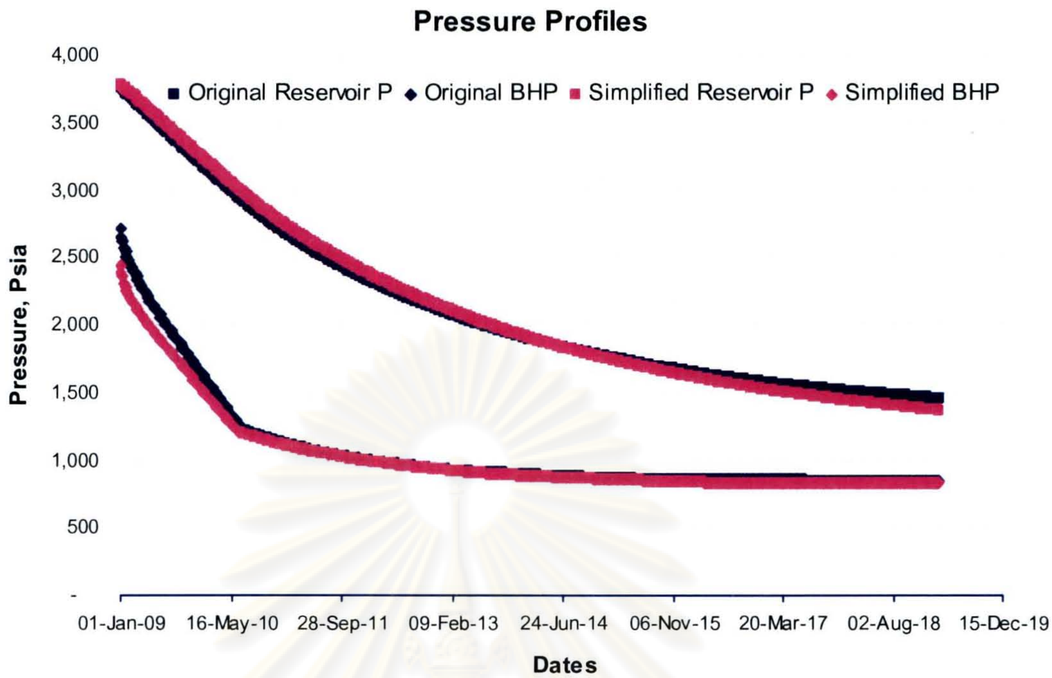

Figure 4.34: Result of model matching, Pressures. Aquifer size = 10 x gas reservoir size

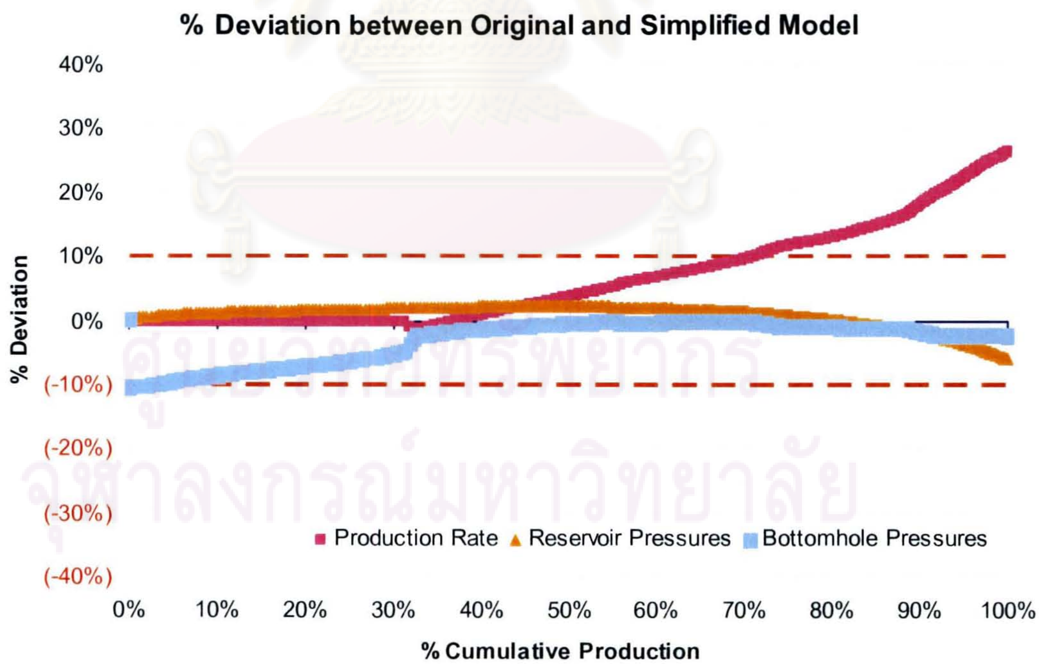

Figure 4.35: Result of model matching, deviation plot. Aquifer size = 10 x gas reservoir size

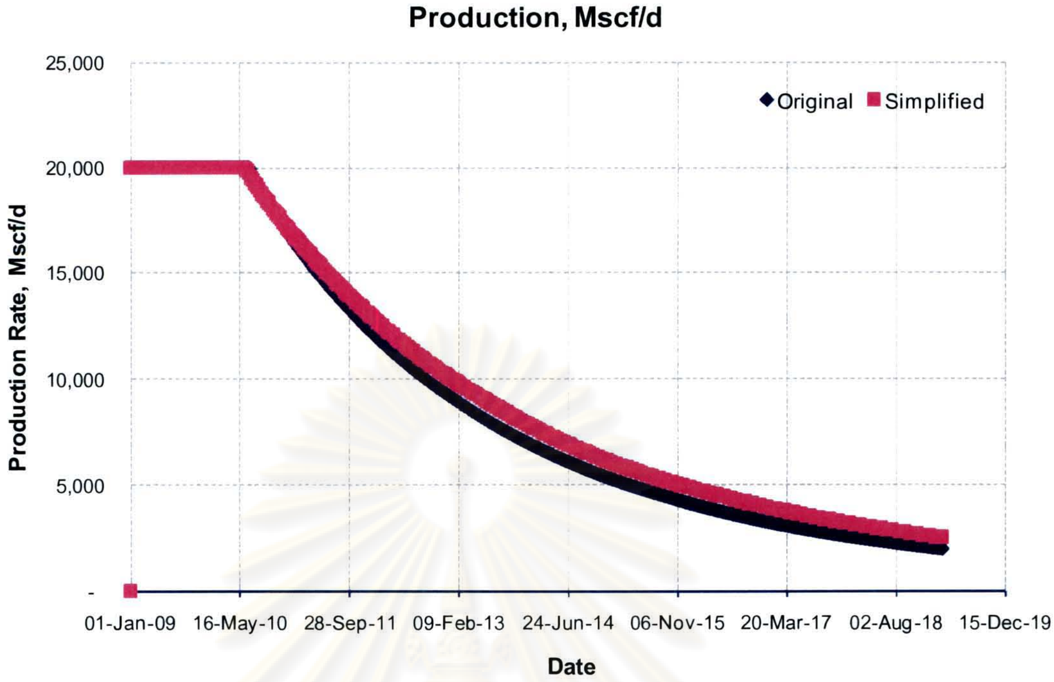

Figure 4.36: Result of model matching, Production rates. Aquifer size = 20 x gas reservoir size

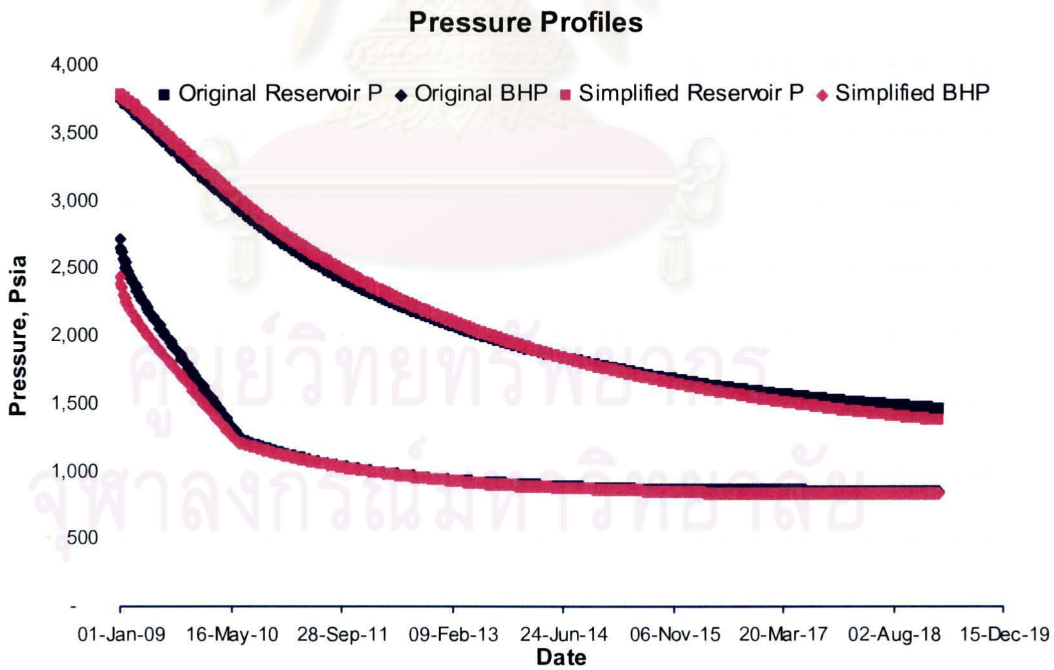

Figure 4.37: Result of model matching, Pressures. Aquifer size = 20 x gas reservoir size

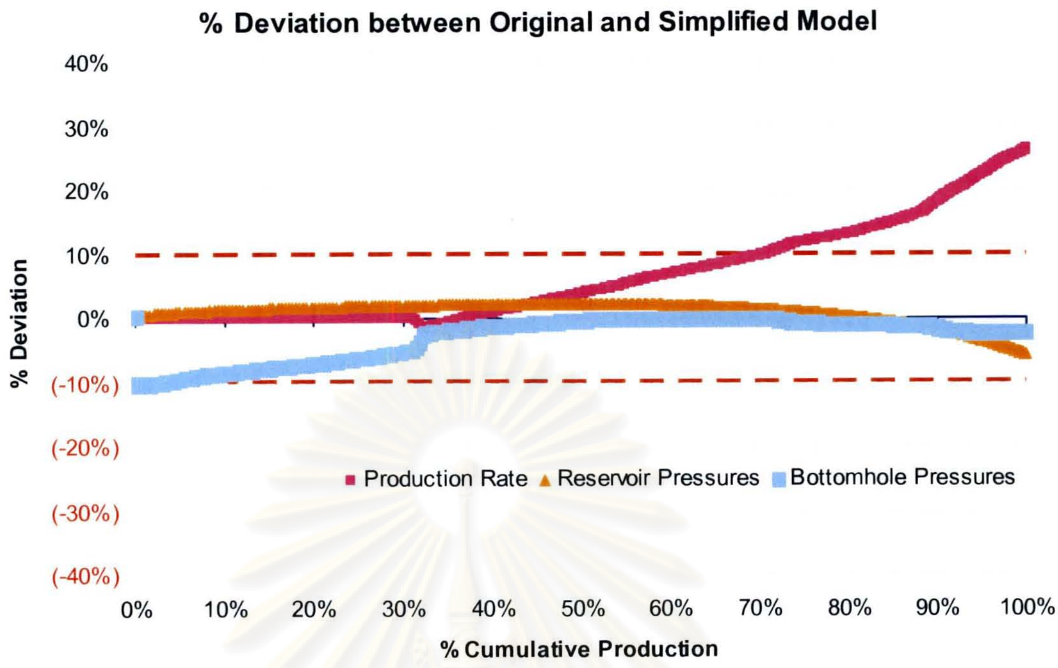

Figure 4.38: Result of model matching, deviation plot. Aquifer size = 20 x gas reservoir size

4.2.5 Matching Conclusions

The matching result for both bar and channel sand reservoirs show that simplified model is matched with small deviations. Since the study is intended to compare the performance of different perforation sequence within same bar and channel model, this deviation is considered acceptable.

The recovery factor for each case is shown in Table 4.7. The differences are all below 10%. For all cases, the deviation is below 5% for cumulative production of up to 90% of ultimate recovery.

Table 4.7: Recovery Factor obtained from model matching

Case	RF, %		
	Original	Simplified	% Difference
Bar Reservoirs	75%	79%	5.6%
Channel Reservoirs, Base case	67%	69%	3.2%
Channel Reservoirs, Aquifer size = 10 x gas reservoir size	68%	72%	6.5%
Channel Reservoirs, Aquifer size = 20 x gas reservoir size	68%	72%	6.5%

From the matching result, it is found that it is possible to generate simplified models which possess similar static and dynamic response to the original reservoirs based on single well approach. Therefore, to use simplified, homogeneous model for further study would give similar results as using original model. The outline of investigation and results is discussed in Chapter V.

CHAPTER V

RESULTS AND DISCUSSION

This chapter presents the results of the study. The effect of production/ perforation approaches on the reservoir recovery efficiency under different drive mechanism and reservoirs arrangement is investigated using the simplified model that tested to match with original bar and channel sand reservoir model.

5.1 Model Arrangement

The simplified model is set up by two main characteristics of the reservoirs that may have an effect on perforation strategy determination:

1. The size of the reservoirs. In the GoT reservoirs there are two types of sand reservoirs, one is big, continuous and thick as mostly encountered in Channel sand type reservoirs. Others is small, thin reservoirs normally called Bar sand type reservoirs.
2. The permeability of the reservoirs.

Therefore, putting these two characteristics together would results in four layered reservoirs. The simplified reservoir model matched in chapter 4 is used as representative model in this study. The matched channel sand reservoirs represent the thick, continuous reservoirs, and the matched bar sands reservoirs represent the small, thin reservoirs. For permeability, 20 mD is chosen for low permeability reservoirs while 200 mD is chosen for high permeability reservoirs. The result combination is shown under Table 5.1. The top depth of the reservoirs is 6,200 feet same as top depth of the original model. Each layer is 100 feet apart, with shale (inactive cells) in between. The initial reservoir pressures are assumed to be hydrostatic.

Table 5.1: Model arrangements

Reservoir	Size	Permeability
1	Thick	200 mD
2	Thin	200 mD
3	Thick	20 mD
4	Thin	20 mD

Due to the combination of each reservoir into multi-layered reservoirs, it is found that single well would not be practical approach to drain the whole reservoirs. For a 3½" production casing, the maximum gas rate is around 20 MMscf/d, which means for a total 104 Bscf reservoir (2 Thick & 2 Thin), it would take 14.3 years to deplete. It is anticipated that 4 wells would be required to deplete the study model.

As both reservoirs (Bar and Channel) are separated from each other in the original model, the overlay of simplified model can be arranged in such manner that well placement can be vertical as possible. Based on production characteristics of 4 wells placed evenly on the reservoirs, each well will produce restricted to its available drainage area, with no flow boundary adjacent to other well's drainage area. Under depletion drive mechanism and homogenous reservoir, the production of each well placed evenly in the reservoir (i.e. similar drainage area) would therefore be similar. Figure 5.1 depicts the well placement in the reservoirs. The red colours represent gas zone and blue colours represent water zone.

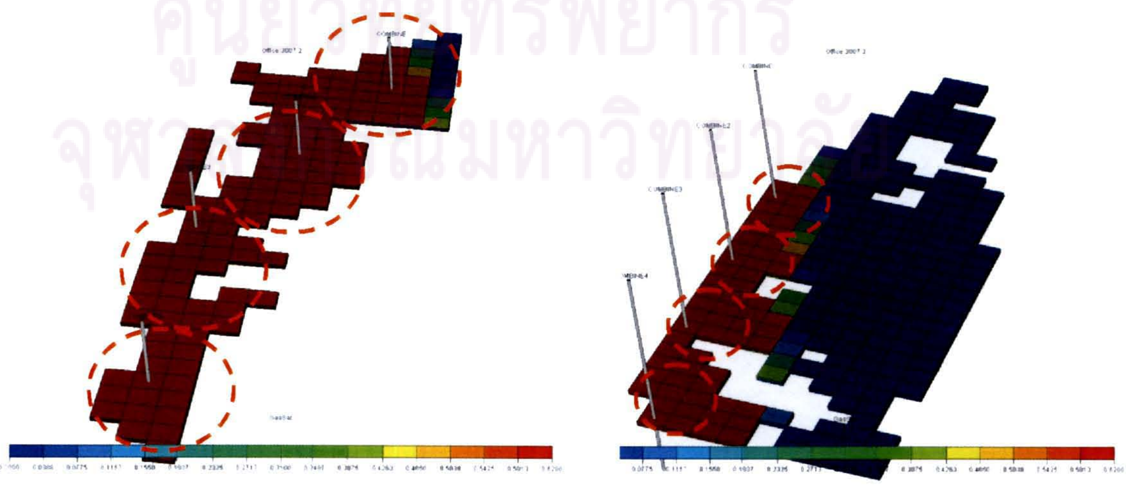

Figure 5.1: Thick and thin reservoirs, well placements and drainage area pattern

Under water drive mechanism studied, the connection of water drive is from the edge of reservoirs as typically found in channel type reservoirs in the GoT. The impact of water expansion and production through each well are shown under Figure 5.2 using thick reservoir as an example. It can be seen that the pattern of water encroaching reservoirs are in subsequent manner, i.e., one well after another starting from the well which is nearest to the water zone and encroach to the next well. This depletion pattern would result in similar depletion from one well to another, only difference is timing.

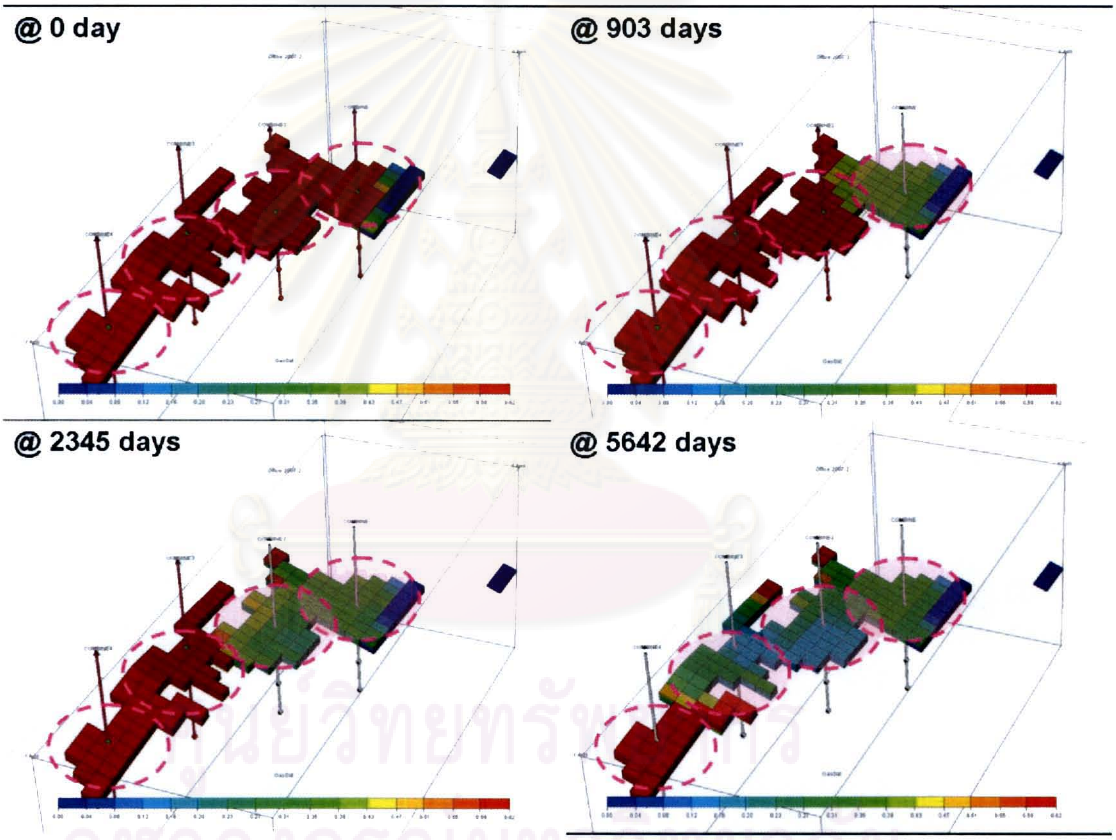

Figure 5.2: Water encroachment pattern in reservoirs

Therefore, to ease the analysis, the reservoirs are cut into single well's drainage area limit. From recovery performance of water drive reservoirs, the result of this reservoir cutting into single well drainage will be conservative because the gas that can not produce after water reaches the well under single well model can actually flow to next well in the 4-wells reservoirs model. However, this phenomenon is not affecting study approach and results as the study is carried out on comparison basis. The result multilayered reservoirs model are shown in Figure 5.3 below.

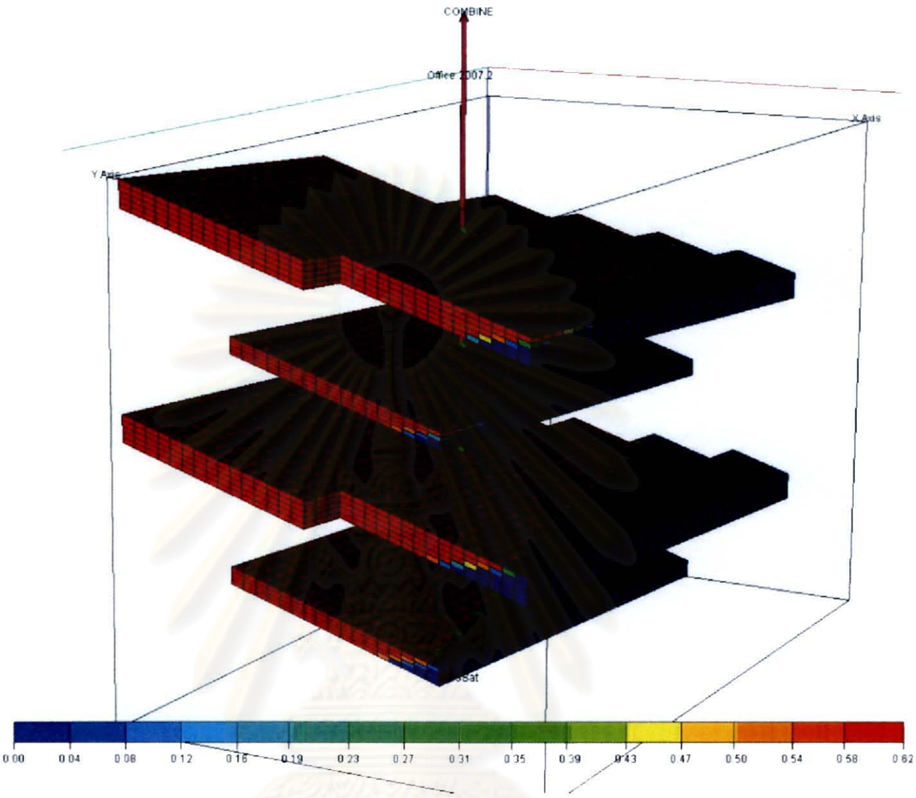

Figure 5.3: Single well model from reservoir model, showing gas saturation distributions

There are three cases to be investigated in this study:

1. Case 1: When all reservoirs are produced under depletion drive mechanism. In this simplest arrangement, the reservoirs are depleted based on the expansion of gas in the reservoirs only. As a result, pressure will plays an important role on production strategy in this case. The case is initiated to study behavior of pressure and their influence on production and crossflow issue.
2. Case 2: When all reservoirs are produced under water drive mechanism. In the second case, the reservoirs are set to be connected with aquifers. As the gas is being produced from well, the reservoir pressure declines and cause the supporting aquifers to expand. As a result there will be an influence

from both pressure and gas saturations that plays role on optimal production/perforation strategy determination in this case.

3. Case 3: Commingled production from both depletion and water drive reservoirs. This case represents more realistic multilayered gas reservoirs in the GoT.

5.2 Study Scenarios

The perforation/production scenarios under this study can be categorized into 3 groups and 1 additional scenario. The first group (scenario 1a-d) is the set of scenario using bottom–up approach. Bottom-up approach is one of the widely used techniques in the gas field in GoT. This method allows the gas to be produced from lowest reservoir first and produce the next upper reservoirs in sequence. This method's strong point is that since it allows the bottom reservoir to be produced first, the shutting-off of the depleted reservoir can be done easily without concerns that the non-depleted reservoirs will have to be isolated from well as found in other scenarios. The scenarios under this group are listed in Table 5.2.

Table 5.2: Scenario studied under Bottom-up approach

Scenario	Description	Explanation
1a	Fully depleted	Produce current reservoir until fully deplete, and then open the next upper layer. Production rate at fully depleted is set at minimum economic limit of 0.5 MMscf/d.
1b	Half depleted	Produce current reservoir until rate decline to half of plateau rate (20 MMscf/d), which equals to 10 MMscf/d, then open the next upper layer.
1b	Maintain production plateau	Produce current reservoir until rate drops below 20 MMscf/d, then open next upper layer.
1d	Water Shut-Off (WSO)	Shut the reservoir once the reservoir produce significant amount of water and less gas to avoid further water production from that reservoir.

As scenarios 1d involves water production, the scenario is tested on water drive and combination drive cases where water production is anticipated only.

The second group concerns with permeability of the reservoirs. It is being investigated because of the importance of permeability on the depletion mechanism of the reservoirs. There are two scenarios under this group, scenario 2a where high permeability reservoirs are depleted first, and scenario 2b where low permeability reservoirs are depleted first.

The third group concerns with the size of reservoirs. The size of reservoirs impacts the rate of depletion in the way that pressure declines are slower in big reservoirs (given same reservoir properties and depletion rate). Therefore, in order to study the multilayered reservoirs, two scenarios are added to the study. Scenario 3a is where the big reservoirs are depleted first. Scenario 3b is where the small reservoirs are depleted first

The summary of scenario 2 and 3 are shown in Table 5.3.

Table 5.3: Summary of scenario 2 and 3 studied

Scenario	Description	Explanation
2a	High permeability first	Produce from high permeability reservoir (reservoir 1 & 2) until rate drops below 20 MMscf/d, then open low permeability reservoirs (reservoir 3 & 4).
2b	Low permeability first	Produce from low permeability reservoir (reservoir 3 & 4) until rate drops below 20 MMscf/d, then open high permeability reservoirs (reservoir 1 & 2).
3a	Thick reservoirs first	Produce from thick reservoir (reservoir 1 & 3) until rate drops below 20 MMscf/d, then open thin reservoirs (reservoir 2 & 4).
3b	Thin reservoirs first	Produce from thin reservoir (reservoir 2 & 4) until rate drops below 20 MMscf/d, then open thick reservoirs (reservoir 1 & 3).

The last scenario is scenario 4. This scenario brings all reservoirs to production altogether since first date of production. The production plateau is set at 20 MMscf/d as previous scenarios.

5.3 Monitoring Parameters

Optimal perforation/production strategy is defined in terms of optimal production out of the multilayered reservoirs. Certain aspects of production are focused in this study. The monitoring parameters include:

1. The level of cross flow through well. The level of crossflow is determined as % of OGIP. In multilayered reservoirs, one of the key issues is the crossflow from one or more reservoirs to others through the well's perforated sections. The crossflow may result in loss or reduced recovery factors if the crossflowed volume cannot be recovered.
2. The time to recover the cross flow volume. Corresponding to the level of crossflow, the time to recovery such crossflowed volume is another concern as the hydrocarbon recovery is delayed by the crossflow effect.
3. The time to achieve designated recovery factors. The time to deplete the reservoirs up to certain recovery factors (depends on study case) is of economic importance as the faster the recovery, the better the economics. Since the RF can be varied among each perforation/production scenarios, certain RF is set for each case for comparison purpose. For Study Case1 (depletion drive) it is set at 70%, For Study Case 2 (water drive) it is set at 30%, and for Study Case 3 (commingled production from depletion and water drive) it is set to 40%. The time to reach ultimate recovery is also monitored.
4. The RF obtained from each scenario. The RF is also of importance as the ability to recover gas from the reservoirs varies with scenarios and study case. The higher RF, the better.

5.4 Multilayered Reservoirs Performance under Depletion Drive

The first case under study is when all reservoirs are under depletion drive mechanism. The study model employs basic single well drainage reservoirs as depicted in Figure 5.3. The model has been put into production under various perforation/ production scenario outlined in section 5.2.

The result from each scenario is shown in Table 5.4 below.

Table 5.4: Depletion drive case simulation results

Scenario	Description	Crossflow (% OGIP)	Time to recover crossflow vol. (days)	time (years) to reach % recovery		RF (%)
				70%	Ultimate	
1 Bottom-Up						
1a	Fully depleted	2.46	1638	17.46	20.59	80.47
1b	Half depleted	0.98	168	6.18	11.79	77.56
1c	Maintain plateau	0.48	105	6.20	11.84	77.11
2 Permeability selective						
2a	High perm. first	0.02	Infinite	6.58	11.02	76.79
2b	Low perm. first	0.01	245	6.27	11.90	77.06
3. Reservoir size selective						
3a	Thick reservoirs first	0.30	35	6.27	12.00	76.95
3b	Thin reservoirs first	0.27	70	6.27	11.90	77.05
4	Produce all since day 1	0.01	231	6.27	11.90	76.85

The following are observed from the table:

1. The level of crossflow is in a range of 0.01%- 2.46% of the OGIP. Based on model (4 reservoirs) OGIP of 30 BCF, the crossflow volume is in a range of 3 MMscf - 0.73 BCF.

   In terms of trends, scenario 1a, has highest crossflow of 2.46%, scenario 1b has crossflow of 0.98%, scenario 1c to 4 has relatively lower level of crossflow (0.48% down to 0.01%) this is directly associated with the level of depletion in the reservoirs. In scenario 1a, at the time next reservoir is open to flow, the current producing reservoir is depleted to minimum flow and hence the reservoir pressure is at minimum. In scenario 1b, the current producing reservoir only half depleted and therefore the reservoir pressure is higher than scenario 1a. In other scenarios each reservoirs is open to flow one after another in a short period of time (because of trying to maintain plateau production) therefore the reservoir pressure is relatively high and crossflow is smaller. The crossflow issue is studied in further details in section 5.4.1.

2. The time to recovery crossflow ranging from unable to recover, to as low as 35 days. The infinite time to recovery indicated in the table does not means that all crossflowed volume is lost in the reservoirs but rather means that only some part of the crossflowed volume can be recovered (but not all of them). Apart from the infinite scenario (scenario 2a), all other scenarios shows definite time to recover the crossflow volume.

   The level of crossflow recovery time depends on the level of reservoir pressure depletion as observed from the table. If the reservoir pressure of the reservoir is lower than the producing well's flowing bottomhole pressure, the gas from higher pressure reservoir would flow into the lower pressure reservoir. If this happens when the reservoir pressure of the crossflowed reservoir is depleted, there will be less chance to recover, and the time spend would be longer than the scenario where reservoir pressure of the crossflowed reservoir is still high.

3. The recovery factor is in the range of 76.79% to 80.47%. The variation in recovery factor between each scenario is low, especially from scenario 1b to 4, where the RF is between 76.79% to 77.85%. This is because of the drive mechanism of the reservoir itself. Under depletion drive mechanism, the recover efficiency of the reservoirs depends on level of depletion. Therefore, if the reservoir is depleted to same abandonment pressure in all scenarios, the RF% would be similar.

   For scenario 1a, the reason the RF% is 80.47%, which is highest among all other scenarios, is because of the late opening (by allowing each reservoir to produce as long as possible up to minimum economic limit) of each reservoirs allows wells to sustain production above wells economic limit compared to other scenarios.

5.4.1 Investigations on Crossflow through Well

A detailed investigation is made on the crossflow issue using the highest crossflow scenario, scenario 1a, as a model. The crossflow rate of each layer is plotted over time in Figure 5.4.

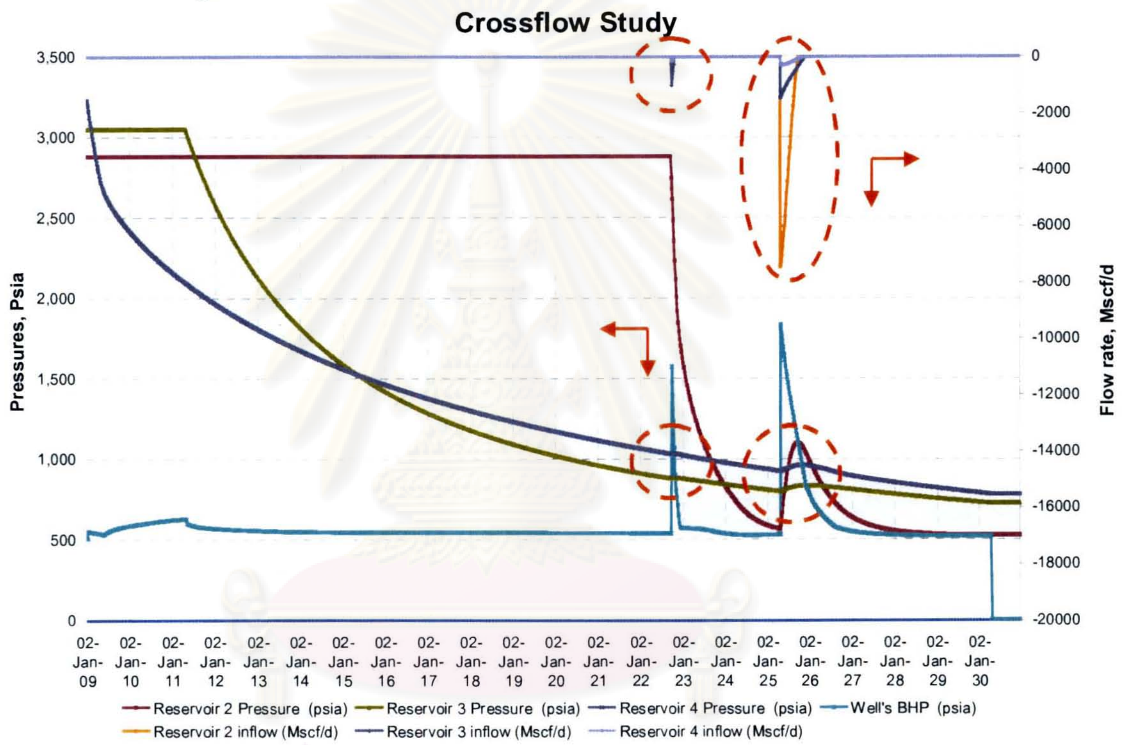

Figure 5.4: Pressure profile and crossflow in reservoirs

Based on the figure, the crossflow occurred whenever the bottomhole pressure exceeds the reservoir pressure, or to be more specific, the near wellbore pressure. This event would unlikely to happen at initial time because the reservoir is not yet depleted and the reservoir pressure is still high. The crossflow will start from middle to late life when one or more of the reservoirs are depleted to near well's bottomhole flowing pressure. As shown under Table 5.4, there is variation in time to recover the crossflow volume. If the crossflow occurs at late life, the time to recover will be long, or even unrecoverable as appear in scenario 2a.

From the darcy's equation for pseudo-steady state gas flow,

$$Q_g = \frac{0.000703kh(P_r^2 - P_{wf}^2)}{\mu ZT \ln(0.472\frac{r_e}{r_w} + S)} \tag{5.1}$$

Which means that for the rate of gas crossflowed into reservoirs, the rate depends on reservoir pressure, well's bottomhole flowing pressure, permeability, reservoir thickness, gas viscosity and compressibility factor, the well's drainage radius and well's tubing radius, and the skin factor. If we compare each reservoir's ability to get crossflowed, it is better to compare in terms of Injectivity Index, $\frac{Q_g}{(P_R^2 - P_{wf}^2)}$, since each reservoir have different pressure and therefore different drawdown. If we rearrange the Darcy's equation into injectivity index form, the result would be,

$$\frac{Q_g}{(P_R^2 - P_{wf}^2)} = \frac{0.000703kh}{\mu ZT \ln(0.472\frac{r_e}{r_w} + S)} \tag{5.2}$$

Figure 5.5 plots the LHS and RHS of this injectivity index equation together. The LHS is obtained from reservoir simulation output, while RHS is calculated. It is found that for low permeability reservoirs, the crossflow injectivity index follows the theory. However, there's variation in the high permeability reservoirs as the injectivity index obtained by model is higher than calculated figures. The cause of this variation needs further investigations.

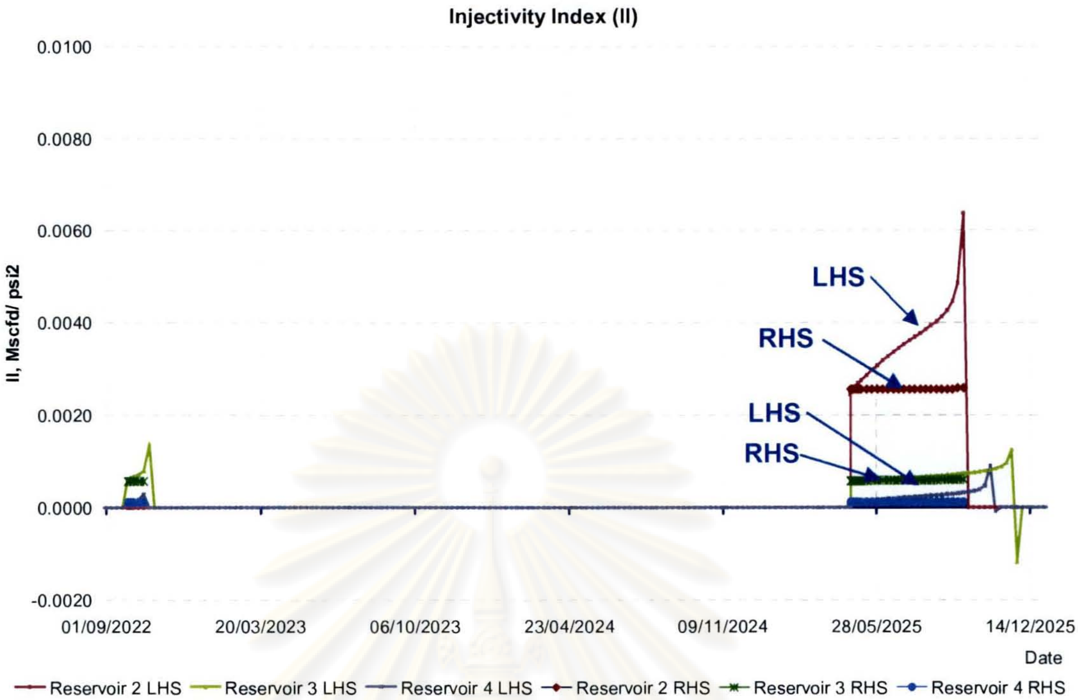

Figure 5.5: Simulation plotted versus calculated injectivity index

From the observations, it is clear that crossflow amount depends on pressure difference, reservoir volume, and how easy or difficult fluid can get into the crossflowed reservoirs (i.e., rock and fluid properties).

Therefore, it is suggested that to minimize crossflow, the reservoir pressure and the rock and fluid property for each reservoir in the multilayered reservoir should be analyzed in accordance with Darcy's equation over the lifetime of the reservoirs.

5.4.2 Conclusions on Depletion Drive Case

As discussed under section 5.4 and 5.4.1. Although the crossflow volume is not large in the model case, it can be larger in reservoir where the rock and fluid properties are good and difference in reservoir pressure between each layer is high. It is suggested to avoid the opening of new layer when the depleted layer(s), or current producing layers's reservoir pressure is low because the crossflowed volume will be difficult to recover.

The recovery efficiency in each case is almost similar. This is due to the depletion drive characteristics of the reservoirs. At similar abandonment pressure of each reservoir, the RF would be similar.

Based on the study results, to produce all reservoir together since day 1 (scenario 4) would provide optimal solution to the depletion drive multilayered reservoirs case. Under this scenario the crossflowed volume is small, the RF is similar to other scenario, and the time to recovery is among the fastest. This scenario also have other practical benefit such as reducing well intervention (i.e., to perforate others reservoirs) and reduce the chance of tool stuck or fish.

5.5 Mutilayered Reservoir Performance under Water Drive

The second case in the study is when all reservoirs are under water drive mechanism. This case is set with an intention to study behavior of multilayered well when all reservoirs are under water drive and subjected to gas/ water flow behavior.

5.5.1 Model Set Up

Numerical aquifers, each with size of 100 times of gas reservoir size of their connected reservoirs is set. The aquifer properties are set to be the same as their connected reservoirs. Aquifer initial pressure is set to be in equilibrium with their reservoirs, i.e., hydrostatic.

Another important concern is that as the simplified model is homogenous, the effect of heterogeneity in the water drive reservoirs can not be taken into account. Heterogeneity in the reservoir creates bypassing of water towards the well and hence trapping of gas behind. As a result, the recovery factor of the reservoirs is reduced. Under homogeneous reservoirs, the water will sweep the gas towards the well and improve recovery factors of the reservoirs.

A model check has been carried out to see if this is the case. The result is shown in Table 5.5. The recovery efficiency is reduced down to 50% when support aquifer is active, which is in-line with typical RF% on water drive gas reservoirs (use scenario 1a as comparison basis). The model is therefore used without further adjustment.

Table 5.5: RF% comparison between depletion and water drive case

Reservoir	Depletion Drive	With Aquifer support
Overall	80.5%	50.5%
1	82%	51%
2	84%	49%
3	79%	51%
4	78%	49%

5.5.2 Study Case Results

The result from each scenario is shown in Table 5.6 below.

Table 5.6: Water drives case simulation results

Scenario	Description	Crossflow (% OGIP)	Time to recover crossflow vol. (days)	Time (years) to reach %recovery		RF (%)
				30%	Ultimate	
1 Bottom-Up						
1a	Fully depleted	0.09	70	6.11	7.04	50.49
1b	Half depleted	0.01	49	1.58	2.09	39.68
1c	Maintain plateau	---	---	1.33	1.84	37.02
1d	WSO	---	---	7.09	8.04	49.40
2 Permeability selective						
2a	High perm. first	---	---	1.39	1.75	34.50
2b	Low perm. first	---	---	1.33	1.79	36.27
3. Reservoir size selective						
3a	Thick reservoirs first	0.09	14	1.31	1.79	36.52
3b	Thin reservoirs first	---	---	1.33	1.76	36.27
4	Produce all since day 1	---	---	1.33	1.79	36.27

The following are observed from the table:

1. The level of crossflow is in a range of 0.09% to none. The level of crossflow is relatively lower than depletion drive case, which is in range of 0.01%- 2.46%.

The low level crossflow is observed to be the result of the supporting aquifers. As the gas is being produced from the reservoirs, the reservoir pressure declined. The declines in reservoir pressure causes supporting aquifers to expand and in turn makes reservoir pressures drops to the lesser extent compared to depletion drive case. As a result, reservoir pressure is almost always higher than well's bottomhole flowing pressure and therefore reduces the chance of crossflow through well experienced in depletion drive case.

Among all scenarios tested, only scenario 1a, 1b and 3a are found to have crossflow. For scenario 1a and 1b, the producing reservoir is allowed to deplete to very low reservoir pressure before open the next upper reservoir layer. Therefore, the crossflow can happen on these two scenarios. For scenario 3a, the crossflow occurred at reservoir 1 which is shallowest, high permeability. As the water is not expanded yet and the thin layer is open to flow, the thin layer which has higher initial pressure (from hydrostatic gradient) causes crossflow into the reservoir 1.

2. The time to recover the crossflowed volume, if occurred, lies in the range of 14 to 70 days which is short period. This is due to the small volume of crossflow.
3. The RF lies in the range of 36.27% to 50.49%. Unlike the depletion drive case, there's significant difference in RF between each scenario in the water drive case. The RF is highest with scenario 1a (50.49%) and lowest with scenario 2b, 3b and 4 (36.27%).

   As will be explained in further details in section 5.5.3, there are two effects from water in the water drive reservoirs. Firstly, water would trap the gas from reaching the well. Secondly, water that reaches the well is being produced through the well to surfaces. This water causes higher pressure drop in the well and hence higher reservoir abandonment pressure (through higher well's bottomhole flowing pressure). These effects reduce reservoir's recovery efficiency.

   When consider the RF variation, it is found that scenario 1a provides highest RF because of this strategy provides least water production over its perforation sequences. The first perforation is on bottommost reservoir

(reservoir 4), which connected with small aquifer and therefore the water production is small. The next upper reservoir, reservoir 3 can depletes more because of small water production in the well at the time it is open to flow. Also, reservoir 3 will not produce water until majority of gas is produced. The higher well bottomhole pressure which reduces drawdown will takes place upon reservoir 1 & 2 only. Therefore, the RF is highest in this case.

The next case is scenario 1d, where the water producing reservoir will be shut off from well. Noted that this scenario provides slightly lower RF than scenario 1a (1d RF = 49.40%). This is because when the water producing zone is shut off from well, some small part of gas that is flowing with that water is also shut off. Therefore, the RF is slightly lower.

Scenario 1b is the next highest recovery (39.68%). This is because it repeats the patterns of scenario 1a, only to the lesser extent. Instead of allowing each reservoir to be depleted to minimum flow rates before open the next upper reservoir, this scenario open the next reservoir at 10 MMscf/d (half of plateau, 20 MMscf/d). The thick reservoir, where water support is large, is open faster than scenario 1a or 1d (because the reservoir is only half depleted to allow next upper layer to open). As a result, the water reaches the well faster and recovery factor is reduced.

Scenario 1c, and scenario 2 through 4 all shares similar recovery efficiency as their production characteristics is similar. The early opening of big aquifer supported reservoirs, especially the high permeability reservoirs leads to early water breakthrough and high reservoir abandonment pressure (through higher flowing bottomhole pressure), which reduced recovery efficiency drastically. The effect of permeability on recovery efficiency is further investigated in section 5.5.4.

5.5.3 Flow of Gas and Water in the Multilayered Reservoirs

The flow of gas and water in the reservoir has been analyzed on the multilayered reservoirs in order to better understand the mechanism of water drive effect to multilayered reservoirs. Scenario 1a (Open next upper reservoir layer when current reservoir producing less gas and more water) is used in the study.

Pressure and gas saturation along the X-axis of the reservoir has been analysed at various timestep. The time steps are chosen according to flow phenomenon in the reservoir as follows:

a) After 3 days of production. Under perforation scenario 1a, the deepest reservoir (reservoir 4) is opened for 3 days. This time step is chosen as initiation of production.
b) After 42 days of production. At this step the pressure declines at edge of reservoir 4 where aquifer is connected is observed.
c) At 728 days of production. At this step the first water production through well is observed.
d) At 1099 days of production. At this step reservoir 4 is decline below 0.5 MMscf/d limit and reservoir 3 starts its production. The interaction between two reservoir is observed.

Figure 5.6 depicts the reservoir shape along X-axis for reservoirs 3 & 4. Notice that since the well is placed at the middle of reservoirs, the X-Axis extent of reservoir 3 starts from cell number 2 to 31 , where reservoir 4 starts from cell 9 to cell 31.

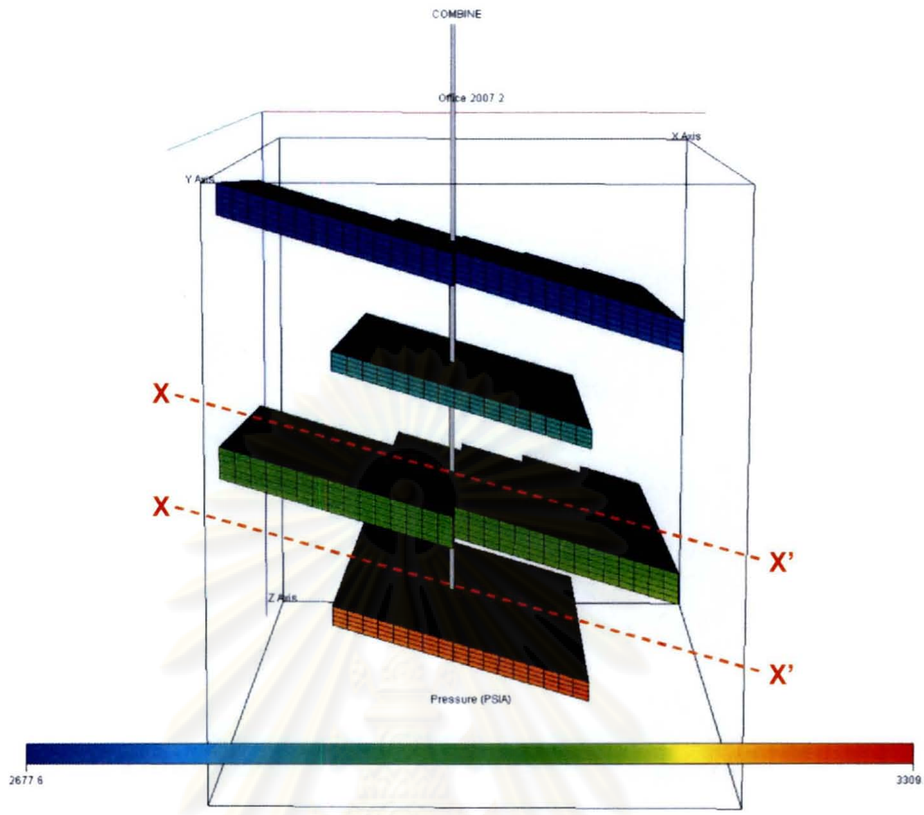

Figure 5.6: Axis for pressure and saturation analysis

Figure 5.7 a) – d) shows the pressure profile and saturation profile along the reservoirs layers. The Y-axis represents pressure, and saturations. The X-axis represents the cell along the X-directions of the reservoirs, the cell number 1 is at updip, and increasing cell number represents location downdip of the reservoirs. At the edge of downdip of reservoirs is where the aquifer is connected.

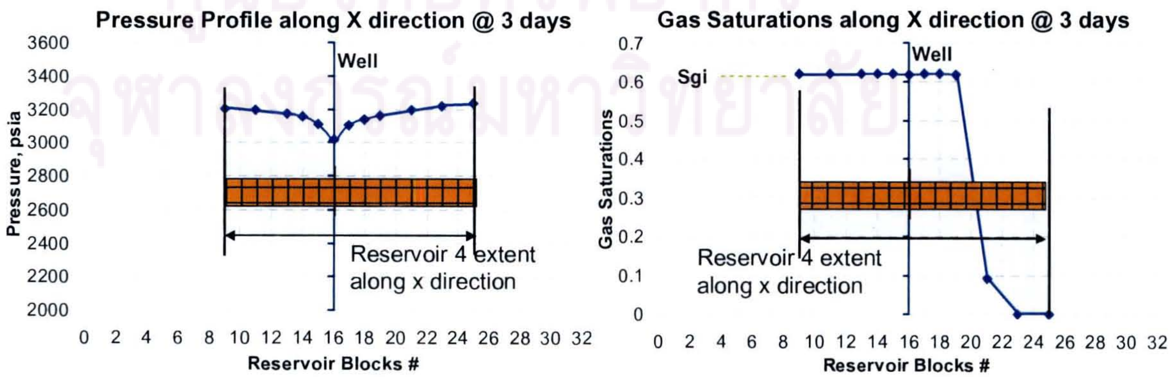

a) at 3 days of Production (Well FBHP = 552.9 psia)

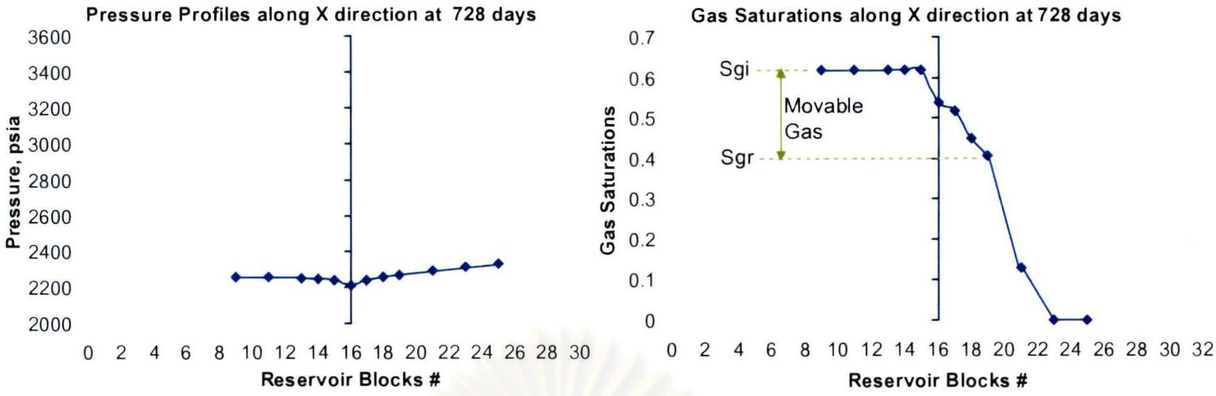

b) at 42 days of Production (well FBHP = 546.6 psia)

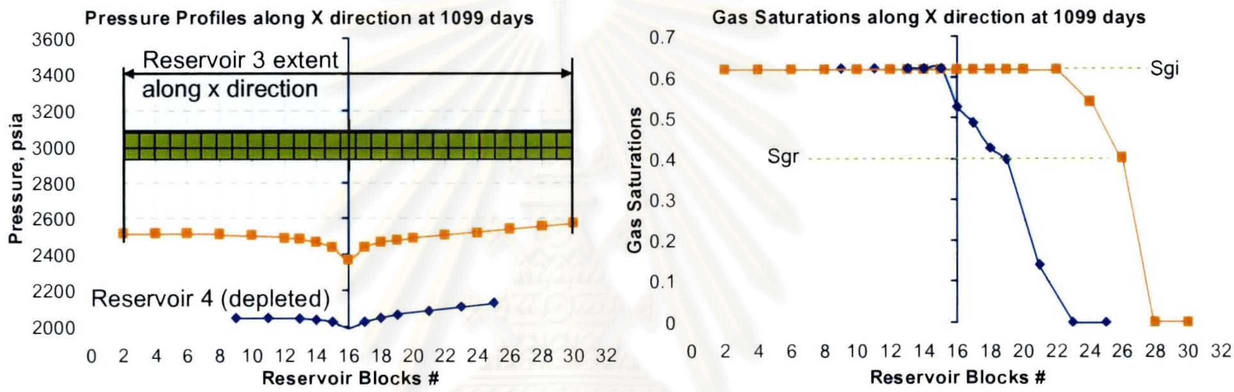

c) at 728 days of Production (well FBHP = 588.60 psia)

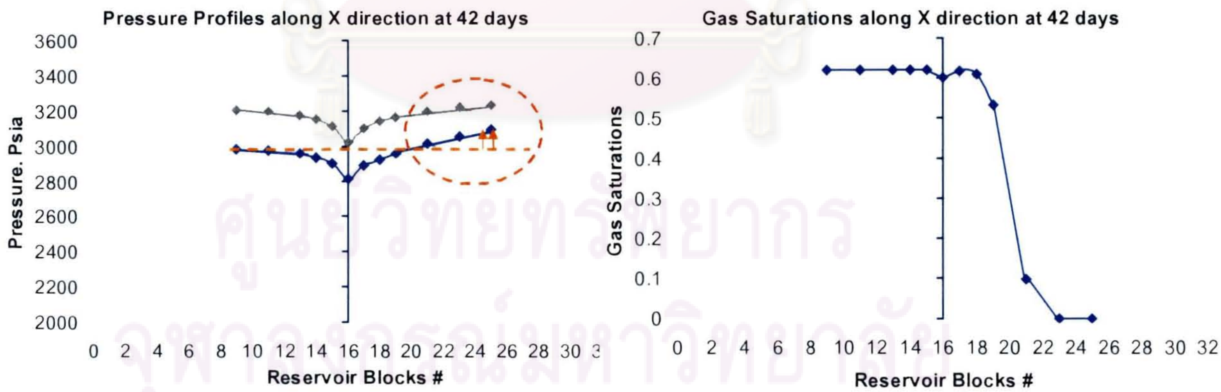

d) at 1099 days of Production (well FBHP = 631.8 psia)

Figure 5.7: a-d) Pressure and Gas saturations along the reservoir at various times

There are 4 timesteps showed to describe the flow behavior in the reservoirs:

a) After 3 days of production (i.e., the time when reservoir 4 flowed for 3 days). This timestep shows the reduction in reservoir pressure as the gas is produced. Water is not expanded yet as the pressure reduction only occurs at near wellbore area.

b) The time when reservoir 4 flowed for 42 days. This timestep shows the reduction in pressure along the reservoir (the gray line represents pressure profile at step a) (3 days), for comparison purpose) to the supporting aquifers. The aquifer expands, and reservoir pressures near them (cell 20-25) gets higher (but not as high as original reservoir pressure). Gas saturation reduced on the downdip side (cell 19-20) as water moves towards the well.

c) The time when reservoir 4 flowed for 728 days. At this timestep the water reaches the well already (as see by reduced gas saturations on wellbore area, cell 16). The reservoir pressure is lowered to around 2200 psia at near wellbore. The water still expands and makes the reservoir pressure at near aquifer side (cell 20-25) higher than no aquifer connection side (cell 9-16).

d) The time when reservoir 4 flowed for 1099 days, and reservoir 3 flowed for 3 days. In this timestep the reservoir 3 is opened to flow. The pressure and gas saturation distribution is similar to reservoir 4 at beginning of production. Except in this case the well's bottomhole flowing pressure is higher than time step b) due to water production from reservoir 4, causing the drawdown on reservoir 3 lesser than if no water is present.

As a summary to the phenomenon observed, the effects of water drive in multilayered reservoirs are two folds: 1; water trapped some gas as it flow towards the well. 2; the water production keeps bottomhole pressure increases, which prevent the wells to produce gas from next layer at full potential.

5.5.4 Factors Effecting Performance of Water Drive in Multilayered Reservoirs

Another study on the mechanism of water drive in multilayered gas reservoirs is the factors affecting the performance of the multilayered reservoirs under water drive. There are 2 parameters that being investigated: The size of aquifers, and the permeability. Table 5.7 shows the %RF of each reservoir in the model under different aquifer size. Table 5.8 shows the %RF of each reservoir in the model under different permeability. For Base Case, the aquifer size is 100 times of the gas in place at reservoir conditions, with the reservoirs permeability of 200 mD in all layers. All other parameters remain unchanged throughout analysis. Scenario 4 (produce from all reservoir together since day1) is used as comparison basis as it provides more insight on how each reservoir contributes to total production.

Table 5.7: Sensitivity on RF on aquifer Size, times of gas in-place at reservoir conditions

	RF (%)		
	Aquifer Size, times of gas in-place		
	50	Base = 100	500
Overall	**54.0%**	**49.2%**	**36.5%**
Reservoir 1	55.0%	47.4%	36.0%
Reservoir 2	51.2%	45.5%	37.7%
Reservoir 3	54.0%	50.3%	35.6%
Reservoir 4	53.3%	54.4%	40.9%

Table 5.8: Sensitivity on RF on reservoir permeability

	RF (%)		
	Reservoir Permeability, mD		
	Base = 200	20	5
Overall	**49.2%**	**33.1%**	**28.2%**
Reservoir 1	47.4%	33.7%	28.5%
Reservoir 2	45.5%	30.0%	26.0%
Reservoir 3	50.3%	34.0%	29.0%
Reservoir 4	54.4%	30.3%	26.3%

In general, the bigger aquifers, the lesser the recovery factors. Because reservoirs 2 and 4 are smaller than reservoirs 1 and 3, their aquifer size is also smaller than reservoir 1 and 3 (because the size of aquifers is relative to reservoir size). This fact makes the change in recovery factors of reservoirs 2 and 4 smaller than change in recovery factors of reservoir 1 and 3.

Despite significant change in Aquifer size, it is found that the highest effect to the recovery performance of the reservoirs lies in the reservoir permeability. Further test is made on permeability to check whether there's threshold where permeability starts to effect recovery performance as found above. The result is shown under table

5.9. At low permeability cases (5 – 100 mD), similar RF are obtained from each reservoirs. At very low permeability (5-20 mD), the RF varies according to reservoir size. RF from reservoir 2 & 4 (same reservoir size) is the same, while RF from reservoir 1 & 3 (same reservoir size) is also the same. At higher permeability, the RF% spread wider between each reservoir.

Table 5.9: Sensitivity on RF for variation in permeability

RF (%)	Reservoir Permeability, mD						
	5	20	50	100	200	500	1000
Overall	**28.2%**	**33.1%**	**40.1%**	**45.2%**	**49.2%**	**52.7%**	**53.0%**
Reservoir 1	28.5%	33.7%	36.8%	42.8%	47.4%	52.1%	50.8%
Reservoir 2	26.0%	30.0%	35.3%	40.3%	45.5%	51.8%	54.2%
Reservoir 3	29.0%	34.0%	43.0%	47.3%	50.3%	52.1%	52.9%
Reservoir 4	26.3%	30.3%	45.0%	49.8%	54.4%	58.2%	59.7%

The result is depicted under Figure 5.8 for overall RF. Note the Sharp change in effect of permeability around 200 mD. Below 200 mD, permeability plays very important role in overall RF. Beyond 200 mD, permeability has relatively small impact to the RF. Further investigation is needed to explain the impact of permeability on overall RF as observed.

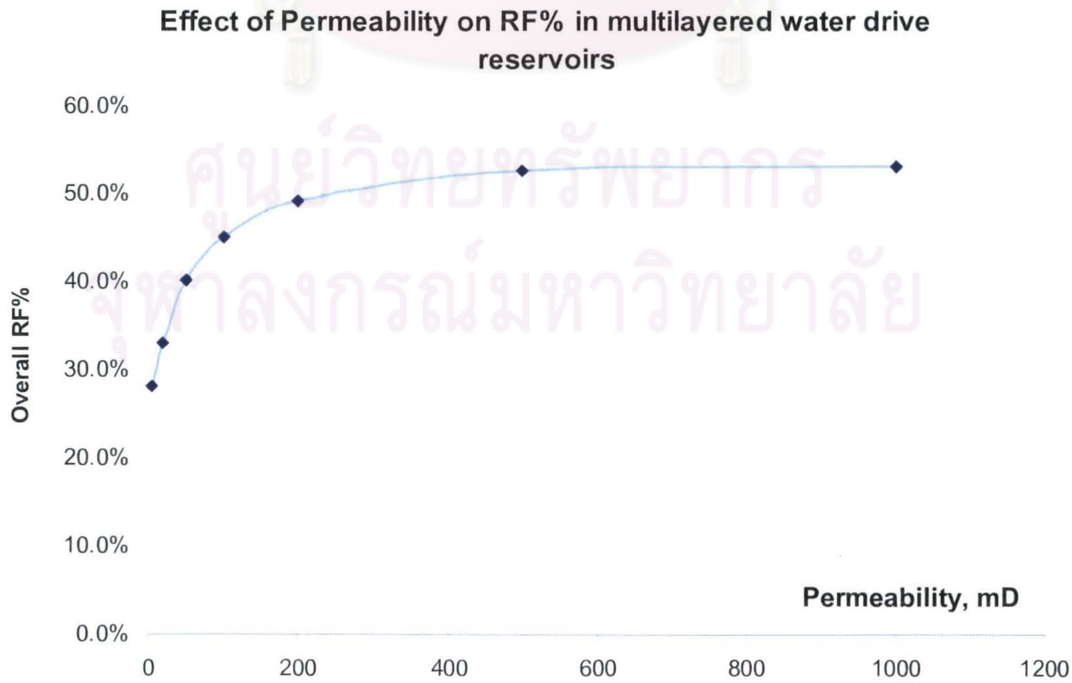

Figure 5.8: Effect of permeability on recovery efficiency in water drive reservoirs

5.5.5 Conclusions on Water Drive Case

Under water drive on all reservoir case, the crossflow is very small in all scenarios and make the issue of less importance. The time to recovery and recovery efficiency is of more concerns.

Scenario 1a (to deplete the reservoir until gas rate is low and water production is high before open next upper reservoir layer) provides highest recovery efficiency, but the time to recovery is the longest. Performing WSO as per scenario 1d did not help improving recovery time either. On the other hand, to open all reservoir to production since day 1 (scenario 4) provide one of the fastest recovery, but the recovery efficiency is low.

Hence, the optimized scenario is to compromise both extremes. This can be achieved by performing early WSO on the producing reservoir once the well's starts to produce significance amount of water. However, the decision on how early such WSO is required (i.e., what is the appropriate level of water production to shut off the zone) is subject to the incremental reserves gain (through allowing the reservoir to produce more water) compared to incremental water production, and the level of prolonged time to recover such reserves. This, in turn, depends on reservoirs characteristics & properties such as permeability, relative permeability to gas and water in the reservoirs, distance from water zone to well, etc. as well as production contribution from updip wells, if any.

An additional case has been investigated to test this concept of early WSO by shutting off the reservoirs when cumulative water production reaches 50% of cumulative water production level observed in scenario 1a (fully depleted). The result shows that Recovery efficiency is increased to 44% with time to reach 30% recovery of 1.39 year, which is much improved from both extreme cases. Therefore, the early WSO of the water producing reservoirs would be the most optimized strategy for water drive reservoirs.

5.6 Mutilayered Reservoir Performance under Combination of Depletion and Water Drive Mechanism

The last case investigated under this study involves multilayered reservoirs where some reservoirs are under depletion drive mechanism and others are under water drive mechanism from connected aquifers. This case is the combination of both case 1 (depletion drive mechanism) and case 2 (water drive mechanism) discussed earlier, and the study result from case 1 and 2 will both be used to explain the results from this case. A separate model is generated for this case. The description of the model is described in next section.

5.6.1 Multilayered Reservoirs under Combination Drive Model Set Up

A new model has been set up for the case. In order to be able to analyze thoroughly, up to 8 reservoirs is created. 4 of the reservoirs are under depletion drive mechanism. Another 4 reservoirs are under water drive mechanism. The reservoir arrangements follow Table 5.10.

Table 5.10: Reservoir arrangements for combination drive model

Reservoir	Size	Permeability	Aquifers connected
1	Thick	200 mD	Yes
2	Thin	200 mD	
3	Thick	20 mD	Yes
4	Thin	20 mD	
5	Thick	200 mD	Yes
6	Thin	200 mD	
7	Thick	20 mD	Yes
8	Thin	20 mD	

Under the 8 reservoirs study model, the OGIP is increased to 60 BCF. Single well approach is still used despite higher OGIP because of the ease on the analysis and improved focus to the effect of recovery mechanism. Based on case 2 study results, the effect of water is more on the thick reservoirs (as the aquifer is bigger), therefore, all the thick reservoirs (reservoirs 1, 3, 5, and 7) are modeled to be connected with supporting aquifer. The aquifer size is 100 times of the gas reservoir size similar to case 2. Fig 5.9 shows the shape and pressure distribution along the reservoirs. Fig 5.10 shows the gas saturations on the reservoirs.

With the modeled arrangement of reservoirs, there are some implications to the production/perforation scenarios. On the scenario 3 where the perforation scenarios are based on type of reservoirs (thick and thin reservoirs), another implications is that this set of scenario is based on drive mechanism, since thick reservoirs are all water drive, and thin reservoirs are depletion drive. Therefore:

Scenario 3a = thick reservoir first = water drive first.

Scenario 3b = thin reservoir first = depletion drive first.

This implication is important because the impact of different drive mechanism can be studied by this set of scenario.

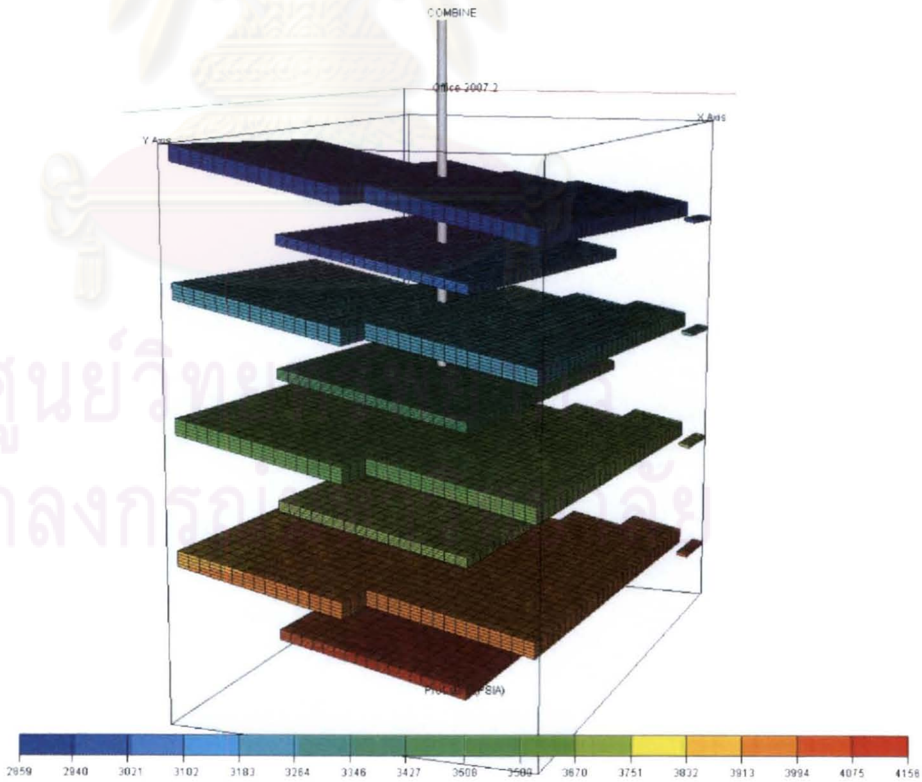

Figure 5.9: Model shape and pressure distribution for combination drive model

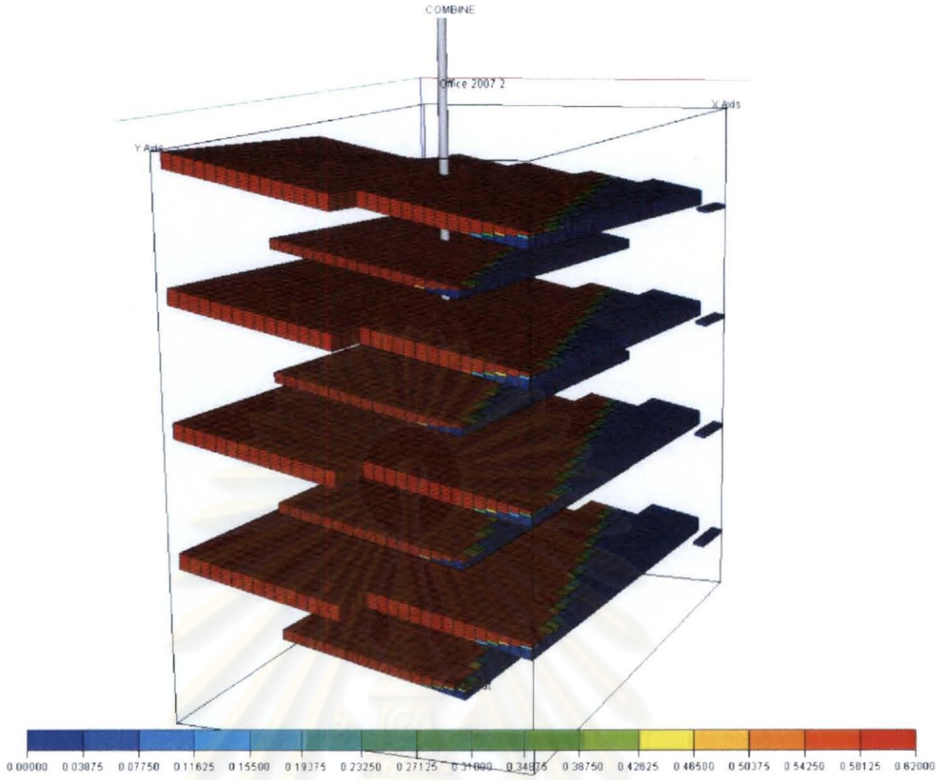

Figure 5.10: Gas saturations for combination drive model

5.6.2 Simulation Results for Multilayered Reservoir Performance under Combination Drive

Table 5.11 listed the simulation results for this case.

Table 5.11: Combination drives case simulation results

Scenario	Description	Crossflow (% OGIP)	Time to recover crossflow vol. (days)	Time (years) to reach % recovery		RF (%)
				40%	Ultimate	
1. Bottom-Up						
1a	Fully depleted	2.66	Infinite	12.81	18.69	55.14
1b	Half depleted	3.01	Infinite	5.30	20.91	52.96
1c	Maintain plateau	2.57	Infinite	4.06	5.69	51.66
1d	WSO	---	---	14.89	21.36	60.61
2. Permeability selective						
2a	High perm. first	1.06	Infinite	4.06	6.60	52.75
2b	Low perm. first	0.62	Infinite	4.06	6.02	52.22
3. Reservoir size selective = Drive Mechanism selective						
3a	Thick (Water drive) reservoirs first	2.05	Infinite	4.06	6.54	51.13
3b	Thin (Depletion drive) reservoirs first	2.63	Infinite	4.06	6.06	52.56
4	Produce all since day 1	0.44	Infinite	4.06	5.58	50.74

The following are observed from the table:

1. The level of crossflow is in a range of none to 3.11%. The level of crossflow is relatively higher than depletion drive case, which is in range of 0.01%- 2.46%. The crossflow in this case is also higher than water drive case where crossflow is minimal (none to 0.09%). The reason for increase

crossflow is due to different drive mechanism, as evidenced by two earlier cases.

The extent of crossflow depends on two factors as discussed in section 5.4.1:

- The pressure difference between the well's bottomhole flowing pressure and reservoir pressure.
- The reservoirs' rock and fluid properties.

Based on these two factors, the depletion drive reservoir are more susceptible to crossflow as their pressure declines upon depletion process, without aquifer support. While for water drive reservoir their pressure declines is partly supported by expansion of aquifers. For depletion drive reservoir in combination with high injectivity index, such as the reservoir with high permeability (reservoirs 2 and 6) the situation is worse. As seen in table 5.12, within single reservoir their crossflow can be as high as 40% of their OGIP.

Table 5.12: % Crossflow by reservoir and scenarios

Size	k, mD	Drive mech.	#	1a	1b	1c	1d	2a	2b	3a	3b	4
				Bottom-Up				High k first	Low k first	Water drive First	Depleti -on drive first	Produc e all from day 1
				fully deplete	half deplete	maintain plateau	WSO					
Overall				**2.7%**	**3.0%**	**2.6%**		**1.1%**	**0.6%**	**2.0%**	**2.6%**	**0.4%**
Thick	200	Water	1			1%		1%	2%	7%		2%
Thin	200	Depletion	2	3%	6%	9%		9%	2%	3%	30%	1%
Thick	20	Water	3									
Thin	20	Depletion	4	1%					2%			
Thick	200	Water	5		3%					3%		
Thin	200	Depletion	6	40%	39%	8%		8%	2%	3%	24%	
Thick	20	Water	7									
Thin	20	Depletion	8	6%								

On the topmost reservoir (reservoir 1), crossflow occurs despite the reservoir is water drive. This is because of the pressure difference between well's bottomhole flowing pressure and reservoir pressure at the time the reservoir is open to flow. As the topmost reservoir is shallowest, its initial pressure (hydrostatic) is lowest among other reservoirs. Depending on each scenario, the reservoir has some crossflow effects.

Another point to be highlight is the effect of different drive mechanism on crossflow. Where the water drive is allowed to produce first, followed by depletion drive (scenario 3a), the crossflow are small on depletion drive reservoir. On the contrary, where depletion drive is allowed to produce first, followed by water drive (scenario 3b) the crossflow is high on depletion drive reservoir.

Table 5.13: Water production (as % of their OGIP) by reservoir and scenarios

Size	k, mD	Drive mech.	#	1a	1b	1c	1d	2	3	4	5	6
				Bottom Up				High k first	Low k first	Water drive First	Depleti-on drive first	Produce all from day 1
				fully deplete	half deplete	maintain plateau	WSO					
Overall				**5%**	**2%**	**1%**	**0%**	**2%**	**1%**	**2%**	**1%**	**1%**
Thick	200	Water	1					2%		1%		
Thin	200	Depletion	2					-1%	-1%	-1%	-1%	
Thick	20	Water	3									
Thin	20	Depletion	4									
Thick	200	Water	5	15%	6%	6%	1%	11%	5%	7%	7%	4%
Thin	200	Depletion	6	-5%				-2%	-1%	-1%	-1%	
Thick	20	Water	7	10%	2%	1%		1%	1%	1%	1%	
Thin	20	Depletion	8									

On the water production aspects, Table 5.13 highlights the water production by reservoirs as a percentage of their OGIP. The yellow cells shows high water production reservoirs while the red value highlight the crossflow of water from wells into the reservoirs. It is found that the high permeability, water drive reservoirs contributes highest water production. Part of this water produced is crossflowed into the high permeability, depletion drive reservoirs (as shown by negative sign). The water production occurs more on the lower side of the model (reservoirs 5 and 7) than upper side. This is contribution from the higher aquifer pressure (according to hydrostatic pressure) at the lower part of the reservoirs.

2. The time to recover crossflowed volume is infinite for all cases except scenario 1d (WSO). Unlike the depletion drive case, the crossflow becomes more difficult to recover in this case because higher flowing bottomhole pressure exists in all cases (except scenario 1d).
   Again, it is to be noted that the unable to recover (infinite) indicated in the table does not means that all crossflowed volume is lost in the reservoirs but rather means that only some part of the crossflowed volume can be recovered (but not all of them).
3. The RF lies in range of 50.74% to 60.61% in this case. The RF is relatively higher than water drive case (36.27% vs. 50.49%) but lower than depletion drive case (76.79% vs. 80.47%). Table 5.14 highlight the RF by reservoirs.

Table 5.14: Recovery Factor (%) by reservoirs and scenarios

Size	k, mD	Drive mech.	#	1a	1b	1c	1d	2	3	4	5	6
				Bottom Up				High k first	Low k first	Water drive First	Depleti -on drive first	Produc e all from day 1
				fully deplete	half deplete	maintain plateau	WSO					
Overall				**55%**	**53%**	**52%**	**61%**	**53%**	**52%**	**51%**	**53%**	**51%**
Thick	200	Water	1	54%	60%	63%	73%	63%	63%	61%	63%	62%
Thin	200	Depletion	2	58%	61%	61%	81%	56%	60%	56%	59%	61%
Thick	20	Water	3	43%	36%	35%	48%	42%	40%	41%	41%	36%
Thin	20	Depletion	4	52%	49%	48%	51%	50%	51%	45%	51%	48%
Thick	200	Water	5	70%	68%	64%	72%	64%	63%	62%	63%	62%
Thin	200	Depletion	6	60%	61%	63%	84%	60%	64%	60%	63%	65%
Thick	20	Water	7	49%	45%	42%	46%	42%	41%	42%	42%	40%
Thin	20	Depletion	8	63%	57%	51%	52%	50%	51%	45%	51%	48%

From the table, the yellow rows are the reservoir with water drive, and white rows are the reservoirs with depletion drive. In general, the RF from depletion drive reservoirs are higher than water drive reservoir as expected. There is no significant difference in RF among each scenario with the exception of WSO scenario (scenario 1d). It can be seen that water shut off has an outstanding advantage in terms of RF improvement by improving the RF of depletion drive reservoirs from 60% to 80% for reservoirs that their RF are hindered by water production from water drive reservoirs.

5.6.3 Conclusion on Combination Drive Case

Under combination drive case, Table 5.15 listed the optimal solution to each issue of concerns. The marks are for scenarios that provide best results for each monitoring parameters.

Table 5.15: Best scenario categorized by issues related to optimal production

Monitoring Parameters	1a	1b	1c	1d	2a	2b	3a	3b	4
	Bottom Up				High k first	Low k first	Water drive First	Depleti -on drive first	Produc e all from day 1
	fully deplete	half deplete	maintain plateau	WSO					
Crossflow				✓					
Time to recovery			✓		✓	✓	✓	✓	✓
Recovery efficiency				✓					

There are two sides of scenario to be compromised. WSO scenario provides favorable solution to the crossflow and recovery efficiency, while other maintaining production scenarios (scenario 1c, and 2 to 4) provides fastest time to recovery.

To compromise between two extremes, the optimal perforation/ production strategy must:-

1. Producing depletion drive without interference of water production.
2. Producing water drive without effect of crossflow into depleted reservoirs.

Therefore, additional scenario is created, using knowledge from the two previous cases to provide insight. This scenario will start by:

1. Producing from depletion drive reservoirs in commingled production until all reservoirs is fully depleted.
2. Then shut-off all depletion drive zones.
3. Produced from water zones, all at once. Early production would provide small amount of water production.
4. WSO on zones which produces half of their expected water production.

The result is as following:

Crossflow: 0.1%

Time to recovery: 8.1 years

RF: 56%

Which is closer to the maximum RF of 62% and time to recovery closer to the minimum time of 4 years (rather than 15 years). The crossflow is also minimal. The case is not a best practice to apply on all other reservoir model in GoT, but it provides general guidelines to achieve optimal solution that can be further developed for specific reservoir of interest.

5.7 Discussions

Based on the study results, it is found that the optimal production strategy varies with drive mechanism.

- For reservoir under depletion drive mechanism, to produce from all reservoirs altogether since day1 would provide optimal result.
- For water drive reservoirs, to produce from all layer altogether, and perform early WSO on water producing zone would provide an optimal results.
- For combination drive reservoirs, to produce from depletion drive layers altogether, shut off the depleted zones, start producing water drive layers and perform early WSO on water producing zone would provide optimal results.

While the solution for depletion drive multilayered reservoirs is obvious, there are a number of items to be discussed on water drive and combination drive reservoirs.

For water drive multilayered reservoirs, there would be an issue of how early WSO should there be in order to reach optimal strategy. The earlier the WSO:

1. More gas is trapped behind in shut off reservoirs. The RF is less.
2. Other reservoirs can produce with lower abandonment pressure because of water producing reservoirs is shut off. The RF is higher.

As a result, how early WSO should be will be a tradeoff between 1 and 2. The answer is subject to specific reservoirs rather than generic since different rock and fluid properties as well as different reservoir geometry would bring difference optimal point.

Under combination drive mechanism, in addition to issue faced with water drive reservoirs, to deplete the depletion drive reservoir first and shutoff the depletion drive zone prior to produce water drive zone would not be practical if there are many depletion drive reservoirs. Therefore, to produce the water drive reservoirs first and early WSO on these reservoirs once they start producing water, then produce from all depletion drive reservoirs altogether would be optimal solution in this case. Vice versa, if there are a number of water drive reservoirs while only few numbers of depletion drive reservoirs, it may be more practical to produce from depletion drive first and shut them off before open the water drive reservoirs.

Under combination drive reservoirs, it is suggested that one should not try to produce from both drive mechanism altogether because it is difficult to know the strength of aquifer drive when production from these reservoir starts. If the aquifer is strong enough as appear to be in study case, the pressure support from the aquifer of these reservoirs would eventually results in crossflow to the depletion drive reservoirs under production.

CHAPTER VI

CONCLUSIONS

This chapter presents the conclusions of the effect of various production/ perforation scenarios over the different types of reservoir drive mechanism for the gas field in the Gulf of Thailand (GoT). The simulation results and the recommendation for future works are outlined.

The reservoir model is built using single well model, based on simplified versions of bar and channel sands that matched original bar and channel reservoirs. Under the model, the channel sand is used as representative of reservoir sands that is thick, continuous and mostly connected with aquifers. The bar sand is used as representative of small, thin sand encountered in the GoT. The model is consisted of 4 reservoirs with equal share of thin and thick reservoirs.

There are 3 major cases in this study. The first case is where all 4 reservoirs in the model are under depletion drive mechanism. The second case is where all 4 reservoirs in the model are under water drive mechanism. The aquifer is set to have the size of 100 times of each reservoir's OGIP. The last case consisted of 8 reservoirs, 4 of them under depletion drive and others of water drive.

In total, 6 main production/ perforation scenarios are put in to study on each of the cases as follows:

1. Bottom-Up production: This scenario produce from deepest reservoirs first followed by the next upper layer one by one. It allows the plugging or patching on the depleted reservoirs without problem on the next producing layers (because the depleted layer(s) are deeper). This method is common practice of the gas field in the GoT.

   In this study there are three criteria to trigger the opening of next upper layers:

   a. Fully depleted. This criterion allows the current producing layer to fully deplete (i.e., reach minimum possible flow of 0.5 MMscf/d) first then open the next layers.
   b. Half depleted. This criterion allows the next upper layer to open whenever the flow from current layer drops below 10 MMscf/d.

c. Maintain production: This criterion opens the next reservoirs layer once the production from current layers drops below 20 MMscf/d.

d. Water shut off: To shut the wells once the reservoir is fully depleted and more water produced to avoid further water production from that reservoir before open the next upper reservoirs.

2a. Produce from high permeability reservoirs first (reservoir 1 & 2).

2b. Produce from low permeability reservoir first (reservoir 3 & 4).

3a. Produce from thick reservoirs first (reservoir 1 & 3).

3b. Produce from thin reservoirs first (reservoir 2 & 4).

4. Produce from every reservoir together since day 1.

From scenario 2 through 4, the criterion to open the next layer is the production maintaining criteria similar to case 1C.

The result is then compared in terms of percentage of cross-flow from one reservoir to another through wells, time to reach certain recovery limits, and recovery efficiency.

Based on the study results, the result can be summarized as follows:

1. The incident of crossflow through well in multilayered gas reservoirs depends on two major factors, one is the difference between reservoir pressure and well bottomhole flowing pressure. Another factor is the reservoir's rock and fluid properties itself. The incident in general fits with the Darcy's equation.
2. The active aquifer creates two effects in the multilayered reservoirs. One is that the aquifers, as it expands through lowering reservoir pressure, traps the gas behind and reduce gas recovery. Another factor is that once the water breakthrough at the well, the pressure drop in well increases. The bottomhole flowing pressure increases and the drawdown is reduced for all reservoirs put into production. The first phenomenon affects individual reservoirs while the second phenomenon affects all reservoirs. The second phenomenon creates difference in recovery efficiency for each perforation/production scenarios studied.
3. Permeability plays an important role in gas – water flows through reservoirs as it has direct effect on recovery efficiency. It is found that

permeability will have less effect on recovery efficiency once the reservoir permeability is above 200 mD.

4. Under depletion drive reservoirs, to put all reservoirs to production since day 1 (scenario 4) would provide optimal solution to the depletion drive multilayered reservoirs case. The crossflowed volume is small, the RF is similar to other scenario, and the time to recovery is among the fastest. Commingled production also have other practical benefit such as reducing well intervention (i.e., to perforate others reservoirs) and reduce the chance of tool stuck or fishing.
5. Under water drive reservoirs, to produce from bottom up by allowing each reservoir to be fully depleted before open another provides highest recovery efficiency, but the time to recovery is the longest. On the other hand, to produce from all reservoirs together since day 1 provides one of the fastest recoveries, but the recovery efficiency is low. Hence, the optimized scenario is to compromise both extremes. This can be achieved by performing early WSO on the producing reservoir once the well's starts to produce significance amount of water.
6. Under water drive reservoirs, the decision on how early such WSO is required (i.e., what is the appropriate level of water production to shut off the zone) is subject to the incremental reserves gain compared to incremental water production, and the level of prolonged time to recover such reserves. This in turns depends on reservoirs characteristics & properties such as permeability, relative permeability of the gas and waters in the reservoirs, distance from water zone to well, etc
7. Under combination drive reservoirs, the observations from both depletion drive and water drive reservoirs are valid.
8. The optimized solution for combination drive reservoirs would be to separate the production between depletion drive reservoirs and the water drive reservoirs. The WSO need to be performed on reservoirs where water production becomes excessive.

References

[1] Arianto, M.A., Susatyo, Y., Srisantoso B. and Sumaryanto, New Completion Solution for Multilayer Gas Fields – A Case History, SPE 10991 presented at at the 2006 SPE Asia Pacific Oil & Gas Conference and Exhibition, Adelaide, Australia, 11–13 September 2006.

[2] Al-Sheri D.A., Rabaa, A.S., Duenas, J.J. and Ramanathan, V, Commingled Production Experience of Multilayer Gas Carbonate reservoirs In Saudi Arabia, SPE 97073 presented at the 2005 SPE Annual Technical Conference and Exhibition, Dallas, Texas, U.S.A., 9 – 12 October 2005.

[3] Fetcovich, M.J., Bradley, M.D., Works, A.M. and Thrasher, T.S., Depletion Performance of the Layered Reservoirs without crossflow, SPE Formation Evaluation paper 18266 first presented at SPE Annual Technical Conferences and Exhibition, Houston, Texas, U.S.A., 2-5 October 1988.

[4] Raghavan, R.: Behavior of wells completed in multiple producing zones, SPE Formation Evaluation paper 14111 presented at SPE International Meeting on Petroleum Engineering, Beijing, People's Republic of China., 13-17 June 1989.

[5] Sangsoo, R., Frantz, J.H. Junior and Lee,W.J., New, Simplified Methods for Modeling Multilayered Reservoirs Performing at Pseudo-Steady State, SPE26831 presented at SPE 69th Annual Tecnhical Conference and Exhibition, New Orleans, LA, U.S.A., 25-28 September 1994.

[6] Gangdan, F., Zhenfeng, Z., Fenzia, Z., Jie, G., Changhao, Y. and Yong, R., A New Completion Technology with Separate Layer Fracturing and Commingled Producing in Gas Field, SPE 104444 presented at 2006 SPE International Meeting on Petroleum Engineering, Beijing, People's Republic of China, 5-7 December 2006.

[7] Jiraratwaro, K., Optimizing Commingled Production Strategy Using Integrated Production Model, Department of Mining and Petroleum Engineering, Faculty of Engineering, Chulalongkorn University, Academic year 2006.

[8] Thirawarapan, C., Buranarachada, D. and Suthipintawong T., Investigation of Partial Perforation Practice in Commingled Gas Production from a Field in the Gulf of Thailand, Department of Mining and Petroleum Engineering, Faculty of Engineering, Chulalongkorn University, Academic year 2005.

[9] Kiatrabile, T., Cheewarunothai, N. and Chutanugarn, D., Production Guidelines for Multilayered Reservoirs, Department of Mining and Petroleum Engineering, Faculty of Engineering, Chulalongkorn University, Academic year 2004.

[10] Panichakul, R., Reserve Evaluation for Multi-Layered Gas Reservoirs Using Material Balance Methods, Department of Mining and Petroleum Engineering, Faculty of Engineering, Chulalongkorn University, Academic year 1997.

[11] Craft, B.C., Hawkins, M.F., Applied Petroleum Reservoir Engineering, New Jersey, U.S.A., Prentice-Hall, 1991.

APPENDICES

APPENDIX A

A1. ECLIPSE definition for simplified model of Bar Sand Reservoirs

a) CASE DEFINITION

```
Simulator:                      Black Oil
Model Dimensions:               Number of cells in the x direction  15
                                Number of cells in the y direction  45
                                Number of cells in the z direction: 4
Grid type:                      Corner Point
Geometry type:                  Block Centered
Oil-Gas-Water Options:          Water, Gas
```

b) GRID

```
X Grid Block Size:              219 ft
Y Grid Block Size:              201 ft
Inclination Angle in X:         10 ft/ 100 ft
Inclination Angle in Y:         2 ft /100 ft
Depth of Top face:              6,206 ft
Shallowest Cell Coordination: 1, 34
```

	# cells in z	Thickness (ft) / layer	ϕ (%)	NTG	k-x (mD)	k-y (mD)	k-z (mD)
Bar Sand Reservoirs	4	15.4	21%	0.25	100	100	10

ACTNUM

	X1	X2	X3	X4	X5	X6	X7	X8	X9	X10	X11	X12	X13	X14	X15
Y1	0	0	0	0	0	1	1	0	0	0	0	0	0	0	0
Y2	0	0	0	0	0	1	1	0	0	0	0	0	0	0	0
Y3	0	0	0	0	1	1	0	0	0	0	0	0	0	0	0
Y4	0	0	0	0	1	1	1	1	0	0	0	0	0	0	0
Y5	0	0	0	0	1	1	1	1	0	0	0	0	0	0	0
Y6	0	0	0	1	1	1	1	1	0	0	0	0	0	0	0
Y7	0	0	0	1	1	0	0	1	0	0	0	0	0	0	0
Y8	0	0	0	1	1	0	0	1	1	0	0	0	0	0	0
Y9	0	0	0	1	1	0	0	0	0	0	0	0	0	0	0
Y10	0	0	1	1	1	1	0	1	1	0	0	0	0	0	0
Y11	0	0	1	1	1	1	1	1	1	1	0	0	0	0	0
Y12	0	0	1	1	1	1	0	1	1	1	0	0	0	0	0
Y13	0	0	1	1	1	0	0	1	1	1	0	0	0	0	0
Y14	0	1	1	1	1	1	1	1	1	1	0	0	0	0	0
Y15	0	1	1	1	1	1	1	1	1	1	0	0	0	0	0
Y16	0	1	1	1	1	1	1	1	1	1	1	0	0	0	0
Y17	0	1	1	1	1	1	1	1	1	1	1	0	0	0	0
Y18	0	1	1	1	1	1	1	1	1	1	1	0	0	0	0
Y19	0	1	1	1	1	1	1	1	1	1	1	0	0	0	0
Y20	0	1	1	1	1	1	1	1	1	1	1	0	0	0	0
Y21	0	1	1	1	1	1	1	1	1	1	1	0	0	0	0
Y22	0	1	1	0	0	1	1	1	1	1	1	0	0	0	0
Y23	0	1	1	0	1	1	1	1	1	1	1	0	0	0	0
Y24	0	1	1	1	1	1	1	1	1	1	1	0	0	0	0
Y25	0	1	1	1	1	1	1	1	1	1	1	0	0	0	0
Y26	0	1	1	1	1	1	1	1	1	1	1	0	0	0	0
Y27	0	1	1	1	1	1	0	1	1	1	1	0	0	0	0
Y28	0	1	0	0	0	1	1	1	1	1	1	0	0	0	0
Y29	0	1	1	0	0	1	0	1	1	1	0	0	0	0	0
Y30	0	1	1	1	0	0	0	0	1	1	0	0	0	0	0
Y31	0	1	1	1	0	0	0	0	0	1	0	0	0	0	0
Y32	0	1	1	1	1	1	1	0	1	1	1	0	0	0	0
Y33	0	0	1	1	1	1	0	1	1	1	1	0	0	0	0
Y34	0	0	1	1	1	1	0	1	1	1	1	0	0	0	0
Y35	0	0	0	0	0	0	0	0	0	0	0	0	0	0	0
Y36	0	0	0	0	0	0	0	0	0	0	0	0	0	0	0
Y37	0	0	0	0	0	0	0	0	0	0	0	0	0	0	0
Y38	0	0	0	0	0	0	0	0	0	0	0	0	0	0	0
Y39	0	0	0	0	0	0	0	0	0	0	0	0	0	0	0
Y40	0	0	0	0	0	0	0	0	0	0	0	0	0	0	0
Y41	0	0	0	0	0	0	0	0	0	0	0	0	0	0	0
Y42	0	0	0	0	0	0	0	0	0	0	0	0	0	0	0
Y43	0	0	0	0	0	0	0	0	0	0	0	0	0	0	0
Y44	0	0	0	0	0	0	0	0	0	0	0	0	0	0	0
Y45	0	0	0	0	0	0	0	0	0	0	0	0	0	0	0

c) PVT

Bar			
Water PVT Properties	Reference pressure(Pref)	4652.5	psia
	Water FVF at Pref	1.0636	rb/stb
	Water viscosity at Pref	0.1907	cp
	Water viscosibility	9.22 E-06	/psi
Fluid Densities at Surface Conditions	Oil density	48.4 (50 °API)	lb/ft^3
	Water density	62.43	lb/ft^3
	Gas density	0.060	lb/ft^3
Rock Properties	Reference Pressure	4230	psia
	Rock Compressibility	5.4029E-6	/psi

d) SCAL

Upper & Lower Bar		
Sw	K_{rg}	K_{rw}
0.4000	1.0000	0.0000
0.4411	0.5549	0.0040
0.4822	0.2846	0.0183
0.5233	0.1317	0.0446
0.5644	0.0529	0.0840
0.6056	0.0173	0.1372
0.6467	0.0041	0.2049
0.6878	0.0005	0.2876
0.7289	0.0000	0.3859
0.7700	0.0000	0.5000
1.0000	0.0000	1.0000

e) INIT

	Ref Depth (ft)	Ref Pressure (psia)	GWC (ft)
Bar Sand Reservoirs	6200	2684.6	6639

f) SCHEDULE

Well	Bar 1
I,J Location	2, 32
Primary Control	Gas Rate
Secondary Control	THP
Primary Target	20 MMscfd
Secondary Target	30 Barg
Well Economic Limit	0.1 MMscfd
Max WGR Limit	1,000,000 STB/ Mscf

Production Starts: 1^{st} Jan 2009
Production Ends: 23^{rd} June 2039
Report Steps: 7 days

A2. ECLIPSE definition for simplified model of Channel Sand Reservoirs

a) CASE DEFINITION

Simulator: Black Oil
Model Dimensions: Number of cells in the x direction 15
Number of cells in the y direction 45
Number of cells in the z direction: 5
Grid type: Corner Point
Geometry type: Block Centered
Oil-Gas-Water Options: Water, Gas

b) GRID

X Grid Block Size: 219 ft
Y Grid Block Size: 201 ft
Inclination Angle in X: 10 ft/ 100 ft
Inclination Angle in Y: 2 ft /100 ft
Depth of Top face: 6,206 ft
Shallowest Cell Coordination: 1, 34

	# cells in z	Thickness (ft)/ layer	ϕ (%)	NTG	k-x (mD)	k-y (mD)	k-z (mD)
Channel Sand Reservoirs	5	18.9	21%	0.4	80	80	8

ACTNUM

	X1	X2	X3	X4	X5	X6	X7	X8	X9	X10	X11	X12	X13	X14	X15
Y1	0	0	0	0	0	0	0	0	0	0	0	0	0	0	0
Y2	0	0	0	0	0	0	0	0	0	0	0	0	0	0	0
Y3	0	0	0	0	0	0	0	0	0	0	0	0	0	0	0
Y4	0	0	0	0	0	0	0	0	0	0	0	0	0	0	0
Y5	0	0	0	0	0	0	0	0	0	0	0	0	0	0	0
Y6	0	0	0	0	0	0	0	0	0	0	0	0	0	0	0
Y7	0	0	0	0	0	0	0	0	0	0	0	0	0	0	0
Y8	0	0	0	0	0	0	0	0	0	0	0	0	0	0	0
Y9	0	0	0	0	0	0	0	0	0	0	0	0	0	0	0
Y10	0	0	0	0	0	0	0	0	0	0	1	0	0	0	0
Y11	0	0	0	0	0	0	0	0	0	1	1	0	0	0	0
Y12	0	0	0	0	0	0	0	0	1	1	1	0	0	0	0
Y13	0	0	0	0	0	0	0	1	1	1	1	0	0	0	0
Y14	0	0	0	0	0	0	0	1	1	1	1	0	0	0	0
Y15	0	0	1	0	0	1	1	1	1	1	1	0	0	0	0
Y16	0	0	1	1	1	1	1	1	1	1	1	0	0	0	0
Y17	0	0	0	1	1	1	1	1	1	1	1	0	0	0	0
Y18	0	0	0	1	1	1	1	1	1	1	1	0	0	0	0
Y19	0	0	0	0	1	1	1	1	1	1	1	0	0	0	0
Y20	0	0	0	0	1	1	1	0	0	0	0	0	0	0	0
Y21	0	0	0	1	1	1	1	0	0	0	0	0	0	0	0
Y22	0	1	0	1	1	1	1	1	0	0	0	0	0	0	0
Y23	0	1	0	0	1	1	1	1	0	0	0	0	0	0	0
Y24	0	1	0	0	1	1	1	1	0	0	0	0	0	0	0
Y25	0	1	0	0	1	1	1	1	0	0	0	0	0	0	0
Y26	0	1	0	1	1	1	1	0	0	0	0	0	0	0	0
Y27	0	1	0	1	1	1	1	0	0	0	0	0	0	0	0
Y28	0	1	1	1	1	1	0	0	0	0	0	0	0	0	0
Y29	0	0	1	1	1	0	0	0	0	0	0	0	0	0	0
Y30	0	0	1	1	0	0	0	0	0	0	0	0	0	0	0
Y31	0	0	1	1	1	0	0	0	0	0	0	0	0	0	0
Y32	0	1	1	1	1	1	0	0	0	0	0	0	0	0	0
Y33	0	1	1	1	0	0	0	0	0	0	0	0	0	0	0
Y34	0	1	1	0	0	0	0	0	0	0	0	0	0	0	0
Y35	0	1	1	0	1	1	0	0	0	0	0	0	0	0	0
Y36	0	1	1	1	1	0	0	0	0	0	0	0	0	0	0
Y37	0	1	1	1	1	0	0	0	0	0	0	0	0	0	0
Y38	0	0	1	1	0	0	0	0	0	0	0	0	0	0	0
Y39	0	0	1	1	0	0	0	0	0	0	0	0	0	0	0
Y40	0	0	1	1	0	0	0	0	0	0	0	0	0	0	0
Y41	0	1	1	1	0	0	0	0	0	0	0	0	0	0	0
Y42	0	1	1	1	0	0	0	0	0	0	0	0	0	0	0
Y43	0	1	1	1	0	0	0	0	0	0	0	0	0	0	0
Y44	0	0	1	1	0	0	0	0	0	0	0	0	0	0	0
Y45	0	0	0	1	0	0	0	0	0	0	0	0	0	0	0

c) PVT

Channel			
Water PVT Properties	Reference pressure(Pref)	3349	psia
	Water FVF at Pref	1.0897	rb/stb
	Water viscosity at Pref	0.1601	cp
	Water viscosibility	1.00 E-05	/psi
Fluid Densities at Surface Conditions	Oil density	48.4 (50 °API)	lb/ft^3
	Water density	62.43	lb/ft^3
	Gas density	0.068	lb/ft^3
Rock Properties	Reference Pressure	3349	psia
	Rock Compressibility	5.4092E-6	/psi

d) SCAL

Upper & Lower Channel		
Sw	K_{rg}	K_{rw}
0.3800	1.0000	0.0000
0.4233	0.5549	0.0040
0.4667	0.2846	0.0183
0.5100	0.1317	0.0446
0.5533	0.0529	0.0840
0.5967	0.0173	0.1372
0.6400	0.0041	0.2049
0.6833	0.0005	0.2876
0.7267	0.0000	0.3859
0.7700	0.0000	0.5000
1.0000	0.0000	1.0000

e) INIT

	Ref Depth (ft)	Ref Pressure (psia)	GWC (ft)
Channel Sand Reservoirs	6200	2684.6	7110

f) SCHEDULE

Well	Channel 1
I,J Location	2, 34
Primary Control	Gas Rate
Secondary Control	THP
Primary Target	20 MMscf/d
Secondary Target	30 Barg
Well Economic Limit	0.1 MMscf/d
Max WGR Limit	1,000,000 STB/ Mscf

Production Starts: 1st Jan 2009

Production Ends: 23rd June 2039

Report Steps: 7 days

A3. ECLIPSE definition for study model of Combination Drive Reservoirs

a) CASE DEFINITION

Simulator:	Black Oil
Model Dimensions:	Number of cells in the x direction 33
	Number of cells in the y direction 33
	Number of cells in the z direction: 43
Grid type:	Corner Point
Geometry type:	Block Centered
Oil-Gas-Water Options:	Water, Gas

b) GRID

X Grid Block Size:	74 ft
Y Grid Block Size:	74 ft
Inclination Angle in X:	10 ft/ 100 ft
Inclination Angle in Y:	2 ft /100 ft
Depth of Top face:	6,206 ft
Shallowest Cell Coordination:	1, 35

CBCB Arrangements	# cells in z	Thickness (ft)/ layer	ϕ (%)	NTG	k-x (mD)	k-y (mD)	k-z (mD)
Thick 1	5	18.9	21%	0.4	200	200	20
Shale 1	1	328	0%	1	0	0	0
Thin 1	4	15.4	21%	0.25	200	200	20
Shale 2	1	328	0%	1	0	0	0
Thick 2	5	18.9	21%	0.4	20	20	2
Shale 3	1	328	0%	1	0	0	0
Thin 2	4	15.4	21%	0.25	20	20	2
Shale 4	1	328	0%	1	0	0	0
Thick 3	5	18.9	21%	0.4	200	200	20
Shale 5	1	328	0%	1	0	0	0
Thin 3	4	15.4	21%	0.25	200	200	20
Shale 6	1	328	0%	1	0	0	0
Thick 4	5	18.9	21%	0.4	20	20	2
Shale 7	1	328	0%	1	0	0	0
Thin 4	4	15.4	21%	0.25	20	20	2

ACTNUM

Thick Reservoirs

	X1	X2	X3	X4	X5	X6	X7	X8	X9	X10	X11	X12	X13	X14	X15	X16	X17	X18	X19	X20	X21	X22	X23	X24	X25	X26	X27	X28	X29	X30	X31	X32	X33
Y1	0	0	0	0	0	0	0	0	0	0	0	0	0	0	0	0	0	0	0	0	0	0	0	0	0	0	0	0	0	0	0	0	0
Y2	0	0	0	0	0	0	0	0	0	0	0	0	0	0	0	0	0	0	0	0	0	0	0	0	0	0	1	1	1	1	1	0	0
Y3	0	0	0	0	0	0	0	0	0	0	0	0	0	0	0	0	0	0	0	0	0	0	0	0	0	0	1	1	1	1	1	0	0
Y4	0	0	0	0	0	0	0	0	0	0	0	0	0	0	0	0	0	0	0	0	0	0	0	0	0	0	1	1	1	1	1	0	0
Y5	0	0	0	0	0	0	0	0	0	0	0	0	0	0	0	0	0	0	0	0	0	1	1	1	1	1	1	1	1	1	1	0	0
Y6	0	0	0	0	0	0	0	0	0	0	0	0	0	0	0	0	0	0	0	0	0	1	1	1	1	1	1	1	1	1	1	0	0
Y7	0	0	0	0	0	0	0	0	0	0	0	0	0	0	0	0	0	0	0	0	0	1	1	1	1	1	1	1	1	1	1	0	0
Y8	0	0	0	0	0	0	0	0	0	0	0	0	0	0	0	0	1	1	1	1	1	1	1	1	1	1	1	1	1	1	1	0	0
Y9	0	0	0	0	0	0	0	0	0	0	0	0	0	0	0	0	1	1	1	1	1	1	1	1	1	1	1	1	1	1	1	0	0
Y10	0	0	0	0	0	0	0	0	0	0	0	0	0	0	0	0	1	1	1	1	1	1	1	1	1	1	1	1	1	1	1	0	0
Y11	0	0	0	0	0	0	0	0	0	0	0	1	1	1	1	1	1	1	1	1	1	1	1	1	1	1	1	1	1	1	1	0	0
Y12	0	0	0	0	0	0	0	0	0	0	0	1	1	1	1	1	1	1	1	1	1	1	1	1	1	1	1	1	1	1	1	0	0
Y13	0	0	0	0	0	0	0	0	0	0	0	1	1	1	1	1	1	1	1	1	1	1	1	1	1	1	1	1	1	1	1	0	0
Y14	0	0	0	0	0	0	0	0	0	0	0	1	1	1	1	1	1	1	1	1	1	1	1	1	1	1	1	1	1	1	1	0	0
Y15	0	0	0	0	0	0	0	0	0	0	0	1	1	1	1	1	1	1	1	1	1	1	1	1	1	1	1	1	1	1	1	0	0
Y16	0	0	0	0	0	0	0	0	0	0	0	1	1	1	1	1	1	1	1	1	1	1	1	1	1	1	1	1	1	1	1	0	0
Y17	0	1	1	1	1	1	1	1	1	1	1	1	1	1	1	1	1	1	1	1	1	1	1	1	1	1	1	1	1	1	1	0	0
Y18	0	1	1	1	1	1	1	1	1	1	1	1	1	1	1	1	1	1	1	1	1	1	1	1	1	1	1	1	1	1	1	0	0
Y19	0	1	1	1	1	1	1	1	1	1	1	1	1	1	1	1	1	1	1	1	1	1	1	1	1	1	1	1	1	1	1	0	0
Y20	0	1	1	1	1	1	1	1	1	1	1	1	1	1	1	1	1	1	1	1	1	1	1	1	1	1	1	1	1	1	1	0	0
Y21	0	1	1	1	1	1	1	1	1	1	1	1	1	1	1	1	1	1	1	1	1	1	1	1	1	1	1	1	1	1	1	0	0
Y22	0	1	1	1	1	1	1	1	1	1	1	1	1	1	1	1	1	1	1	1	1	1	1	1	1	1	1	1	1	1	1	0	0
Y23	0	1	1	1	1	1	1	1	1	1	1	1	1	1	1	1	1	1	1	1	1	1	1	1	1	1	1	1	1	1	1	0	0
Y24	0	1	1	1	1	1	1	1	1	1	1	1	1	1	1	1	1	1	1	1	1	1	1	1	1	1	1	1	1	1	1	0	0
Y25	0	1	1	1	1	1	1	1	1	1	1	1	1	1	1	1	1	1	1	1	1	1	1	1	1	1	1	1	1	1	1	0	0
Y26	0	1	1	1	1	1	1	1	1	1	1	1	1	1	1	1	1	1	1	1	1	1	1	1	1	1	1	1	1	1	1	0	0
Y27	0	1	1	1	1	1	1	1	1	1	1	1	1	1	1	1	1	1	1	1	1	1	1	1	1	1	1	1	1	1	1	0	0
Y28	0	1	1	1	1	1	1	1	1	1	1	1	1	1	1	1	1	1	1	1	1	1	1	1	1	1	1	1	1	1	1	0	0
Y29	0	1	1	1	1	1	1	1	1	1	1	1	1	1	1	1	1	1	1	1	1	1	1	1	1	1	1	1	1	1	1	0	0
Y30	0	1	1	1	1	1	1	1	1	1	1	1	1	1	1	1	1	1	1	1	1	1	1	1	1	1	1	1	1	1	1	0	0
Y31	0	1	1	1	1	1	1	1	1	1	1	1	1	1	1	1	0	0	0	0	0	0	0	0	0	0	0	0	0	0	0	0	0
Y32	0	1	1	1	1	1	1	1	1	1	1	1	1	1	1	1	0	0	0	0	0	0	0	0	0	0	0	0	0	0	0	0	0
Y33	0	1	1	1	1	1	1	1	1	1	1	1	1	1	1	1	0	0	0	0	0	0	0	0	0	0	0	0	0	0	0	0	0

Thin Reservoirs

	X1	X2	X3	X4	X5	X6	X7	X8	X9	X10	X11	X12	X13	X14	X15	X16	X17	X18	X19	X20	X21	X22	X23	X24	X25	X26	X27	X28	X29	X30	X31	X32	X33
Y1	0	0	0	0	0	0	0	0	0	0	0	0	0	0	0	0	0	0	0	0	0	0	0	0	0	0	0	0	0	0	0	0	0
Y2	0	0	0	0	0	0	0	0	0	0	0	0	0	0	0	0	0	0	0	0	0	0	0	0	0	0	0	0	0	0	0	0	0
Y3	0	0	0	0	0	0	0	0	0	0	0	0	0	0	0	0	0	0	0	0	0	0	0	0	0	0	0	0	0	0	0	0	0
Y4	0	0	0	0	0	0	0	0	0	0	0	0	0	0	0	0	0	0	0	0	0	0	0	0	0	0	0	0	0	0	0	0	0
Y5	0	0	0	0	0	0	0	0	1	1	1	1	1	1	1	1	1	1	1	1	1	1	1	1	1	0	0	0	0	0	0	0	0
Y6	0	0	0	0	0	0	0	0	1	1	1	1	1	1	1	1	1	1	1	1	1	1	1	1	1	0	0	0	0	0	0	0	0
Y7	0	0	0	0	0	0	0	0	1	1	1	1	1	1	1	1	1	1	1	1	1	1	1	1	1	0	0	0	0	0	0	0	0
Y8	0	0	0	0	0	0	0	0	1	1	1	1	1	1	1	1	1	1	1	1	1	1	1	1	1	0	0	0	0	0	0	0	0
Y9	0	0	0	0	0	0	0	0	1	1	1	1	1	1	1	1	1	1	1	1	1	1	1	1	1	0	0	0	0	0	0	0	0
Y10	0	0	0	0	0	0	0	0	1	1	1	1	1	1	1	1	1	1	1	1	1	1	1	1	1	0	0	0	0	0	0	0	0
Y11	0	0	0	0	0	0	0	0	1	1	1	1	1	1	1	1	1	1	1	1	1	1	1	1	1	0	0	0	0	0	0	0	0
Y12	0	0	0	0	0	0	0	0	1	1	1	1	1	1	1	1	1	1	1	1	1	1	1	1	1	0	0	0	0	0	0	0	0
Y13	0	0	0	0	0	0	0	0	1	1	1	1	1	1	1	1	1	1	1	1	1	1	1	1	1	0	0	0	0	0	0	0	0
Y14	0	0	0	0	0	0	0	0	1	1	1	1	1	1	1	1	1	1	1	1	1	1	1	1	1	0	0	0	0	0	0	0	0
Y15	0	0	0	0	0	0	0	0	1	1	1	1	1	1	1	1	1	1	1	1	1	1	1	1	1	0	0	0	0	0	0	0	0
Y16	0	0	0	0	0	0	0	0	1	1	1	1	1	1	1	1	1	1	1	1	1	1	1	1	1	0	0	0	0	0	0	0	0
Y17	0	0	0	0	0	0	0	0	1	1	1	1	1	1	1	1	1	1	1	1	1	1	1	1	1	0	0	0	0	0	0	0	0
Y18	0	0	0	0	0	0	0	0	1	1	1	1	1	1	1	1	1	1	1	1	1	1	1	1	1	0	0	0	0	0	0	0	0
Y19	0	0	0	0	0	0	0	0	1	1	1	1	1	1	1	1	1	1	1	1	1	1	1	1	1	0	0	0	0	0	0	0	0
Y20	0	0	0	0	0	0	0	0	1	1	1	1	1	1	1	1	1	1	1	1	1	1	1	1	1	0	0	0	0	0	0	0	0
Y21	0	0	0	0	0	0	0	0	1	1	1	1	1	1	1	1	1	1	1	1	1	1	1	1	1	0	0	0	0	0	0	0	0
Y22	0	0	0	0	0	0	0	0	1	1	1	1	1	1	1	1	1	1	1	1	1	1	1	1	1	0	0	0	0	0	0	0	0
Y23	0	0	0	0	0	0	0	0	1	1	1	1	1	1	1	1	1	1	1	1	1	1	1	1	1	0	0	0	0	0	0	0	0
Y24	0	0	0	0	0	0	0	0	1	1	1	1	1	1	1	1	1	1	1	1	1	1	1	1	1	0	0	0	0	0	0	0	0
Y25	0	0	0	0	0	0	0	0	1	1	1	1	1	1	1	1	1	1	1	1	1	1	1	1	1	0	0	0	0	0	0	0	0
Y26	0	0	0	0	0	0	0	0	1	1	1	1	1	1	1	1	1	1	1	1	1	1	1	1	1	0	0	0	0	0	0	0	0
Y27	0	0	0	0	0	0	0	0	1	1	1	1	1	1	1	1	1	1	1	1	1	1	1	1	1	0	0	0	0	0	0	0	0
Y28	0	0	0	0	0	0	0	0	1	1	1	1	1	1	1	1	1	1	1	1	1	1	1	1	1	0	0	0	0	0	0	0	0
Y29	0	0	0	0	0	0	0	0	1	1	1	1	1	1	1	1	1	1	1	1	1	1	1	1	1	0	0	0	0	0	0	0	0
Y30	0	0	0	0	0	0	0	0	1	1	1	1	1	1	1	1	1	1	1	1	1	1	1	1	1	0	0	0	0	0	0	0	0
Y31	0	0	0	0	0	0	0	0	0	0	0	0	0	0	0	0	0	0	0	0	0	0	0	0	0	0	0	0	0	0	0	0	0
Y32	0	0	0	0	0	0	0	0	0	0	0	0	0	0	0	0	0	0	0	0	0	0	0	0	0	0	0	0	0	0	0	0	0
Y33	0	0	0	0	0	0	0	0	0	0	0	0	0	0	0	0	0	0	0	0	0	0	0	0	0	0	0	0	0	0	0	0	0

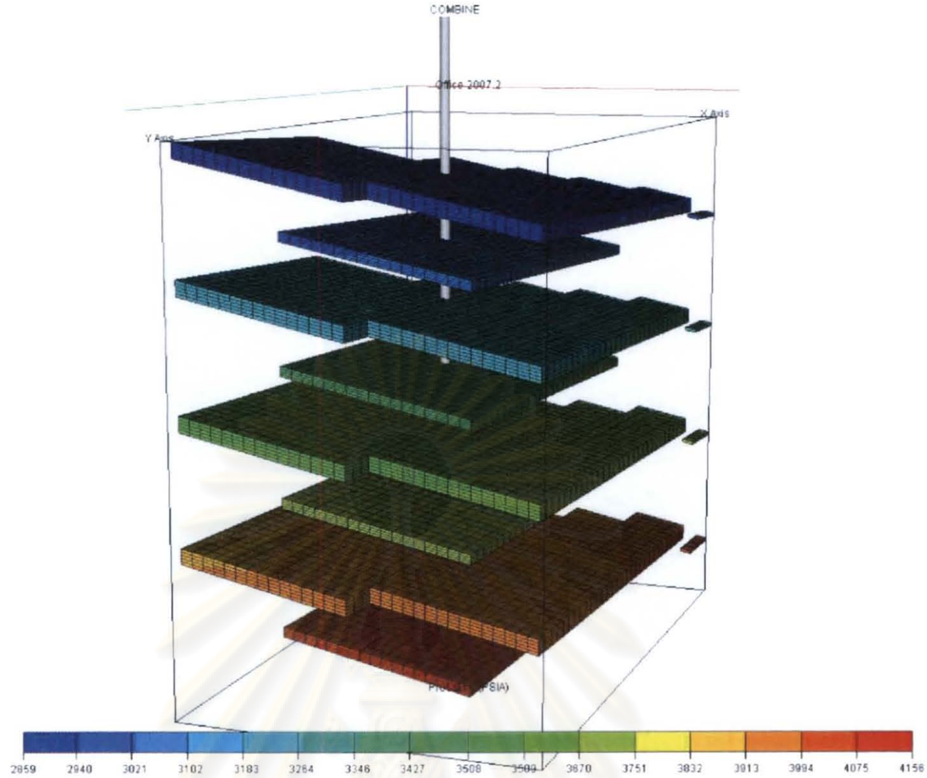

Figure A1: Model shape and pressure distribution for combination drive model

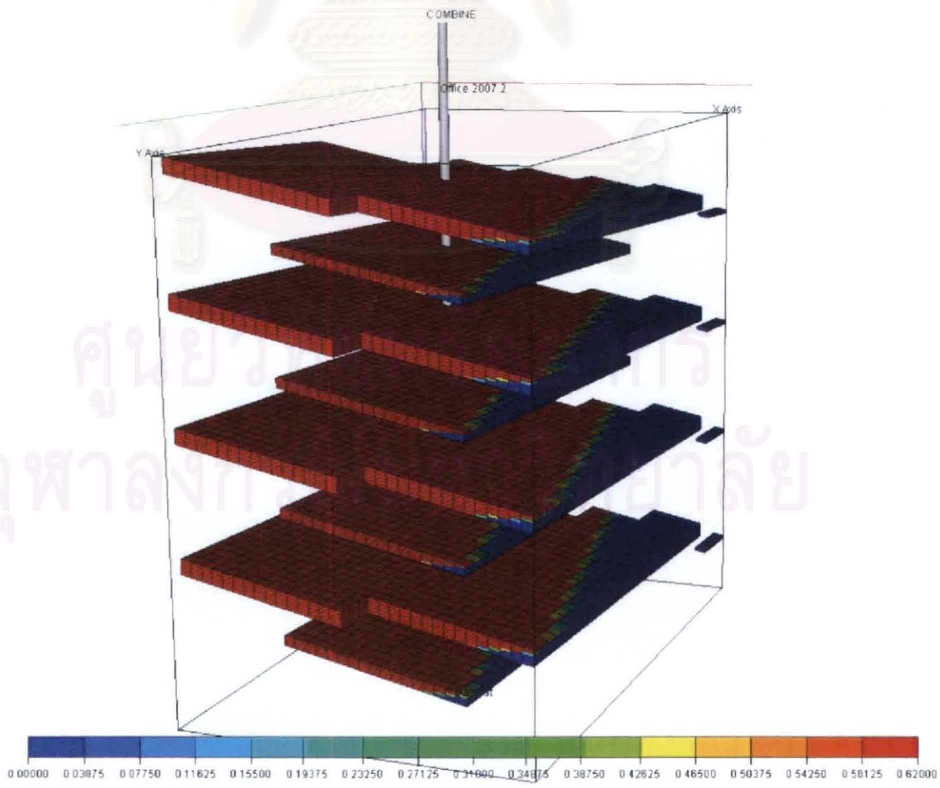

Figure A2: Gas saturations for combination drive model

c) PVT

Thick Reservoirs			
Water PVT Properties	Reference pressure(Pref)	3349	psia
	Water FVF at Pref	1.0897	rb/stb
	Water viscosity at Pref	0.1601	cp
	Water viscosibility	1.00 E-05	/psi
Fluid Densities at Surface Conditions	Oil density	48.4 (50 °API)	lb/ft^3
	Water density	62.43	lb/ft^3
	Gas density	0.068	lb/ft^3
Rock Properties	Reference Pressure	3349	psia
	Rock Compressibility	5.4092E-6	/psi

Thin Reservoirs			
Water PVT Properties	Reference pressure(Pref)	4652.5	psia
	Water FVF at Pref	1.0636	rb/stb
	Water viscosity at Pref	0.1907	cp
	Water viscosibility	9.22 E-06	/psi
Fluid Densities at Surface Conditions	Oil density	48.4 (50 °API)	lb/ft^3
	Water density	62.43	lb/ft^3
	Gas density	0.060	lb/ft^3
Rock Properties	Reference Pressure	4230	psia
	Rock Compressibility	5.4029E-6	/psi

d) SCAL

Thick Reservoirs

Sw	K_{rg}	K_{rw}
0.3800	1.0000	0.0000
0.4044	0.5549	0.0296
0.4289	0.2846	0.0838
0.4533	0.1317	0.1540
0.4778	0.0529	0.2370
0.5022	0.0173	0.3313
0.5267	0.0041	0.4355
0.5511	0.0005	0.5487
0.5756	0.0000	0.6704
0.6000	0.0000	0.8000
1.0000	0.0000	1.0000

Thin Reservoirs		
Sw	K_{rg}	K_{rw}
0.4000	1.0000	0.0000
0.4411	0.5549	0.0040
0.4822	0.2846	0.0183
0.5233	0.1317	0.0446
0.5644	0.0529	0.0840
0.6056	0.0173	0.1372
0.6467	0.0041	0.2049
0.6878	0.0005	0.2876
0.7289	0.0000	0.3859
0.7700	0.0000	0.5000
1.0000	0.0000	1.0000

e) INIT

Arrangements	Ref Depth (ft)	Ref Pressure (psia)	GWC (ft)
Thick 1	6732	2915	6668
Thin 1	7050	3052	6998
Thick 2	7548	3268	7484
Thin 2	7866	3406	7815
Thick 3	8364	3622	8305
Thin 3	8682	3759	8631
Thick 4	9180	3975	9117
Thin 4	9484	4106	9442

f) Schedule

Well	Combine 1
I,J Location	16, 21
Primary Control	Gas Rate
Secondary Control	THP
Primary Target	20 MMscf/d
Secondary Target	30 Barg
Well Economic Limit	0.1 MMscfd
Max WGR Limit	1,000,000 STB/ Mscf

Production Starts: 1st Jan 2009
Production Ends: 23rd June 2039
Report Steps: 7 days

A4. ACTIONX keywords for production/perforation scenarios.

Scenario 1a

```
ACTIONX
ACT1 10000 /
WGPR 'COMBINE' < 600 /
/
COMPDAT
'COMBINE' 2* 34 34 'OPEN' 2* 0.2552 1* 5 1* 'Z' 1* /
/
WELOPEN
'COMBINE' /
/
ENDACTIO

ACTIONX
ACT2 10000 /
WGPR 'COMBINE' < 600 AND /
RPR 7 < 3900 /
/
COMPDAT
'COMBINE' 2* 29 29 'OPEN' 2* 0.2552 1* 5 1* 'Z' 1* /
/
WELOPEN
'COMBINE' /
/
ENDACTIO

ACTIONX
ACT3 10000 /
WGPR 'COMBINE' < 600 AND /
RPR 7 < 3900 AND /
RPR 6 < 3697 /
/
COMPDAT
'COMBINE' 2* 23 23 'OPEN' 2* 0.2552 1* 5 1* 'Z' 1* /
/
WELOPEN
'COMBINE' /
/
ENDACTIO

ACTIONX
ACT4 10000 /
WGPR 'COMBINE' < 600 AND /
RPR 7 < 3900 AND /
RPR 6 < 3697 AND /
RPR 5 < 3548 /
/
```

```
COMPDAT
'COMBINE' 2* 18 18 'OPEN' 2* 0.2552 1* 5 1* 'Z' 1* /
/
WELOPEN
'COMBINE' /
/
ENDACTIO

ACTIONX
ACT5 10000 /
WGPR 'COMBINE' < 600 AND /
RPR 7 < 3900 AND /
RPR 6 < 3697 AND /
RPR 5 < 3548 AND /
RPR 4 < 3345 /
/
COMPDAT
'COMBINE' 2* 12 12 'OPEN' 2* 0.2552 1* 5 1* 'Z' 1* /
/
WELOPEN
'COMBINE' /
/
ENDACTIO

ACTIONX
ACT6 10000 /
WGPR 'COMBINE' < 600 AND /
RPR 7 < 3900 AND /
RPR 6 < 3697 AND /
RPR 5 < 3548 AND /
RPR 4 < 3345 AND /
RPR 3 < 3196 /
/
COMPDAT
'COMBINE' 2* 7 7 'OPEN' 2* 0.2552 1* 5 1* 'Z' 1* /
/
WELOPEN
'COMBINE' /
/
ENDACTIO

ACTIONX
ACT7 10000 /
WGPR 'COMBINE' < 600 AND /
RPR 7 < 3900 AND /
RPR 6 < 3697 AND /
RPR 5 < 3548 AND /
RPR 4 < 3345 AND /
RPR 3 < 3196 AND /
RPR 2 < 2991 /
```

```
/
COMPDAT
'COMBINE' 2* 1 1 'OPEN' 2* 0.2552 1* 5 1* 'Z' 1* /
/
WELOPEN
'COMBINE' /
/
ENDACTIO
```

```
Scenario 1b
ACTIONX
ACT1 10000 /
WGPR 'COMBINE' < 10000 /
/
COMPDAT
'COMBINE' 2* 34 34 'OPEN' 2* 0.2552 1* 5 1* 'Z' 1* /
/
WELOPEN
'COMBINE' /
/
ENDACTIO

ACTIONX
ACT2 10000 /
WGPR 'COMBINE' < 10000 AND /
RPR 7 < 3900 /
/
COMPDAT
'COMBINE' 2* 29 29 'OPEN' 2* 0.2552 1* 5 1* 'Z' 1* /
/
WELOPEN
'COMBINE' /
/
ENDACTIO

ACTIONX
ACT3 10000 /
WGPR 'COMBINE' < 10000 AND /
RPR 7 < 3900 AND /
RPR 6 < 3697 /
/
COMPDAT
'COMBINE' 2* 23 23 'OPEN' 2* 0.2552 1* 5 1* 'Z' 1* /
```

```
/
WELOPEN
'COMBINE' /
/
ENDACTIO

ACTIONX
ACT4 10000 /
WGPR 'COMBINE' < 10000 AND /
RPR 7 < 3900 AND /
RPR 6 < 3697 AND /
RPR 5 < 3548 /
/
COMPDAT
'COMBINE' 2* 18 18 'OPEN' 2* 0.2552 1* 5 1* 'Z' 1* /
/
WELOPEN
'COMBINE' /
/
ENDACTIO

ACTIONX
ACT5 10000 /
WGPR 'COMBINE' < 10000 AND /
RPR 7 < 3900 AND /
RPR 6 < 3697 AND /
RPR 5 < 3548 AND /
RPR 4 < 3345 /
/
COMPDAT
'COMBINE' 2* 12 12 'OPEN' 2* 0.2552 1* 5 1* 'Z' 1* /
/
WELOPEN
'COMBINE' /
/
ENDACTIO

ACTIONX
ACT6 10000 /
WGPR 'COMBINE' < 10000 AND /
RPR 7 < 3900 AND /
RPR 6 < 3697 AND /
RPR 5 < 3548 AND /
RPR 4 < 3345 AND /
RPR 3 < 3196 /
/
COMPDAT
'COMBINE' 2* 7 7 'OPEN' 2* 0.2552 1* 5 1* 'Z' 1* /
/
WELOPEN
```

```
'COMBINE' /
/
ENDACTIO

ACTIONX
ACT7 10000 /
WGPR 'COMBINE' < 10000 AND /
RPR 7 < 3900 AND /
RPR 6 < 3697 AND /
RPR 5 < 3548 AND /
RPR 4 < 3345 AND /
RPR 3 < 3196 AND /
RPR 2 < 2991 /
/
COMPDAT
'COMBINE' 2* 1 1 'OPEN' 2* 0.2552 1* 5 1* 'Z' 1* /
/
WELOPEN
'COMBINE' /
/
ENDACTIO
```

Scenario 1c

```
ACTIONX
ACT1 10000 /
WGPR 'COMBINE' < 20000 /
/
COMPDAT
'COMBINE' 2* 34 34 'OPEN' 2* 0.2552 1* 5 1* 'Z' 1* /
/
WELOPEN
'COMBINE' /
/
ENDACTIO

ACTIONX
ACT2 10000 /
WGPR 'COMBINE' < 20000 AND /
RPR 7 < 3900 /
/
COMPDAT
'COMBINE' 2* 29 29 'OPEN' 2* 0.2552 1* 5 1* 'Z' 1* /
/
WELOPEN
'COMBINE' /
/
ENDACTIO

ACTIONX
ACT3 10000 /
```

```
WGPR 'COMBINE' < 20000 AND /
RPR 7 < 3900 AND /
RPR 6 < 3697 /
/
COMPDAT
'COMBINE' 2* 23 23 'OPEN' 2* 0.2552 1* 5 1* 'Z' 1* /
/
WELOPEN
'COMBINE' /
/
ENDACTIO

ACTIONX
ACT4 10000 /
WGPR 'COMBINE' < 20000 AND /
RPR 7 < 3900 AND /
RPR 6 < 3697 AND /
RPR 5 < 3548 /
/
COMPDAT
'COMBINE' 2* 18 18 'OPEN' 2* 0.2552 1* 5 1* 'Z' 1* /
/
WELOPEN
'COMBINE' /
/
ENDACTIO

ACTIONX
ACT5 10000 /
WGPR 'COMBINE' < 20000 AND /
RPR 7 < 3900 AND /
RPR 6 < 3697 AND /
RPR 5 < 3548 AND /
RPR 4 < 3345 /
/
COMPDAT
'COMBINE' 2* 12 12 'OPEN' 2* 0.2552 1* 5 1* 'Z' 1* /
/
WELOPEN
'COMBINE' /
/
ENDACTIO

ACTIONX
ACT6 10000 /
WGPR 'COMBINE' < 20000 AND /
RPR 7 < 3900 AND /
RPR 6 < 3697 AND /
RPR 5 < 3548 AND /
RPR 4 < 3345 AND /
```

```
RPR 3 < 3196 /
/
COMPDAT
'COMBINE' 2* 7 7 'OPEN' 2* 0.2552 1* 5 1* 'Z' 1* /
/
WELOPEN
'COMBINE' /
/
ENDACTIO

ACTIONX
ACT7 10000 /
WGPR 'COMBINE' < 20000 AND /
RPR 7 < 3900 AND /
RPR 6 < 3697 AND /
RPR 5 < 3548 AND /
RPR 4 < 3345 AND /
RPR 3 < 3196 AND /
RPR 2 < 2991 /
/
COMPDAT
'COMBINE' 2* 1 1 'OPEN' 2* 0.2552 1* 5 1* 'Z' 1* /
/
WELOPEN
'COMBINE' /
/
ENDACTIO
```

Scenario 1d

```
ACTIONX
ACT1 10000 /
WGPR 'COMBINE' < 600 /
/
COMPDAT
'COMBINE' 2* 40 40 'SHUT' 2* 0.2552 1* 5 1* 'Z' 1* /
'COMBINE' 2* 34 34 'OPEN' 2* 0.2552 1* 5 1* 'Z' 1* /
/
WELOPEN
'COMBINE' /
/
ENDACTIO

ACTIONX
ACT2 10000 /
WGPR 'COMBINE' < 600 AND /
RPR 7 < 3900 /
/
COMPDAT
'COMBINE' 2* 34 34 'SHUT' 2* 0.2552 1* 5 1* 'Z' 1* /
'COMBINE' 2* 29 29 'OPEN' 2* 0.2552 1* 5 1* 'Z' 1* /
```

```
/
WELOPEN
'COMBINE' /
/
ENDACTIO

ACTIONX
ACT3 10000 /
WGPR 'COMBINE' < 600 AND /
RPR 7 < 3900 AND /
RPR 6 < 3697 /
/
COMPDAT
'COMBINE' 2* 29 29 'SHUT' 2* 0.2552 1* 5 1* 'Z' 1* /
'COMBINE' 2* 23 23 'OPEN' 2* 0.2552 1* 5 1* 'Z' 1* /
/
WELOPEN
'COMBINE' /
/
ENDACTIO

ACTIONX
ACT4 10000 /
WGPR 'COMBINE' < 600 AND /
RPR 7 < 3900 AND /
RPR 6 < 3697 AND /
RPR 5 < 3548 /
/
COMPDAT
'COMBINE' 2* 23 23 'SHUT' 2* 0.2552 1* 5 1* 'Z' 1* /
'COMBINE' 2* 18 18 'OPEN' 2* 0.2552 1* 5 1* 'Z' 1* /
/
WELOPEN
'COMBINE' /
/
ENDACTIO

ACTIONX
ACT5 10000 /
WGPR 'COMBINE' < 600 AND /
RPR 7 < 3900 AND /
RPR 6 < 3697 AND /
RPR 5 < 3548 AND /
RPR 4 < 3345 /
/
COMPDAT
'COMBINE' 2* 18 18 'SHUT' 2* 0.2552 1* 5 1* 'Z' 1* /
'COMBINE' 2* 12 12 'OPEN' 2* 0.2552 1* 5 1* 'Z' 1* /
/
WELOPEN
```

```
'COMBINE' /
/
ENDACTIO

ACTIONX
ACT6 10000 /
WGPR 'COMBINE' < 600 AND /
RPR 7 < 3900 AND /
RPR 6 < 3697 AND /
RPR 5 < 3548 AND /
RPR 4 < 3345 AND /
RPR 3 < 3196 /
/
COMPDAT
'COMBINE' 2* 12 12 'SHUT' 2* 0.2552 1* 5 1* 'Z' 1* /
'COMBINE' 2* 7 7 'OPEN' 2* 0.2552 1* 5 1* 'Z' 1* /
/
WELOPEN
'COMBINE' /
/
ENDACTIO

ACTIONX
ACT7 10000 /
WGPR 'COMBINE' < 600 AND /
RPR 7 < 3900 AND /
RPR 6 < 3697 AND /
RPR 5 < 3548 AND /
RPR 4 < 3345 AND /
RPR 3 < 3196 AND /
RPR 2 < 2991 /
/
COMPDAT
'COMBINE' 2* 7 7 'SHUT' 2* 0.2552 1* 5 1* 'Z' 1* /
'COMBINE' 2* 1 1 'OPEN' 2* 0.2552 1* 5 1* 'Z' 1* /
/
WELOPEN
'COMBINE' /
/
ENDACTIO
```

Scenario 2a

```
ACTIONX
ACT1 10000 /
WGPR 'COMBINE' < 20000 /
/
COMPDAT
'COMBINE' 2* 12 12 'OPEN' 2* 0.2552 1* 5 1* 'Z' 1* /
'COMBINE' 2* 18 18 'OPEN' 2* 0.2552 1* 5 1* 'Z' 1* /
'COMBINE' 2* 34 34 'OPEN' 2* 0.2552 1* 5 1* 'Z' 1* /
'COMBINE' 2* 40 40 'OPEN' 2* 0.2552 1* 5 1* 'Z' 1* /
/
WELOPEN
'COMBINE' /
/
ENDACTIO
```

Scenario 2b

```
ACTIONX
ACT1 10000 /
WGPR 'COMBINE' < 20000 /
/
COMPDAT
'COMBINE' 2* 1 1 'OPEN' 2* 0.2552 1* 5 1* 'Z' 1* /
'COMBINE' 2* 7 7 'OPEN' 2* 0.2552 1* 5 1* 'Z' 1* /
'COMBINE' 2* 23 23 'OPEN' 2* 0.2552 1* 5 1* 'Z' 1* /
'COMBINE' 2* 29 29 'OPEN' 2* 0.2552 1* 5 1* 'Z' 1* /
/
WELOPEN
'COMBINE' /
/
ENDACTIO
```

Scenario 3a

```
ACTIONX
ACT1 10000 /
WGPR 'COMBINE' < 20000 /
/
COMPDAT
'COMBINE' 2* 7 7 'OPEN' 2* 0.2552 1* 5 1* 'Z' 1* /
'COMBINE' 2* 18 18 'OPEN' 2* 0.2552 1* 5 1* 'Z' 1* /
'COMBINE' 2* 29 29 'OPEN' 2* 0.2552 1* 5 1* 'Z' 1* /
'COMBINE' 2* 40 40 'OPEN' 2* 0.2552 1* 5 1* 'Z' 1* /
/
WELOPEN
'COMBINE' /
/
ENDACTIO
```

Scenario 3b

```
ACTIONX
ACT1 10000 /
WGPR 'COMBINE' < 20000 /
/
COMPDAT
'COMBINE' 2* 1 1 'OPEN' 2* 0.2552 1* 5 1* 'Z' 1* /
'COMBINE' 2* 12 12 'OPEN' 2* 0.2552 1* 5 1* 'Z' 1* /
'COMBINE' 2* 23 23 'OPEN' 2* 0.2552 1* 5 1* 'Z' 1* /
'COMBINE' 2* 34 34 'OPEN' 2* 0.2552 1* 5 1* 'Z' 1* /
/
WELOPEN
'COMBINE' /
/
ENDACTIO
```

APPENDIX B

Selected Simulation Results

Case 1: Scenario 1a, Combination drive model

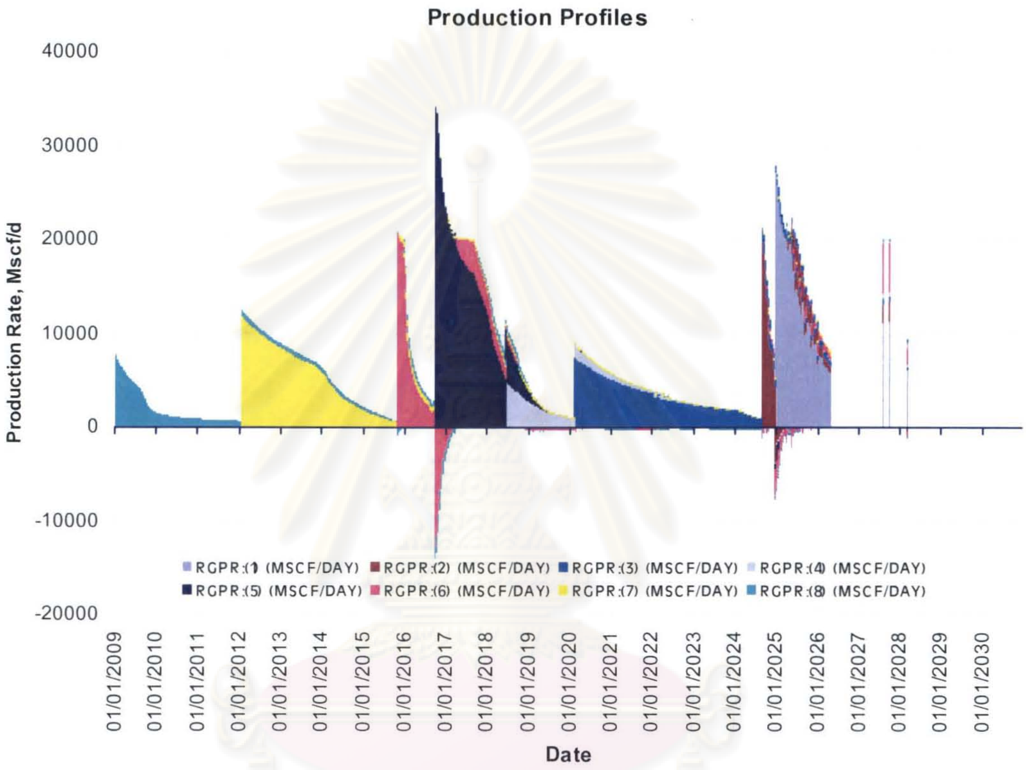

Figure B1: Gas Production Profiles

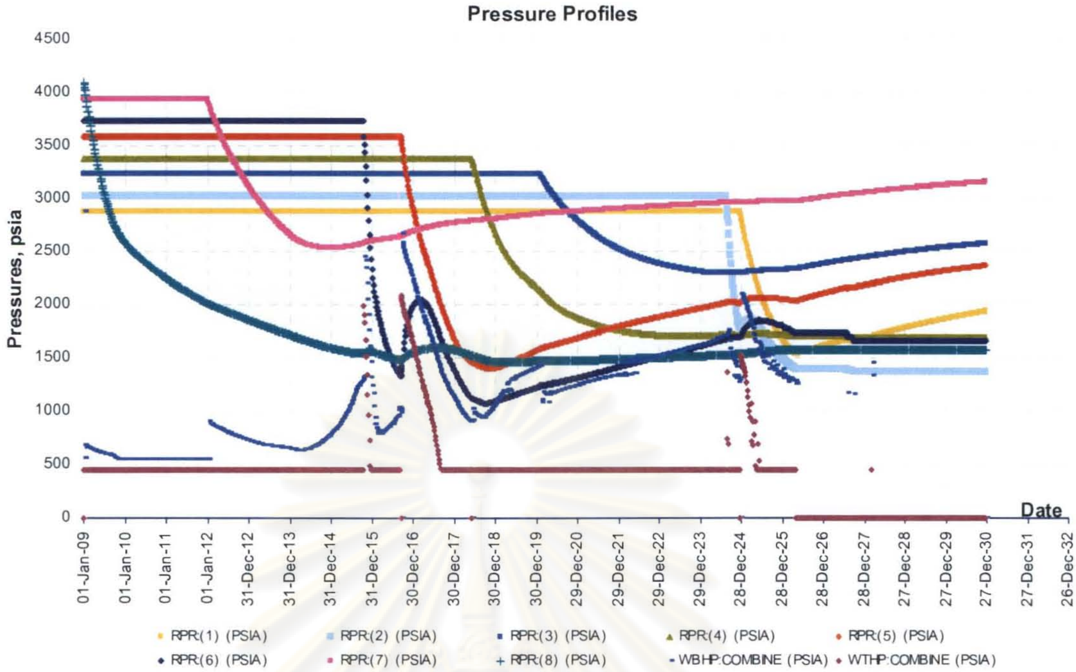

Figure B2: Pressure Profiles

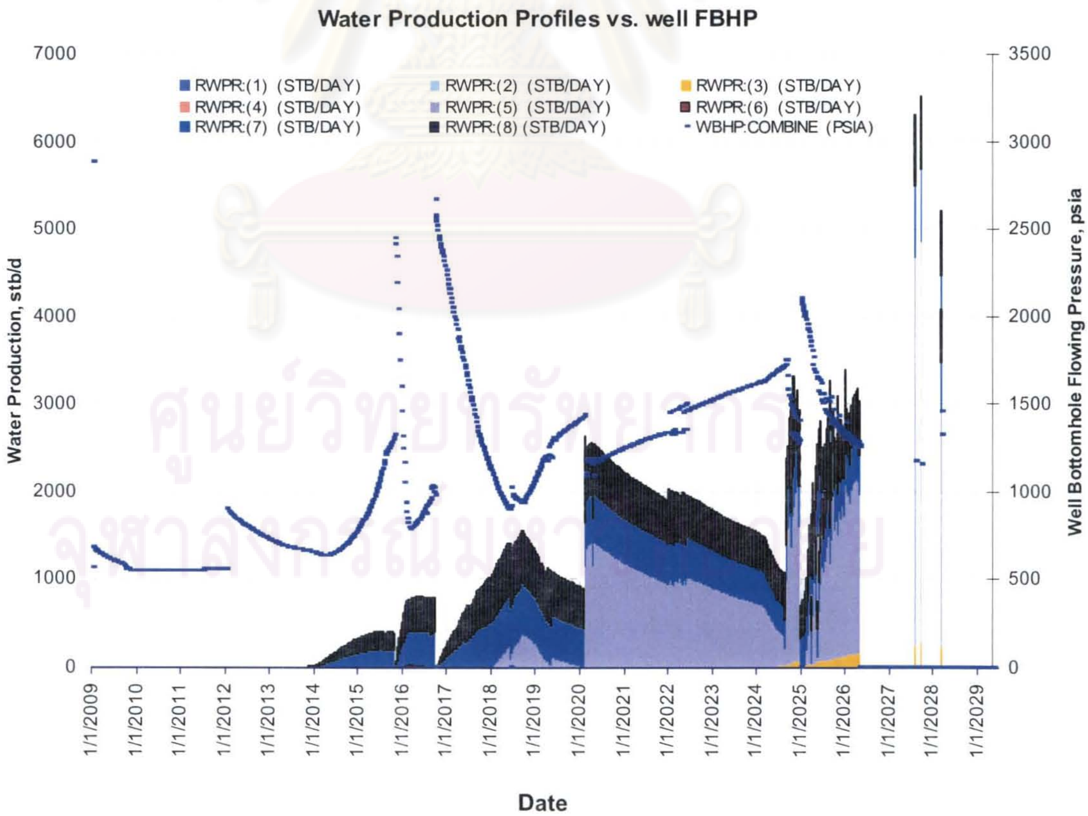

Figure B3: Water Production Profiles vs. Well's Flowing Bottomhole Pressures

Case 2: Scenario 1b, Combination drive model

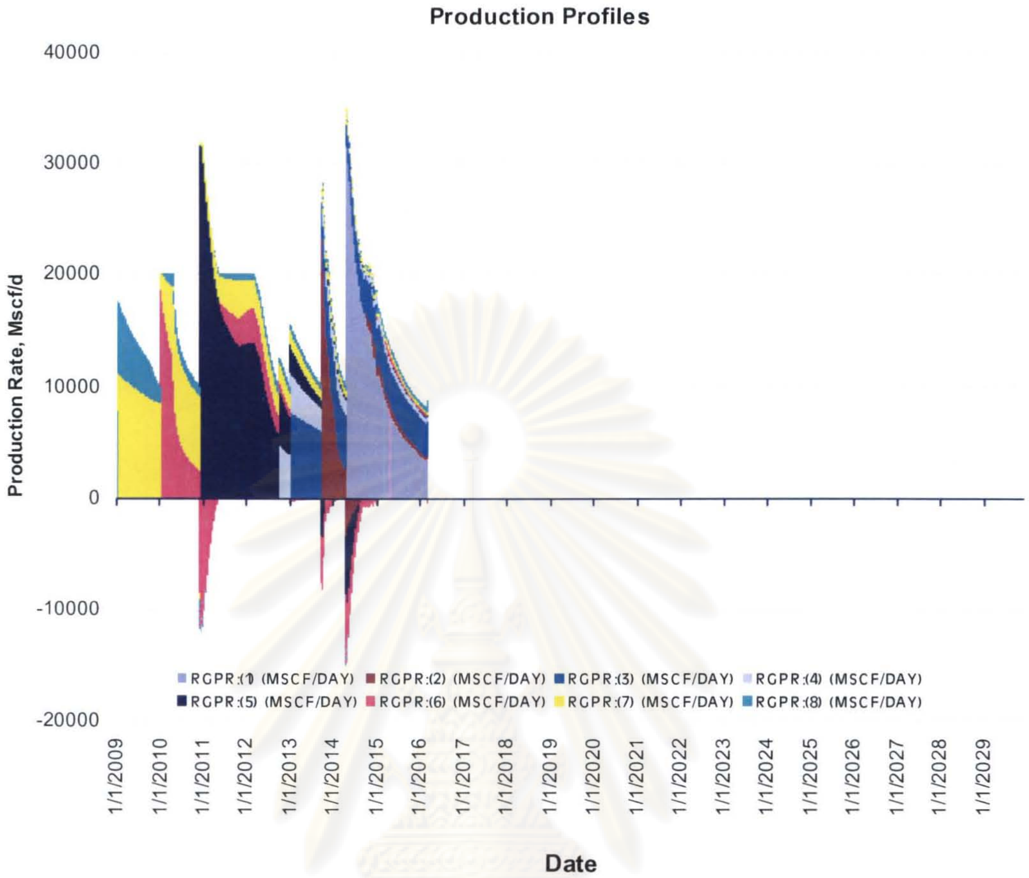

Figure B4: Gas Production Profiles

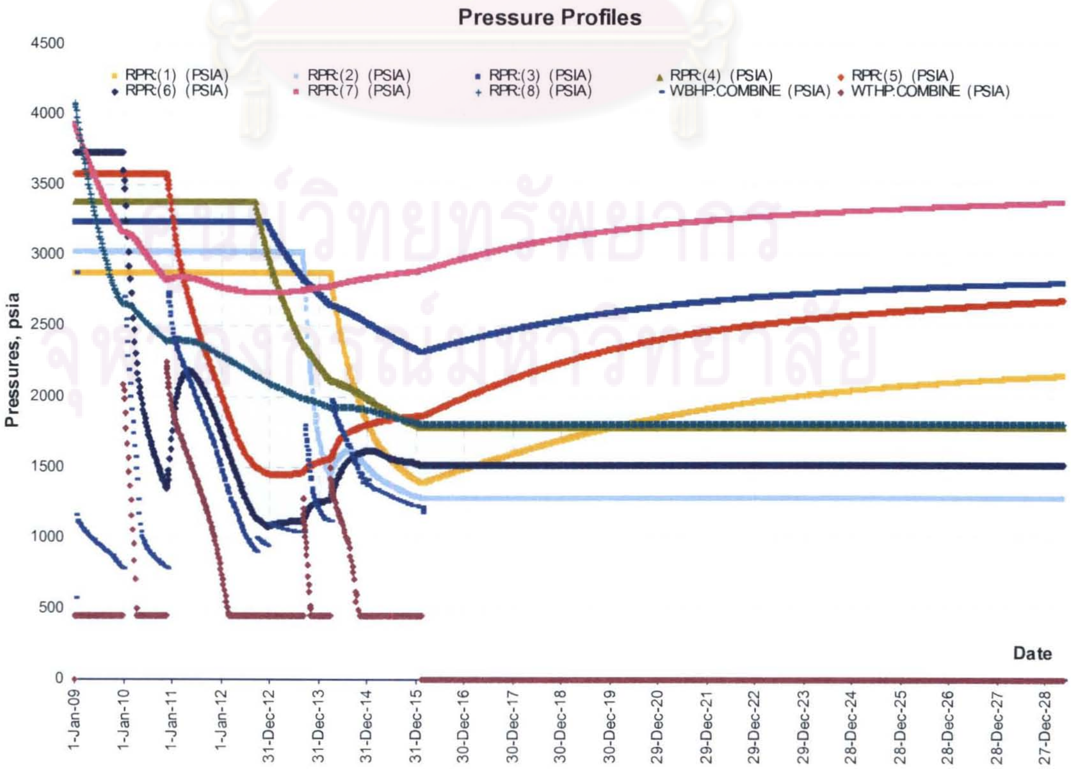

Figure B5: Pressure Profiles

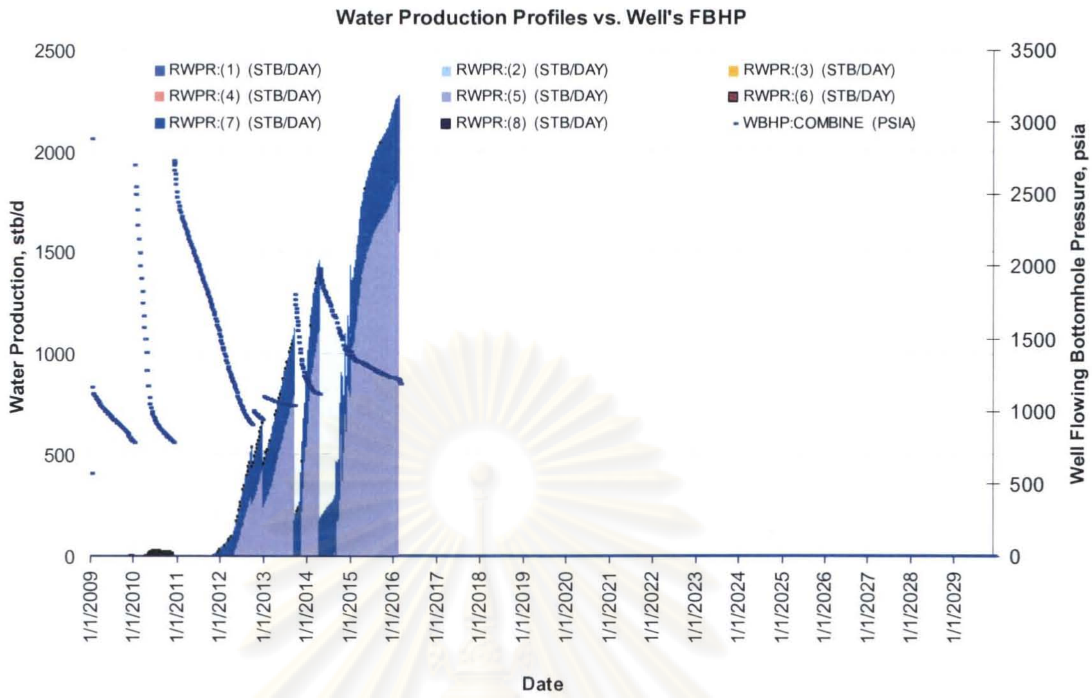

Figure B6: Water Production Profiles vs. Well's Flowing Bottomhole Pressures

Case 3: Scenario 1c, Combination drive model

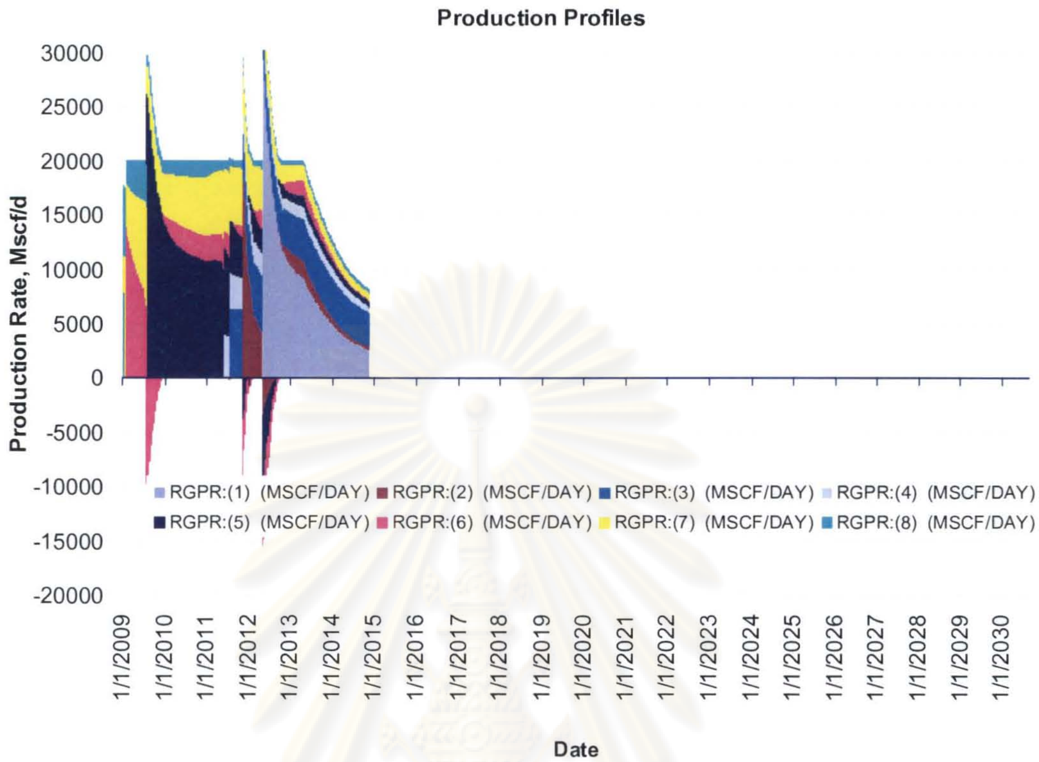

Figure B7: Gas Production Profiles

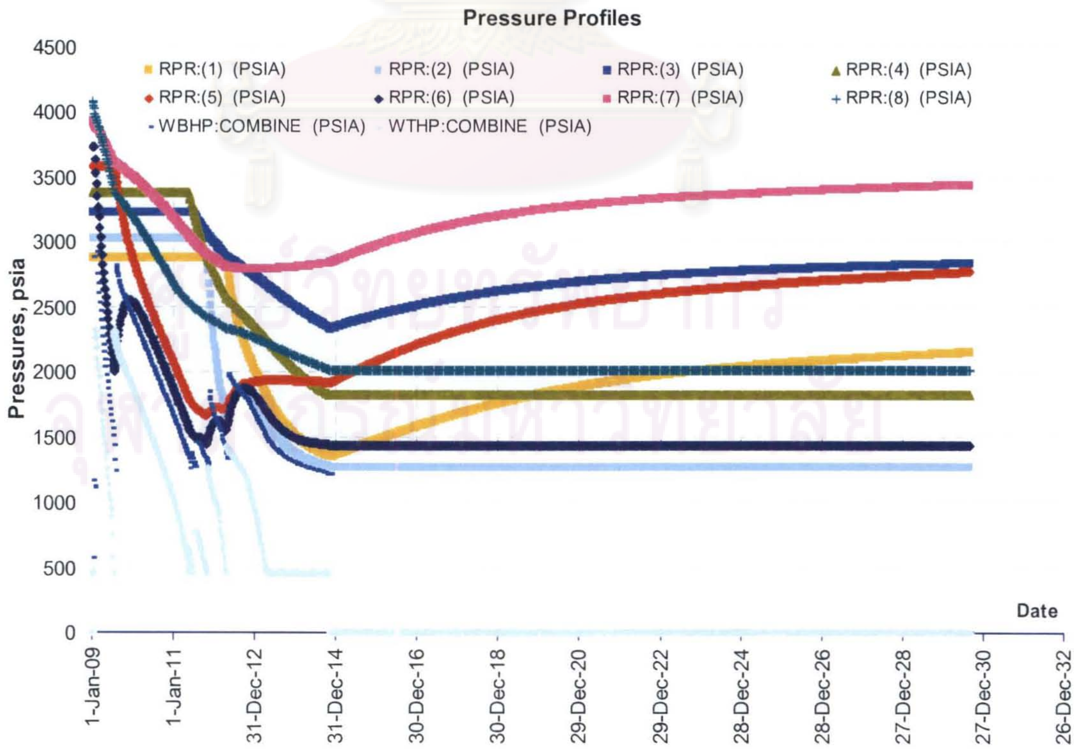

Figure B8: Pressure Profiles

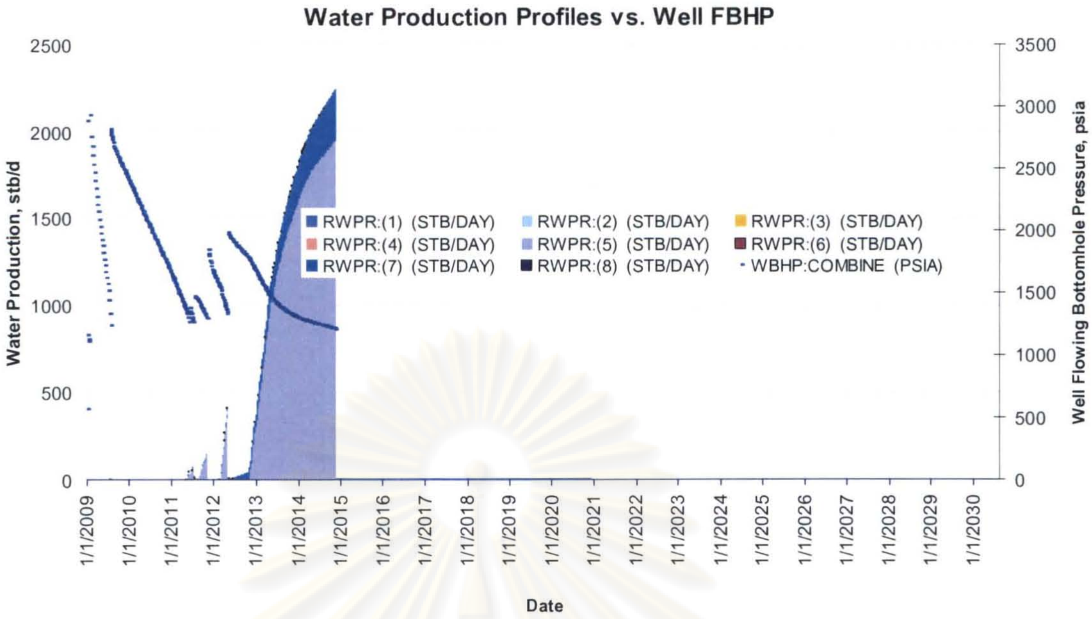

Figure B9: Water Production Profiles vs. Well's Flowing Bottomhole Pressures

Case 4: Scenario 1d, Combination drive model

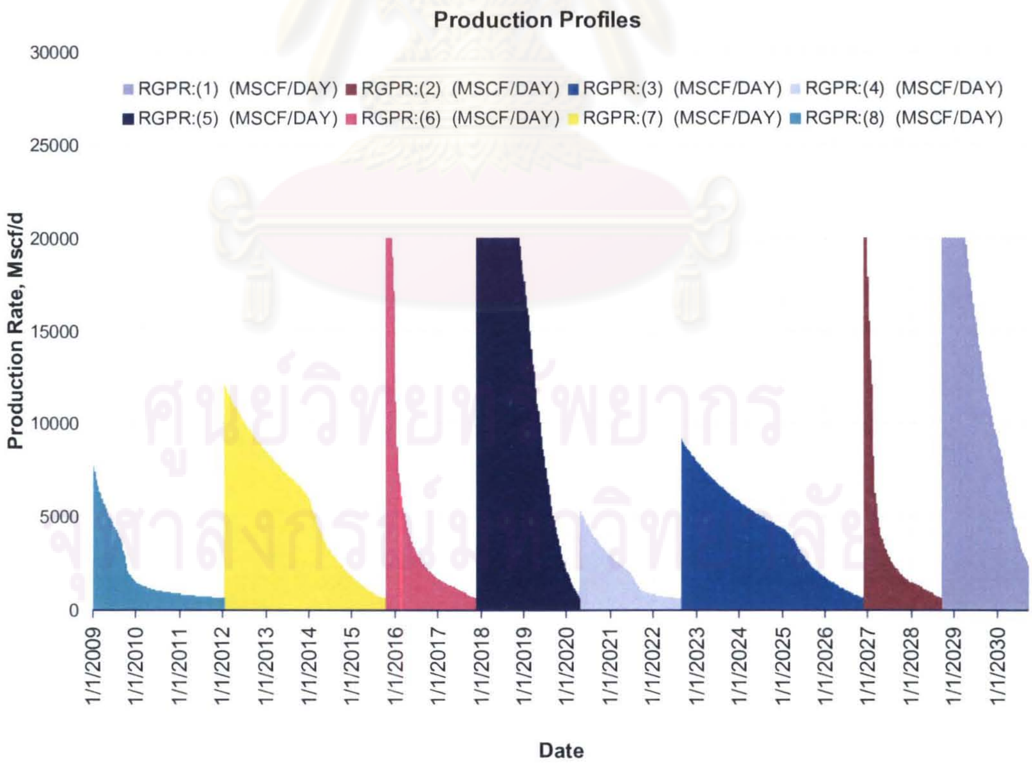

Figure B10: Gas Production Profiles

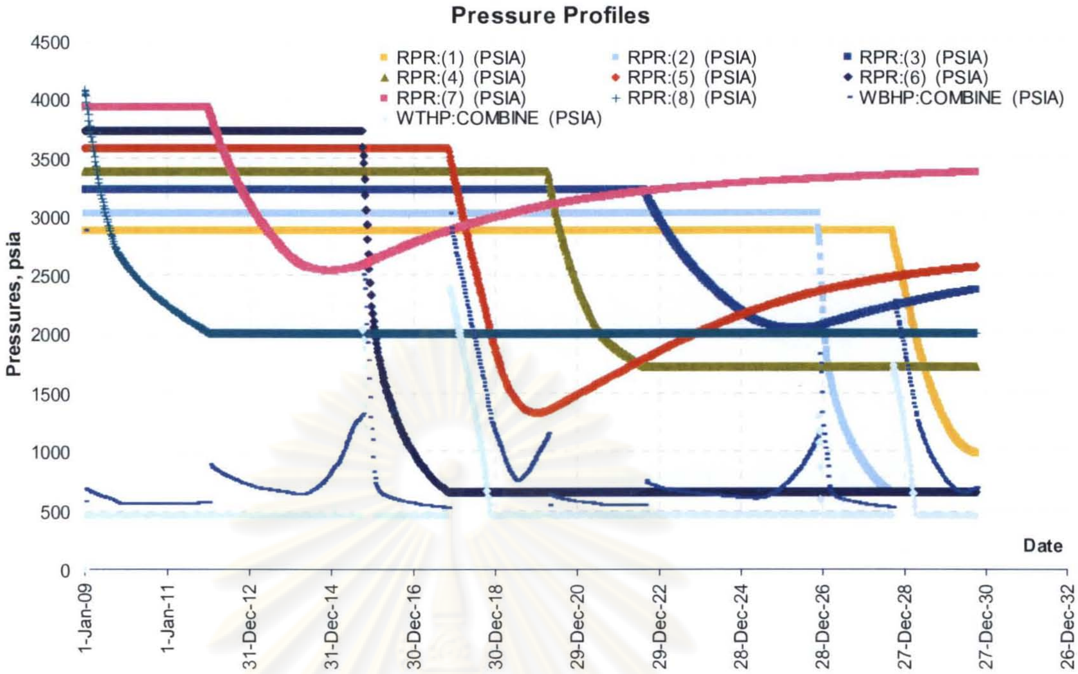

Figure B11: Pressure Profiles

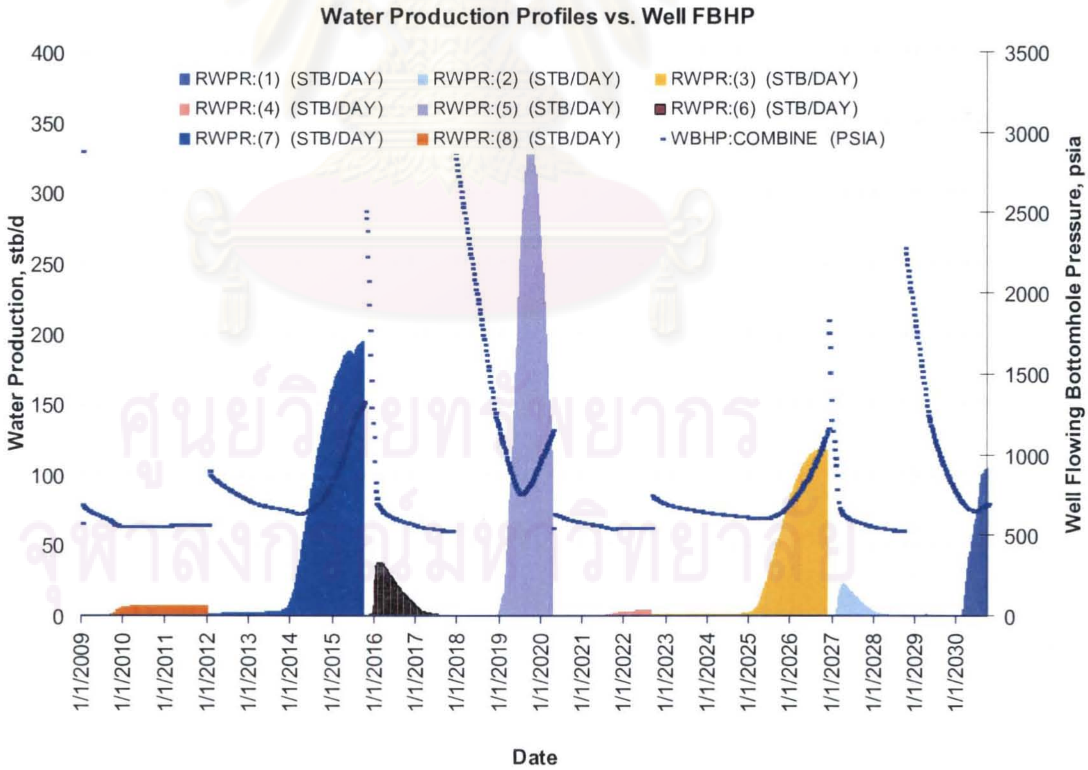

Figure B12: Water Production Profiles vs. Well's Flowing Bottomhole Pressures

Case 5: Scenario 2a, Combination drive model

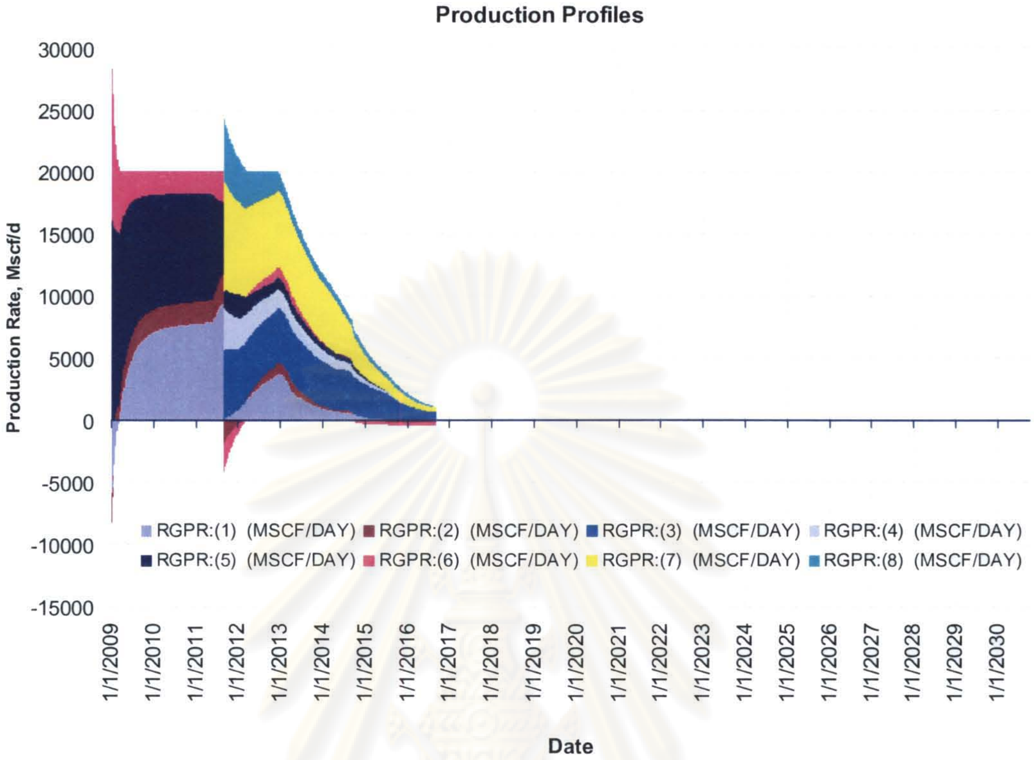

Figure B13: Gas Production Profiles

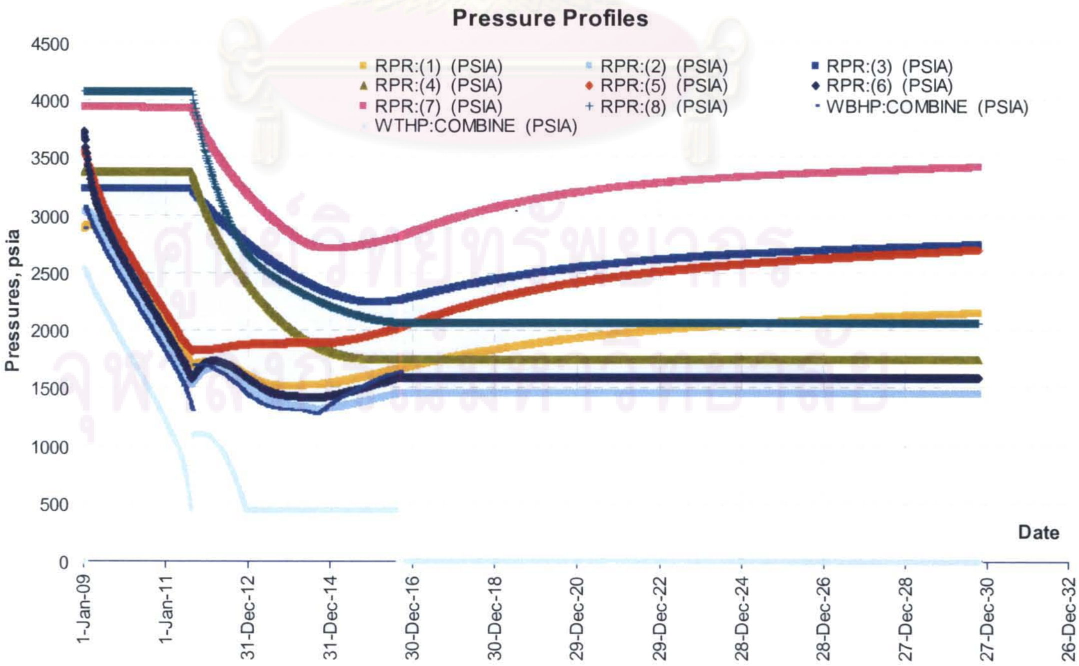

Figure B14: Pressure Profiles

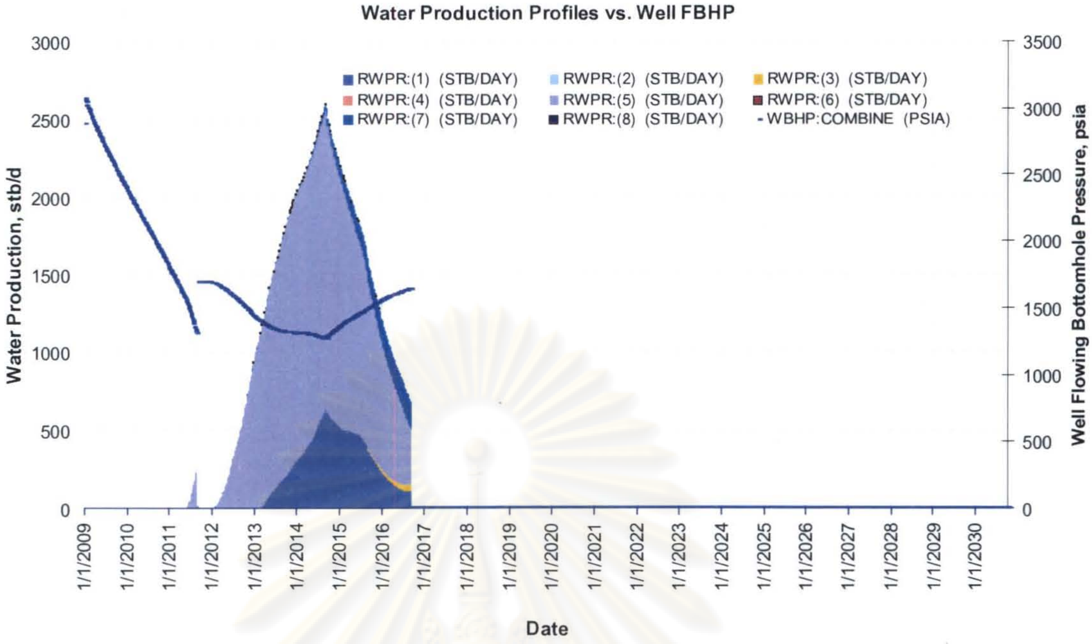

Figure B15: Water Production Profiles vs. Well's Flowing Bottomhole Pressures

Case 6: Scenario 2b, Combination drive model

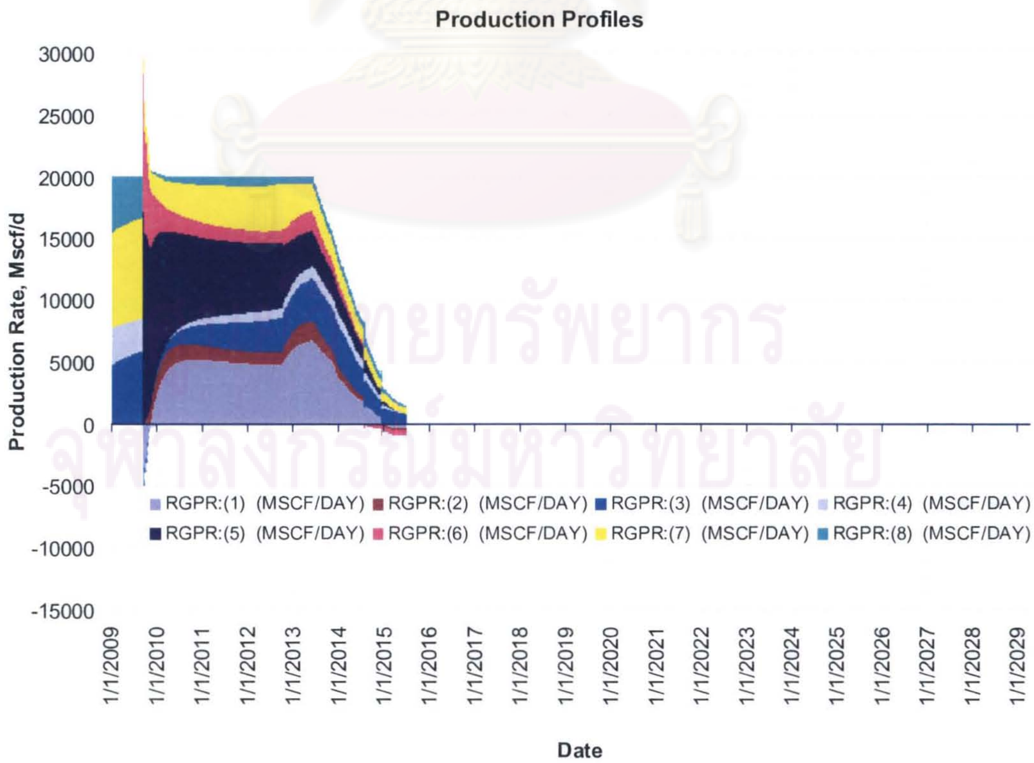

Figure B16: Gas Production Profiles

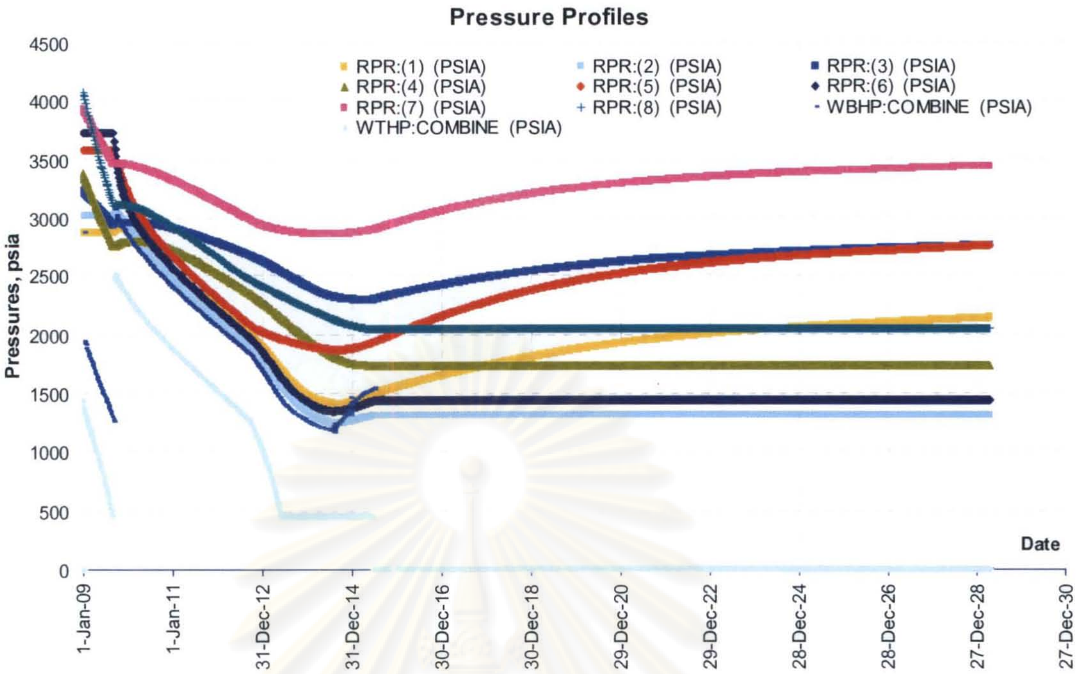

Figure B17: Pressure Profiles

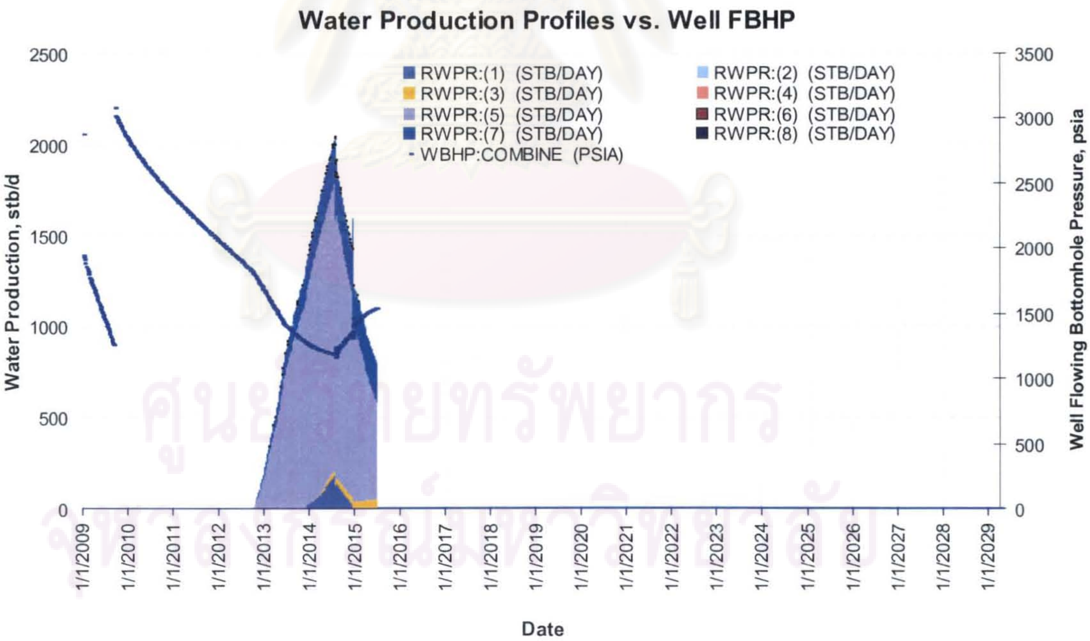

Figure B18: Water Production Profiles vs. Well's Flowing Bottomhole Pressures

Case 7: Scenario 3a, Combination drive model

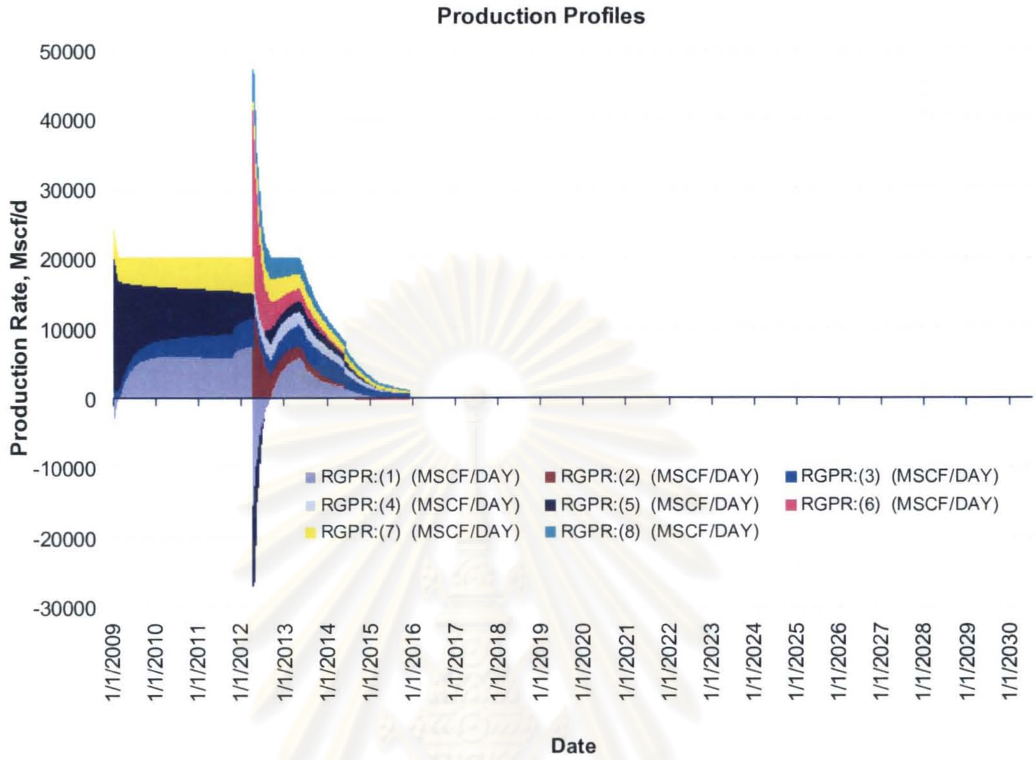

Figure B19: Gas Production Profiles

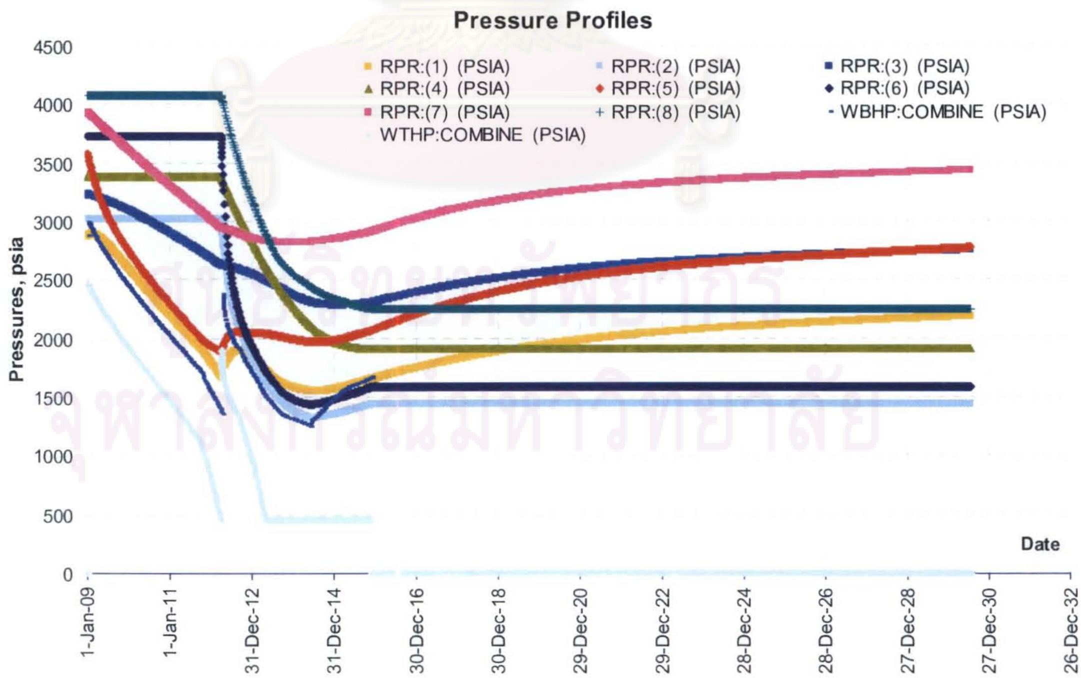

Figure B20: Pressure Profiles

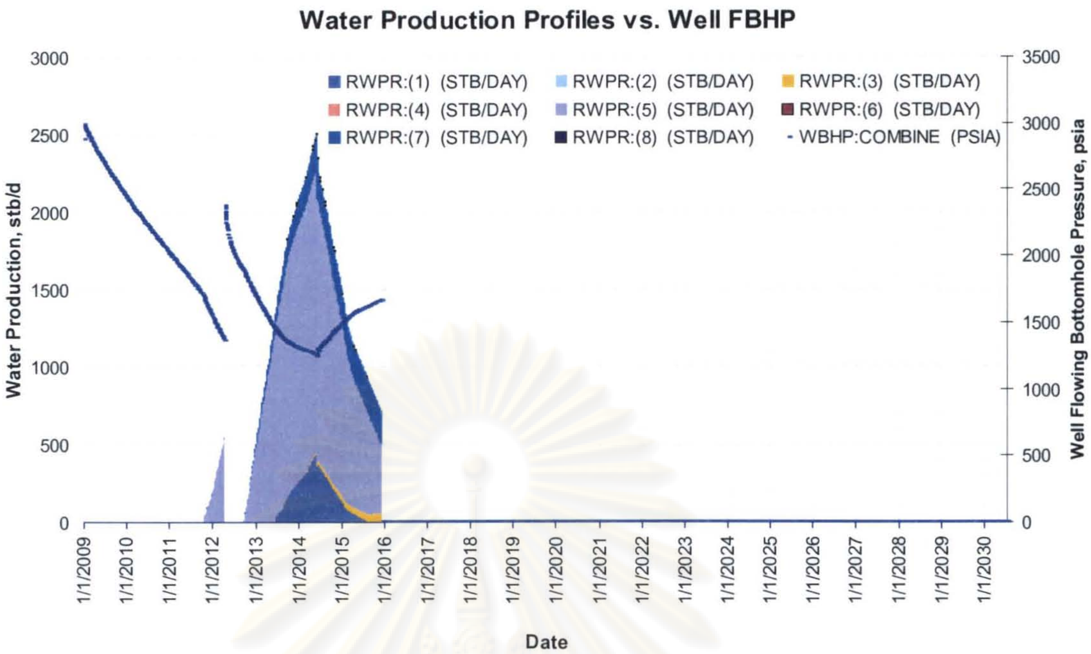

Figure B21: Water Production Profiles vs. Well's Flowing Bottomhole Pressures

Case 8: Scenario 3b, Combination drive model

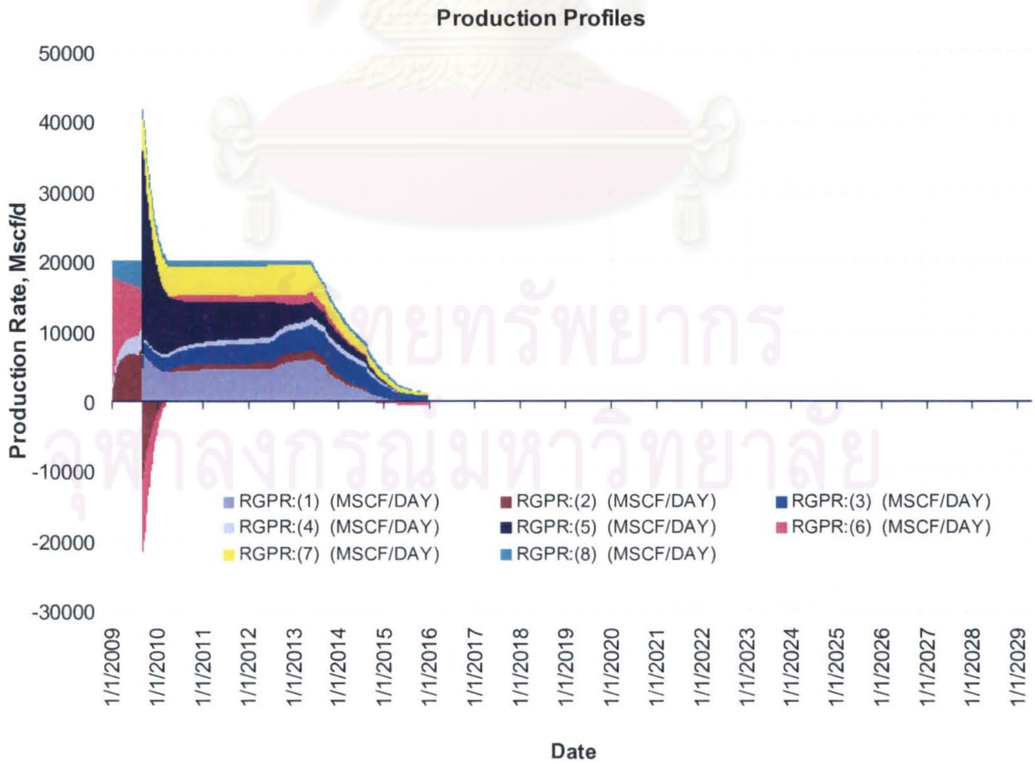

Figure B22: Gas Production Profiles

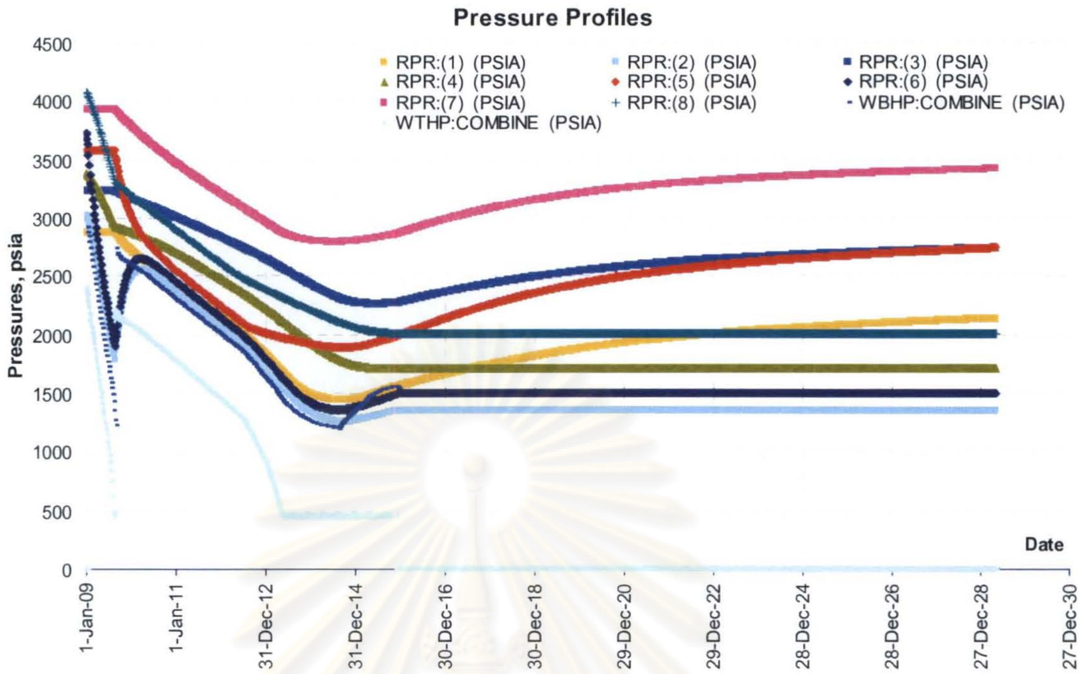

Figure B23: Pressure Profiles

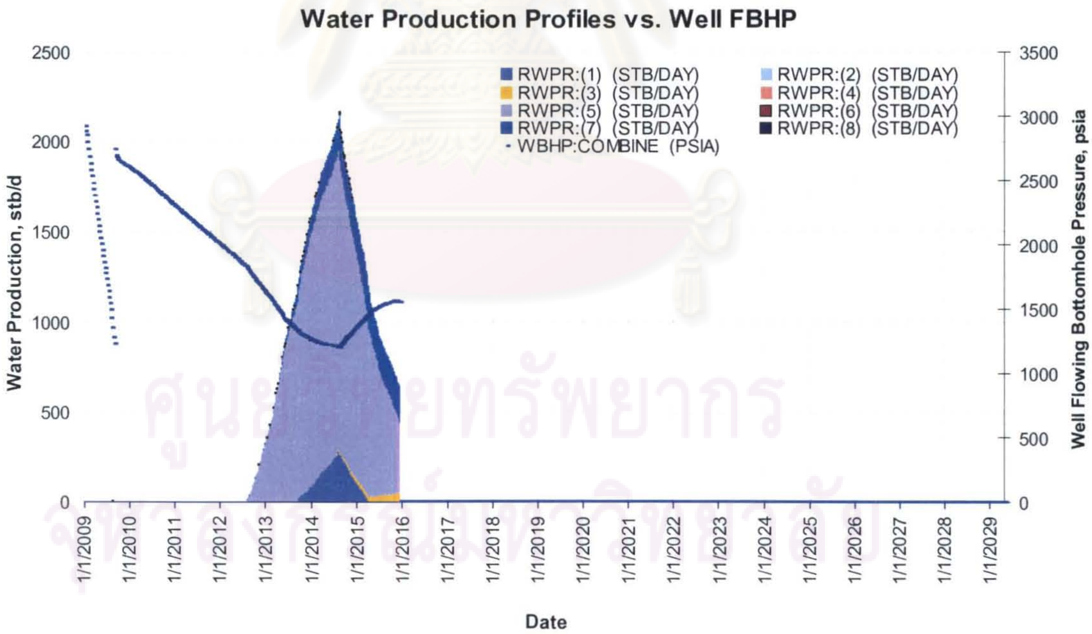

Figure B24: Water Production Profiles vs. Well's Flowing Bottomhole Pressures

Case 9: Scenario 4, Combination drive model

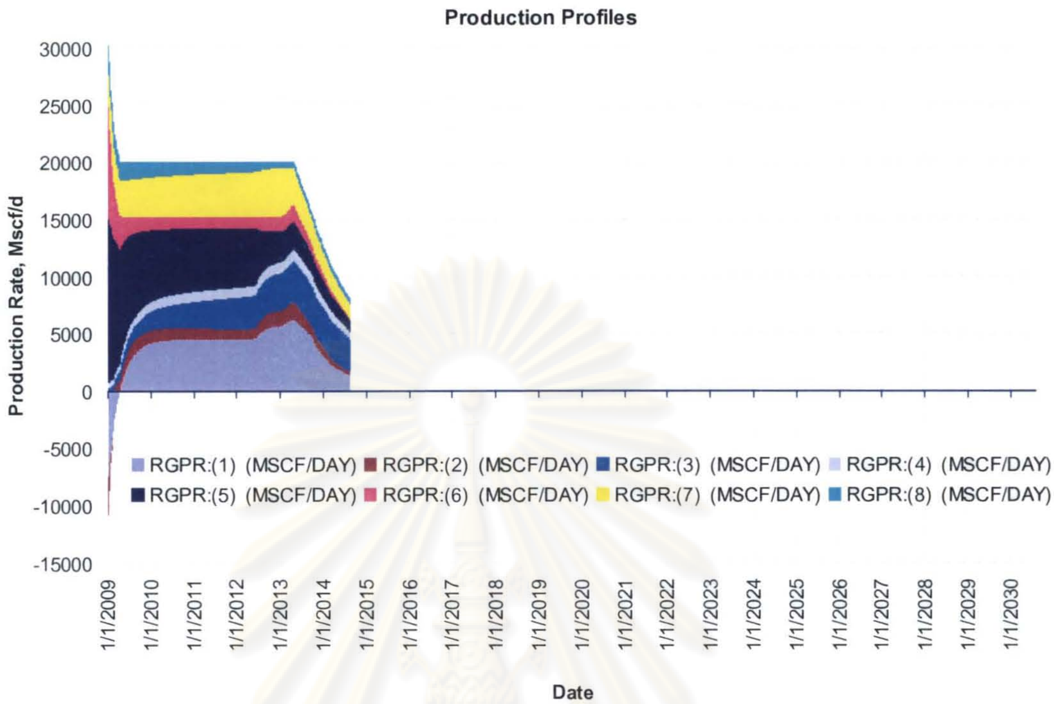

Figure B25: Gas Production Profiles

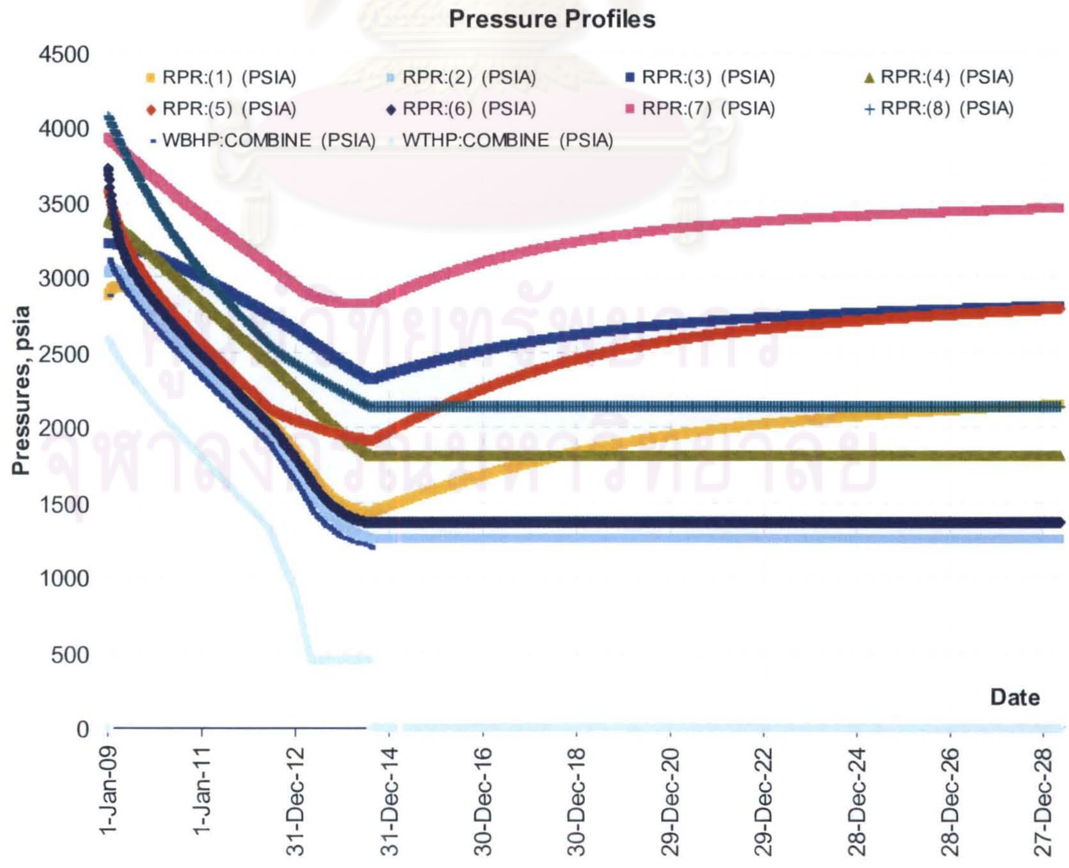

Figure B26: Pressure Profiles

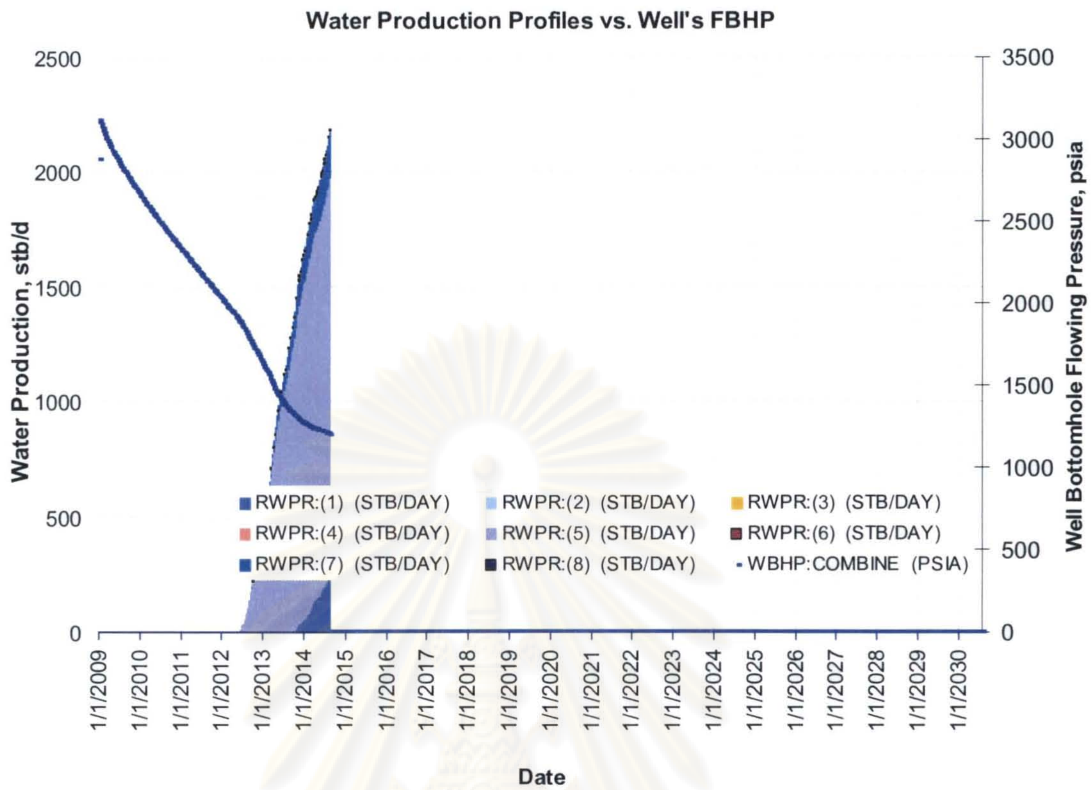

Figure B27: Water Production Profiles vs. Well's Flowing Bottomhole Pressure

Vitae

Ronasak Momin was born on January 31st, 1974 in Bangkok, Thailand. He received his Bachelor of Engineering (2nd class honors) in Chemical Engineering from the Faculty of Engineering, King Mongkot's University of Technology North Bangkok in 1996 and MBA from Thammasat University in 2004. He has been a graduate student in the Master's Degree Program in Petroleum Engineering of the Department of Mining and Petroleum Engineering, Chulalongkorn University since 2006.